From observation well to model area

Estimating groundwater levels spatially using time series analysis

S.A. Klop

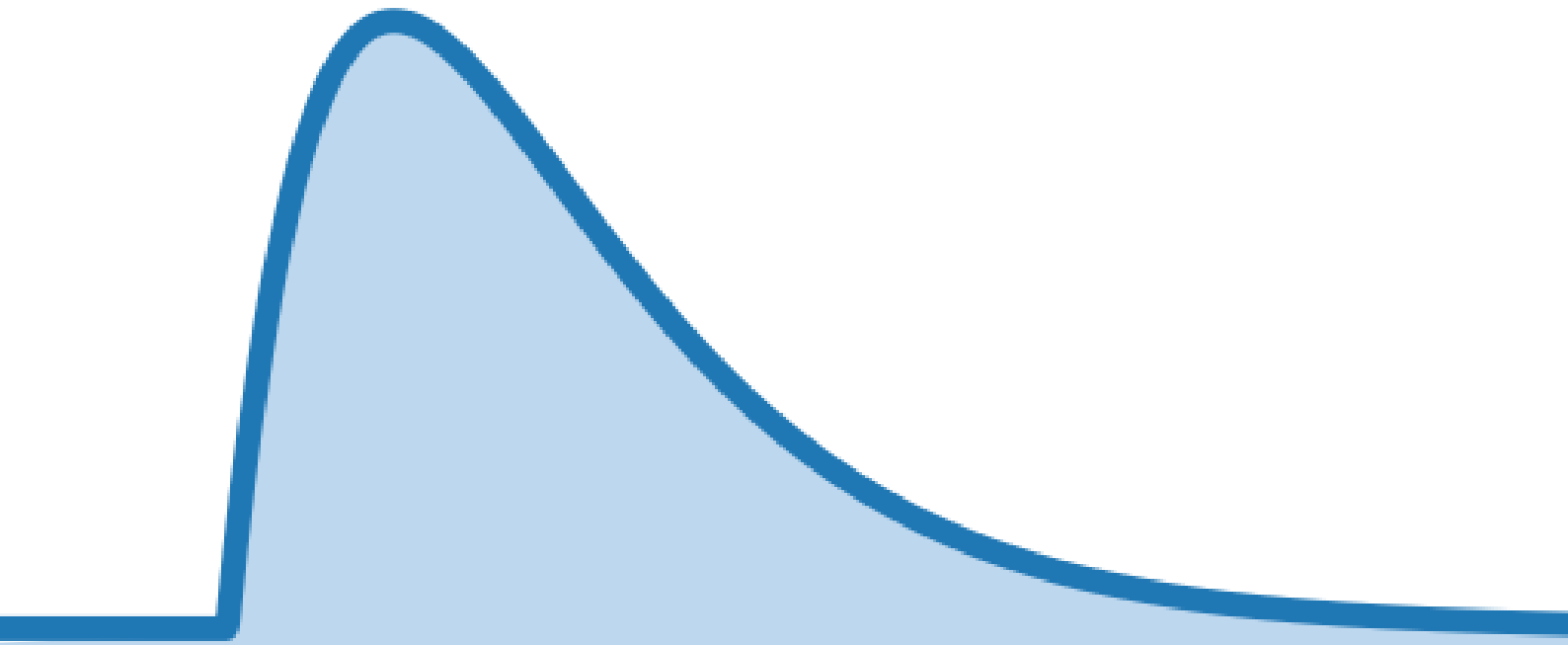

TU Delft

From observation well to model area

Estimating groundwater levels spatially using time series analysis

by

S.A. Klop

to obtain the degree of Master of Science
at the Delft University of Technology,
to be defended publicly on Thursday January 17, 2019 at 14:30 PM.

Student number:	4096843	
Thesis committee:	Prof. dr. ir. M. Bakker,	TU Delft
	Ir. F. Schaars,	Artesia
	Dr. Ir. G.H.W. Schoups,	TU Delft
	Dr. Ir. C.C.J.M. Tiberius,	TU Delft

TU Delft Delft University of Technology

Abstract

Groundwater is an important aspect of water management. A groundwater level that is too high or too low can result in damages to, for example, agriculture or structures. It is therefore important to manage groundwater levels in an area. Measures can be taken to adjust the groundwater level, for example, adjusting a weir or dredging canals. Groundwater levels need to be monitored so that effects of water management measures can be assessed. Groundwater levels are monitored with a network of monitoring wells. The observations from these monitoring wells can be analysed to get a better understanding of the groundwater dynamics. Time series analysis can be used to analyse measured groundwater levels. Time series analysis is a statistical method to simulate a hydrological time series using the stresses on a system and the response functions to these stresses. No additional knowledge on the groundwater system, like aquifer parameters, is required. The effect of different stresses can be determined with this method. This provides information at a single point, but the groundwater level will, of course, vary spatially. It is important to know how the groundwater level varies spatially in order to better manage the groundwater.

The objective of this study is to use time series analysis to spatially simulate groundwater levels based on measurements at one or more observation wells. A method is proposed to use the information obtained from time series analysis to calibrate a conceptual groundwater model to spatially simulate groundwater levels. The proposed method is first tested in a synthetic environment. Several synthetic groundwater models are defined with different layouts. Using these models, synthetic groundwater observations are simulated, which are analysed with time series analysis. The resulting response function is used to calibrate the conceptual groundwater model. The conceptual model is used to simulate the groundwater level. The simulated groundwater level is compared to the groundwater level of the synthetic model. The conceptual model is able to correctly simulate the groundwater level at multiple locations in the area. The explained variance percentages of the simulations is generally higher than 90% for the cases studied.

The proposed method is applied to a case study in The Netherlands in nature area "The Pannenhoef" where multiple observations wells are located. Time series analysis is performed on the groundwater observation series starting with one well in the study area. The response function is determined with time series analysis, and is used to calibrate the conceptual model. The conceptual model is used to simulate the groundwater level in the study area. The simulated groundwater level is compared to the observations at the other observation wells. This process is then repeated for each observation well. The results show that there is a consistent shift between the conceptual model simulation and the observed groundwater levels. No logical pattern is detected between the mean measured heads and the surrounding observations or estimated surface water levels. This makes it impossible to create an accurate spatial conceptual model to simulate the observed heads. However, the conceptual model is reasonably good at simulating the fluctuations of the groundwater level at some locations in the system, but not at all locations. No correlation is found between the goodness of fit of the simulation of the fluctuations and other parameters of the conceptual model.

From the results of the synthetic study it is concluded that the proposed method can be applied to simulate the groundwater level spatially for the tested synthetic models. The explained variance percentage of these simulations is high at most locations in the studied systems. However, more research is needed to identify what the limits of the method are in a synthetic environment. The results from the case study show that the conceptual model is not able to simulate the groundwater head in the area of the case study. A consistent shift between the conceptual model simulations and the observed groundwater head suggests that the base level of the conceptual model is incorrect. The data of the case study did not prove to be sufficient to estimate a reasonable groundwater base level at the location of the observation wells. However, the results do show that the conceptual model is able to simulate the fluctuations of the groundwater level at several locations in the area. It could not be determined why the simulated fluctuations do not match the observed fluctuations at some locations. The proposed method is a promising approach for the spatial simulation of groundwater fluctuations, but good and consistent data is needed to simulate the base level in an area.

Preface

This report is the result of my master thesis research in fulfilment of my Master degree Water Management at Delft University of technology. This research has given me more insight in groundwater modelling and has taught me many more valuable skills. This result could not have been achieved without the support and guidance of many people.

First, I would like to thank my graduation committee for their guidance and feedback during the process of my thesis. Without their support I would not have been able to complete this research. Special thanks go to Mark Bakker, who, as my daily supervisor, helped me with all my Python problems and guided me in the right direction. I would also like to thank Frans Schaars for always providing a fresh take on my research and giving me advice on my work. I thank Gerrit Schoups and Cristian Tiberius for giving me comments of my research which greatly improved the final product.

Next, I would like to thank Tjalda who was always there to support me and give me advice on my thesis. Without her support I would have not been able to finish my thesis. I would also like to thank all my colleagues from Hokje 1, who supported me during the long hours at the university. Without the occasional coffee break and sparing session, I would not have completed this research.

I have thoroughly enjoyed the time working on my master thesis. It has been a great learning experience.

S.A. Klop
January 10, 2019

Contents

1 Introduction

Groundwater levels are an important aspect of water management. This is especially true in the Netherlands where the groundwater table is generally close to the surface. Groundwater plays a key role in, for example, the agricultural sector and urban water management. In the agricultural sector it is key that the groundwater level is not too high, which can cause rotting in the roots of crops or make it impossible for machines to work the fields, or too low, which can mean that the crops are not able to extract enough water from the subsurface. In urban water management, different aspects determine the desired groundwater levels, for example, high groundwater can result in water on the streets or flooded basements, while too low water levels can result in damage to foundations of houses. Numerous examples of this exist in The Netherlands, like in Gouda in 2017[1] or in Amsterdam[2].

Because of this, it is important to understand the groundwater dynamics in an area. Groundwater levels are monitored extensively in The Netherlands. A network of monitoring wells provide information about the groundwater table. The groundwater head is recorded by these wells[3] often at multiple locations in a water system. Using this data the groundwater table can be monitored and managed. When the groundwater level is too high, it can be lowered by for example lowering the water levels in surrounding water bodies or by extracting groundwater. A too low groundwater table can be adjusted by, for example, adjusting a weir so the surrounding water levels increase. These are all examples of active groundwater management. Groundwater is also managed passively by implementing rules and regulations. For instance, waterboards regulate permits for groundwater extractions therefore managing the volume of water extracted from an aquifer.

It is important to know the impact of these measures. The data that is obtained from monitoring wells, does not always directly show how a groundwater system is behaving and reacting to measures that are taken to adjust the groundwater levels. This is because the groundwater level is not constant, the groundwater level changes due to natural processes such as seasonal changes and drought periods. It can therefore be hard to identify the effect of these measures. Time series analysis can be used to compute these effects on the groundwater table. Time series analysis is a method to simulate a hydrological time series using the stress series[4] and their response functions. In this case the method aims to simulate the observed groundwater table using the precipitation, evaporation and any additional stresses like groundwater extractions. The response function of a system is the change in groundwater due to a certain unit of stress. Different response functions can describe the behaviour of different types of systems. Fast responding systems will have a different response function compared to a system which reacts slower to a certain stress. The method of time series analysis is widely applied in The Netherlands using the software Menyanthes (Von Asmuth et al., 2012; Box et al., 2015), which is specifically designed for time series analysis of groundwater series. Since 2017 an alternative for the Menyanthes software was developed called Pastas (Bakker et al., 2018), which is an open

[1] `https://www.ad.nl/gouda/schadeclaim-voor-gouda-over-niveau-van-waterpeil~aa8cb227/`

[2] `https://www.parool.nl/amsterdam/palen-onder-amsterdam-verpulveren~a264596/`

[3] Groundwater is usually measured as a hydraulic head, meaning the water level above a datum. The unit for the groundwater head is meters.

[4] A stress series is defined as an influence on the groundwater system like precipitation and evaporation.

source software written in Python.

Even though the monitoring network in the Netherlands is considerable and time series analysis can provide substantial information about the groundwater system and its response, there still are some limitations. One of these is that groundwater levels are measured at a point. However, groundwater levels can vary spatially due to heterogeneous soil characteristics and different boundary conditions. Because of this and because different land uses have different groundwater requirements, it is important to know how the groundwater table varies spatially. In areas where there are only a limited number of wells, the spatial variation of the groundwater levels is largely unknown. Currently this issue can be solved by creating a groundwater model using groundwater modelling software like ModFlow (Hughes et al., 2017) or Ttim (Bakker, 2013b,a). With these models it is possible to model the groundwater table in an area. However, this requires data about aquifer parameters and a heavy time investment. Second, this requires the creation of a new groundwater model for each area, making this option less viable when multiple areas need to be evaluated and a quick assessment is needed.

Performing time series analysis on an observation series of a monitoring well often provides excellent information about the ground water level at a point with a relatively low data requirement and time investment, while making a groundwater model can provide information on a larger spatial scale but requires a relatively large time investment and data requirement. For management decisions it would be beneficial to be able to understand the spatially varying groundwater level without the need to invest in a complete groundwater model. This research aims to find a method to use the information gained from time series analysis together with a simple conceptual groundwater model to determine groundwater levels on a spatial scale. The primary research question for this study is:

Can time series analysis be used to estimate groundwater levels in an area?

The following sub questions are formulated:

- Can the response function at an observation well be determined with time series analysis?
- Can a single layer conceptual model be used to reproduce the response function at an observation well obtained with time series analysis?
- Can a calibrated single layer conceptual model be used to estimate the response at other observation wells?

This report is structured as follows. In Chapter 2 the time series analysis is explained. In this chapter the theory behind the time series analysis method is discussed. In Chapter 3 the synthetic study is explained. The method used for the synthetic models is described, after which the results from the synthetic study are presented. The case study is presented in Chapter 4. The method of the case study is explained and the results are presented. In the final chapters the results conclusions about the results are drawn, the research questions are answered, and recommendations are given.

2

Time series analysis Methodology

In this chapter the method of time series analysis is described. The different response functions used in this method are briefly presented. After this the different response functions are tested on a set of groundwater observation series from different observation wells.

2.1. Time series analysis using transfer function noise modelling

Groundwater observation series can be simulated using time series analysis. The method is used to explain head variations in a groundwater monitoring well using a mathematical approach with transfer function noise modelling (TFN) (Von Asmuth et al., 2002, 2008). This method uses a response function to simulate a observed head series. The time series analysis in this study is performed using the Pastas software (Bakker et al., 2018). Pastas is a recently developed open source software, developed by Artesia and The Technical University of Delft. For this research Pastas is favoured compared to, for example, Menyanthis because it is open source, meaning that changes or additions can be made. The data that is needed for the time series analysis is a data series with observed groundwater levels and data about any stresses which have an influence on the observed series; this can be precipitation, evaporation or an extraction well. No additional data is required with regards to soil characteristics or information about the water system. For time series analysis the assumption is that the system behaves linearly. Because of this, the influence of each stress series on the observed head series is computed using the principle of convolution. This means that the observed head can be simulated as

$$h(t) = \sum_{i=1}^{k} h_i(t) + d + n(t) \tag{2.1}$$

where $h(t)$ is the observed head, $\sum_{i=1}^{k} h_i(t)$ is the contribution to the head from each stress where k is the number of stresses, d is the head when no stresses are present in the system (the base level), and $n(t)$ is the noise series (Von Asmuth et al., 2008). The contribution of stress i to the observed head is calculated with the response function of each stress. This yields the following formula:

$$h_i(t) = \sum_{j=1}^{\infty} N_j b_j(t) \tag{2.2}$$

where $h_i(t)$ is the head as a result of stress i, N_j is the stress (for example mm of rain) in the time interval j (from t_{j-1} to t_j) and $b_j(t)$ is the block response at time t due to the unit stress in time interval j (Bakker et al., 2008).

2.2. Response functions

Three response functions are distinguished; the block response function and the step response function and the impulse response function. The step response function is the result of a continuous unit stress on the system (e.g., a constant precipitation of 1 mm/day or pumping of 1 m^3/day). For long enough periods this function will reach an equilibrium state. The block response function is the result of one unit of stress on a single time step (this can be one day, hour, minute depending on the system). The impulse response function is the head as a result of a unit stress for an infinitely small time step. The step response, $s(t)$, is defined as :

$$s(t) = \int_0^t \theta(\tau) d\tau \tag{2.3}$$

with $\theta(\tau)$ is the impulse response of the system. The block response, $b(t)$, is related to the step response as:

$$b(t) = s(t) - s(t - \Delta t) \text{ for } t \geq \Delta t \tag{2.4}$$

Response functions are functions that describe the behaviour of the groundwater head due to a certain stress, the shape of these functions is dependent on the type of stress and the water system. Some response functions can be derived from simple groundwater problems. Several different response functions are used in this research. The exponential response function is the simplest response function used in this research. The formula for the Exponential step response function is

$$s(t) = A\frac{1}{a}\int_0^t e^{-\tau/a} d\tau = A(1 - e^{-t/a}) \tag{2.5}$$

where A [L] is the head which the function approaches when $t \to \infty$, and a is a scaling parameter with dimension [T]. The function has two parameters A and a. Examples of the exponential step and block response are shown in Figure 2.1, the responses are plotted using different parameters, which yield different shapes for the step response.

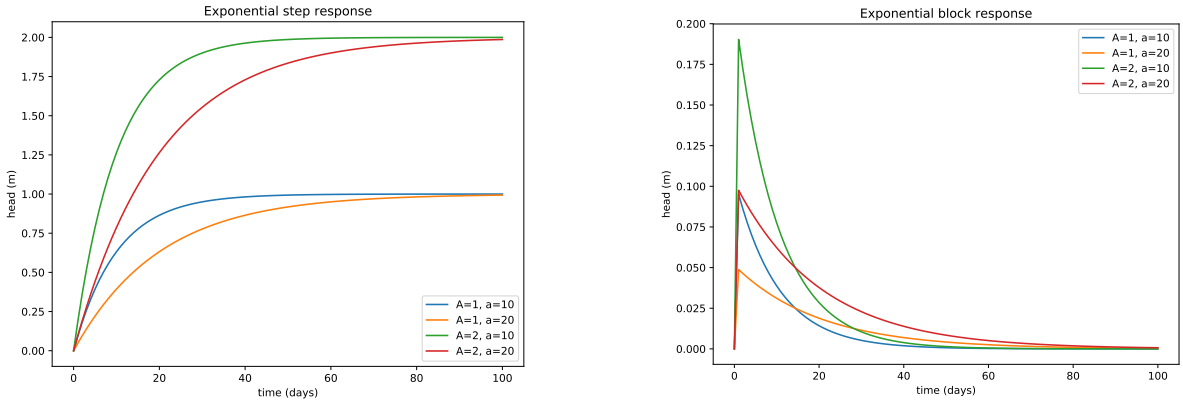

Figure 2.1: Examples of the Exponential response functions with different parameters.

The Gamma step response function is one of the most commonly used response function for precipitation and evaporation stress series. This response function is based on the Gamma function. The formula for the Gamma step response is:

$$s(t) = A\frac{1}{\Gamma(n)}\int_0^t \tau^{n-1} \cdot e^{-\tau/a} d\tau = A\Gamma_{inc}(n, t/a) \tag{2.6}$$

where A [L] is the head that the function approaches when $t \to \infty$, and a is a scaling parameter with dimension [T]. The Gamma function has three parameters A, a and n. In Figure 2.2 different examples of the Gamma response functions are shown.

Extraction or discharge wells have different effect on the groundwater head in a well than precipitation or evaporation have. For this type of stress the Hantush function can be used. This function is based on the analytical solution found by Hantush and Jacob (1955) for pumping tests, and also used by Von Asmuth et al. (2008) and Veling and Maas (2010). The Hantush formula is based on a well in an infinite aquifer, with

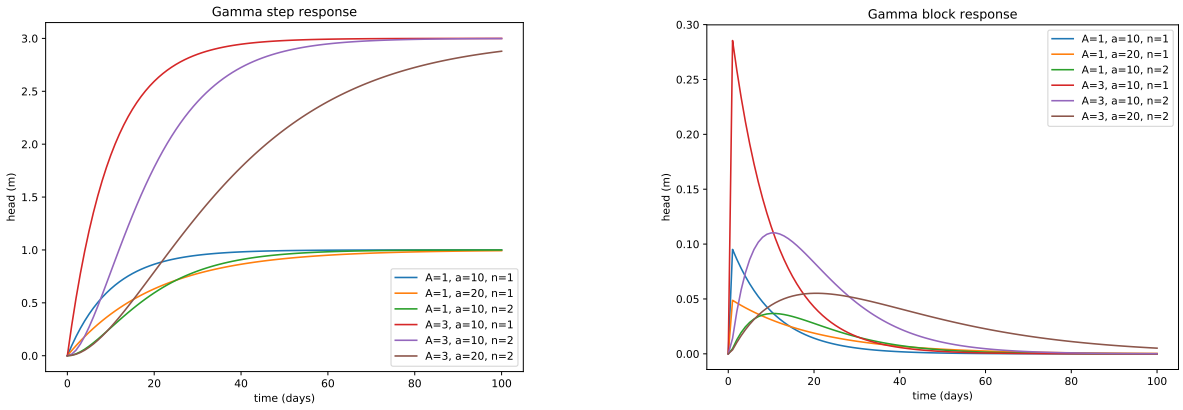

Figure 2.2: Examples of Gamma response functions for several parameter combinations

a thickness D, a hydraulic conductivity k and a storage coefficient S. The aquifer is covered with an aquitard with a resistance c. The Hantush function is:

$$s(t) = A\frac{1}{\int_0^\infty \tau^{-1} e^{-\tau/a - b/\tau} d\tau} \int_0^t \tau^{-1} e^{-\tau/a - b/\tau} d\tau \tag{2.7}$$

where A [L] is the head that the function approaches when $t \to \infty$, a is a scaling parameter with dimension [T] and b is another scaling parameter with dimension [T] (Veling and Maas, 2010). Examples for the Hantush response function using different parameters are shown in Figure 2.3.

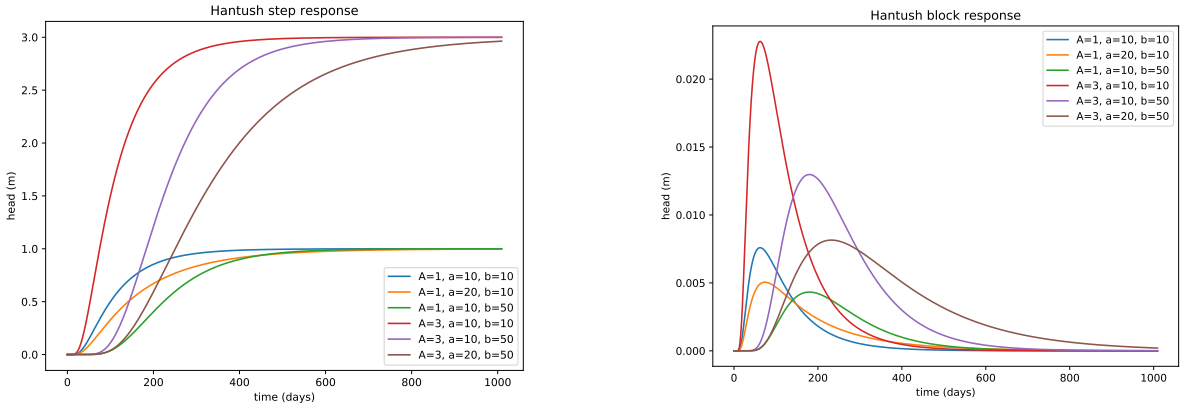

Figure 2.3: Examples of the Hantush response functions for several parameter combinations

A new response function proposed in this research is the Double Exponential function. The formula for the double exponential response function is:

$$s(t) = A\left(1 - \left((1-\alpha)\cdot e^{-t/a} + \alpha \cdot e^{-t/b}\right)\right) \tag{2.8}$$

where A and a are the same parameters as in the normal exponential function, b with dimension [T] is the weighing parameter for the second exponential and α is a ratio parameter between both exponentials. In Figure 2.4 examples for the Double Exponential response function are shown.

A second new response function used in this research is the Four-Parameter response function. The Four-Parameter function is based on Bakker et al. (2008). The formula for this response function is:

$$s(t) = A\frac{1}{\int_0^\infty \tau^{n} \cdot e^{-\tau/a - b/\tau} d\tau} \int_0^t \tau^{n} \cdot e^{-\tau/a - b/\tau} d\tau \tag{2.9}$$

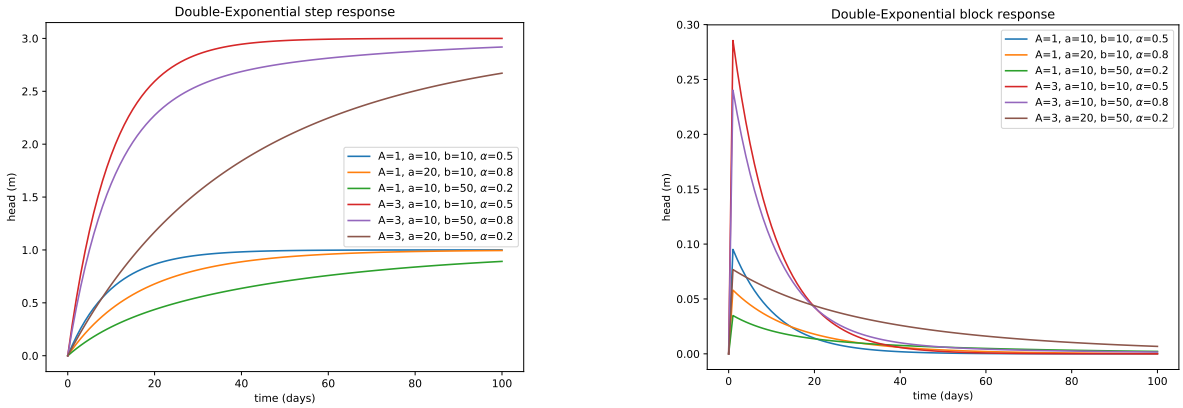

Figure 2.4: Examples of the Double Exponential response functions for several parameter combinations

where A is the equilibrium parameter and a [T], b [T], and n are scaling parameters. The function is scaled with an integral to make sure the response function approaches A when $t \rightarrow \infty$. These response functions can have different shapes compared to the standard response functions described above. Examples of the Four-Parameter response functions are shown in figure 2.5.

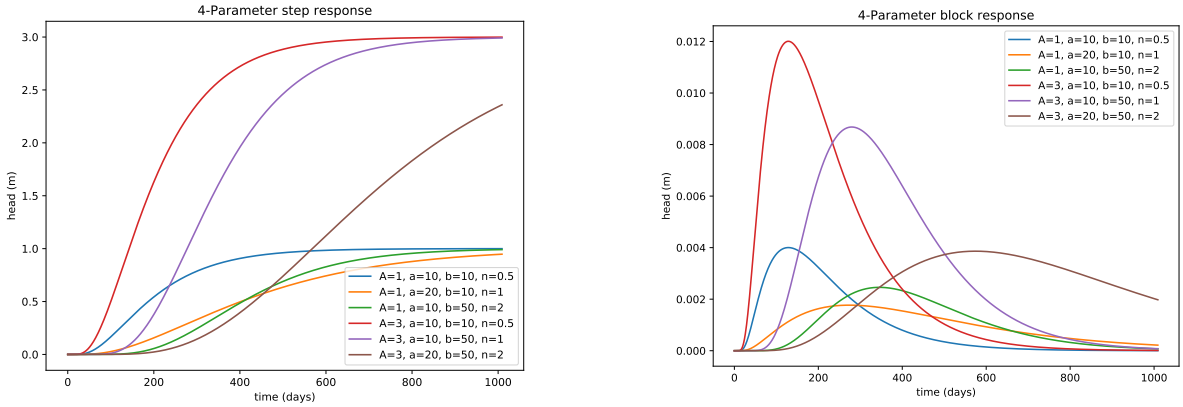

Figure 2.5: Examples of the Four-Parameter response functions for several parameter combinations

In Table 2.1 an overview of all the response functions is presented together with the parameters of each function. When Equation 2.9 is compared to equations 2.5, 2.6 and 2.7, it can be seen that all of these equations are special cases of the Four-Parameter function. Therefore the Four-Parameter function is always able to produce the same behaviour as the Exponential, Gamma and Hantush functions.

2.3. Noise model

One of the response functions is selected for each stress, different stresses can have different response functions depending on the type of stress. With this information the time series analysis will optimize the parameters for all of the response functions to simulate the observed head. Optimization in Pastas is done with the least squares method. The parameters of all the response functions are optimized to simulate the observed head series. Time series analysis can either minimize the residuals or the noise. The residuals are defined as

$$r(t) = h_o(t) - h_s(t) \tag{2.10}$$

where h_o is the observed groundwater head and h_s is the simulated groundwater head. The noise is a series obtained from the residuals of the simulation through the noise model. Noise is introduced in the model, for example, when head observations contain errors or when the stress series contain errors. This can be caused

Name	Step response	Parameters
Exponential	$s(t) = A\frac{1}{a}\int_0^t e^{-\tau/a}d\tau$	A, a
Gamma	$s(t) = A\frac{1}{\Gamma(n)}\int_0^t \tau^{n-1}e^{-\tau/a}d\tau$	A, a, n
Hantush	$s(t) = A\frac{1}{\int_0^\infty \tau^{-1}\cdot e^{-\tau/a-b/\tau}d\tau}\int_0^t \tau^{-1}\cdot e^{-\tau/a-b/\tau}d\tau$	A, a, b
Double Exponential	$s(t) = A\left(1-\left((1-\alpha)\cdot e^{-t/a}+\alpha\cdot e^{-t/b}\right)\right)$	A, a, b, α
Four-parameter	$s(t) = A\frac{1}{\int_0^\infty \tau^{n}\cdot e^{-\tau/a-b/\tau}d\tau}\int_0^t \tau^{n}\cdot e^{-\tau/a-b/\tau}d\tau$	A, a, b, n

Table 2.1: Overview of the different response functions and their formulas.

for example when a rain gauge is at some distance from the observation well and records precipitation when at the actual location of the observation well there is no precipitation. The noise is not independent for each time step, it is correlated. The base formula for the noise model is:

$$n(t_1) = r(t_1) - r(t_0)e^{-(t_1-t_0)/\alpha} \tag{2.11}$$

where $n(t_1)$ is the noise at time t_1, $r(t_1)$ is the residual at time t_1, $r(t_0)$ is the residual at time t_0 and α is the decay rate for the noise [T] (Von Asmuth and Bierkens, 2005). The noise model assumes exponential decay of the noise. By calculating the innovations from the residuals, it can be determined what the actual noise is by filtering the correlation in the residual series. The noise series is minimized to obtain the optimal parameters for the response functions, the base level and any additional parameters. When the simulation of the observed head is completed and the parameters of all the response functions are determined, the response function (both step and block) for each stress is known and the contribution of each individual stress series to the observations.

2.4. Comparing response functions

Time series analysis for this study is performed using the Pastas software. Two different response functions are added to the response functions available in Pastas; the Double Exponential and the Four-Parameter response function. The response functions are compared with a set of 76 observation wells, located around the city Utrecht. The observation wells that are used only have a single stress series; the recharge. The recharge is calculated as

$$R = P - f \cdot E \tag{2.12}$$

where P is the precipitation, E is the evaporation and f is the evaporation factor. The parameter f is optimized with time series analysis. In order to evaluate the time series analysis simulation, several statistical parameters are calculated. The explained variance percentage (EVP) is calculated for the simulation. The EVP is calculated as:

$$EVP = \frac{\sigma_{h_o}^2 - \sigma_r^2}{\sigma_{h_o}^2} \cdot 100 \tag{2.13}$$

Where $\sigma_{h_o}^2$ is the variance of the observations and σ_r^2 is the variance of the residuals (Von Asmuth et al., 2002). An EVP of 100% means the simulation is a perfect match to the observations. An EVP of 0% means the simulation is not able to simulate the observations. Furthermore, the root mean squared error (RMSE) and the root mean squared noise (RMSN) are calculated. The RSME and RMSN are calculated as:

$$RMSE = \sqrt{\frac{\sum_{i=1}^{k}(h_s(t_i) - h_o(t_i))^2}{k}} \qquad RSMN = \sqrt{\frac{\sum_{i=1}^{k} n(t_i)^2}{k}} \tag{2.14}$$

where h_s is the simulated groundwater series, h_o is the observed groundwater, k is the number of observations and n is the noise series. A high RMSE or RMSN indicates that there are large deviations between the simulated and observed series. These parameters are calculated with Pastas.

Well B38E1615_2 is used as an example well. The time series analysis is performed using 4 types of response functions: the Exponential, Gamma, Double exponential and the Four-Parameter function. The Hantush response function is not used in this comparison, since this is commonly used for stresses from an extraction well. The results of the four response functions are shown in Figure 2.6, 2.7, 2.8 and 2.9. It can be seen that the EVP is lowest using the Exponential response function. For the Gamma response function the EVP is slightly higher. The Double Exponential and the Four-Parameter functions yield the highest EVP's of 79.66% and 82.18% respectively.

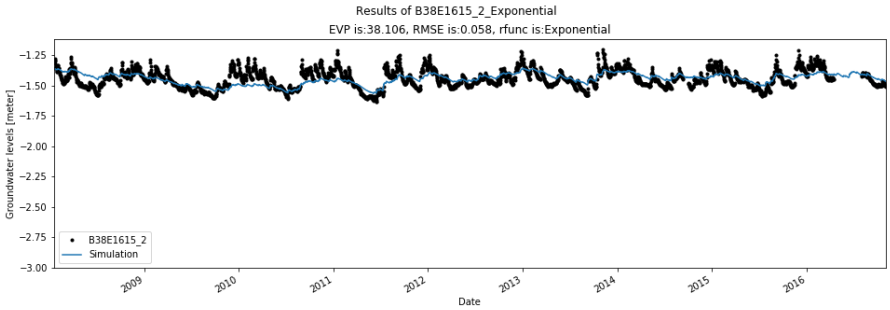

Figure 2.6: Time series analysis simulation using the Exponential response function on the example well

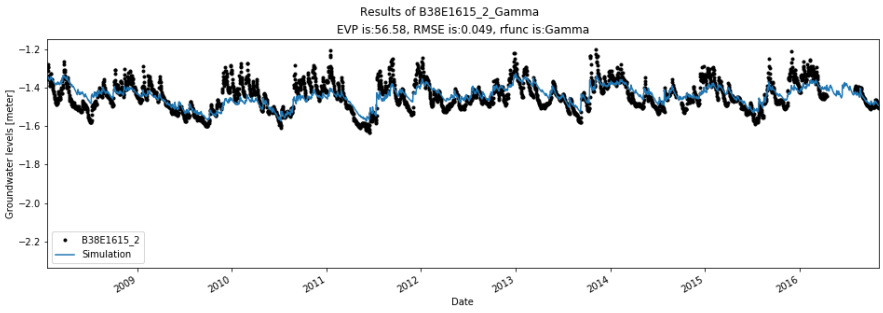

Figure 2.7: Time series analysis simulation using the Gamma response function on the example well

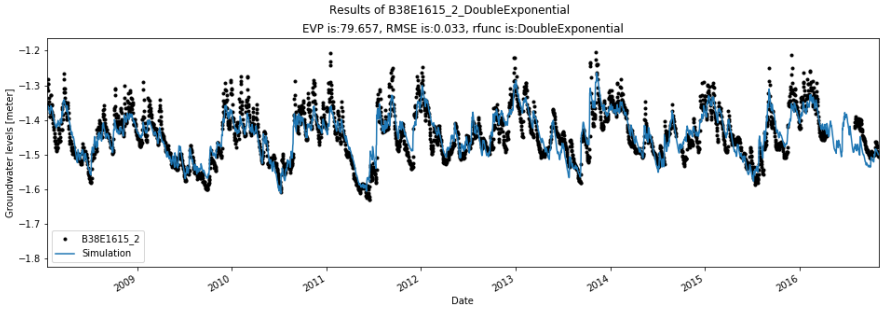

Figure 2.8: Time series analysis simulation using the Double Exponential response function on the example well

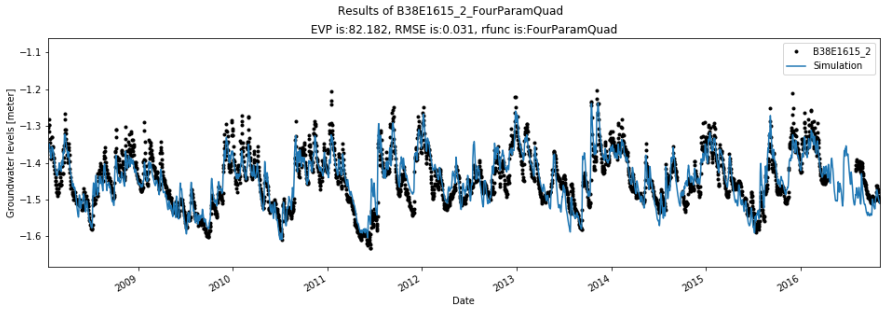

Figure 2.9: Time series analysis simulation using the Four-Parameter response function on the example well

Time series analysis is performed on each of the 76 observation wells using the 4 types of response function. For each simulation the EVP, RMSE and RMSN are calculated. The EVP results are shown in Figure 2.10, the RMSE in Figure 2.11 and the RMSN in Figure 2.12. As can be seen in the figure, the EVP is different for each simulation. The EVP of some wells is low for all response functions, time series analysis is not able to simulate the observed groundwater levels well. The Four-Parameter response function is often the response function with the highest EVP. In some cases the simulation with the Double Exponential function has the highest EVP value. The Gamma function and the Exponential function have a lower EVP value in most cases. Based on the equation of the response functions, the Gamma function should always perform better or equal to the Exponential function and the Four-Parameter function should perform better or equal to the Gamma function. This is not always the case as is shown in Figure 2.10. This can be explained by the least squares optimization not being able to find the optimal solution for the parameters or the noise model is not able to filter the noise correctly. This only occurs in very few cases. The RMSE and the RMSN are lowest for the Four-Parameter function, this is in line with the EVP values. The RSME and RMSN have a similar pattern. The Gamma function is expected to perform better than the Exponential function, 15% of the wells have at least a 10% increase in EVP compared to the Exponential response function. For the simulations with the Four-Parameter function, 35% of the wells have at least a 10% increase in EVP compared to the Gamma response function. The Double Exponential function has the highest EVP for 23% of the simulations.

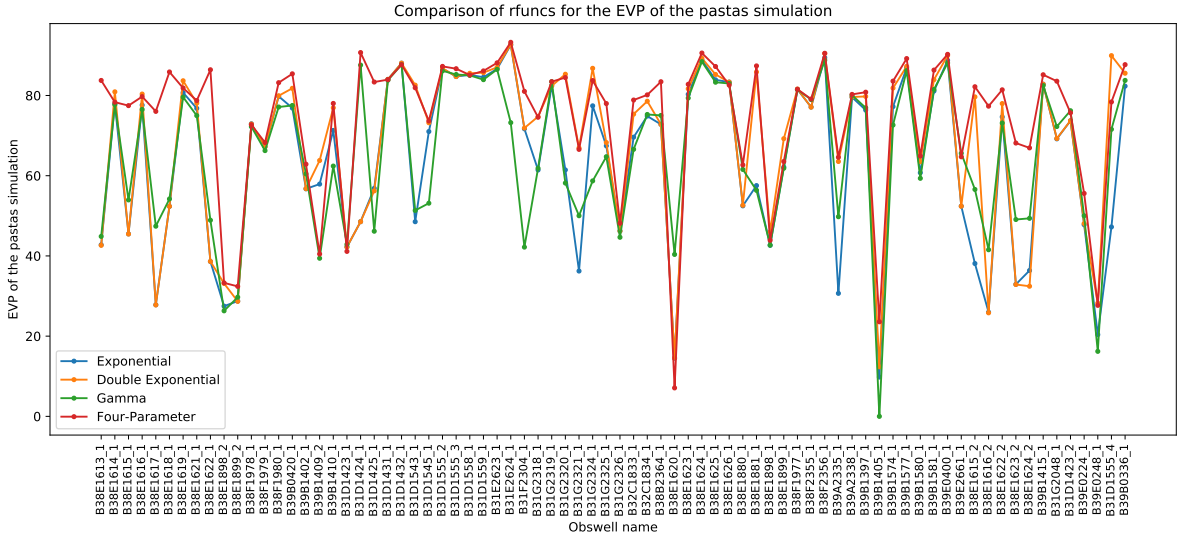

Figure 2.10: EVP comparison for different response functions

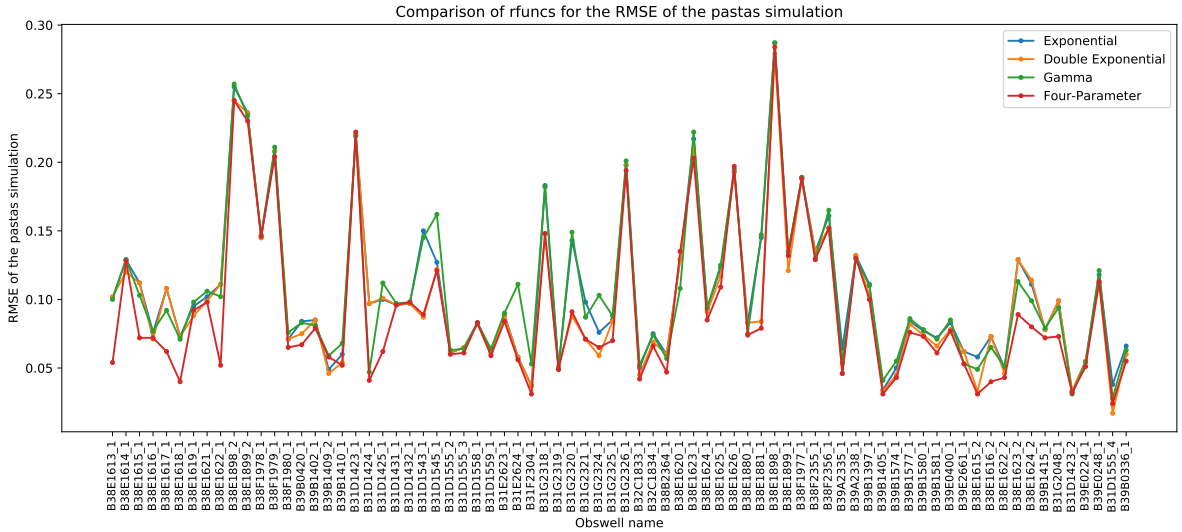

Figure 2.11: RMSE comparison for different response functions

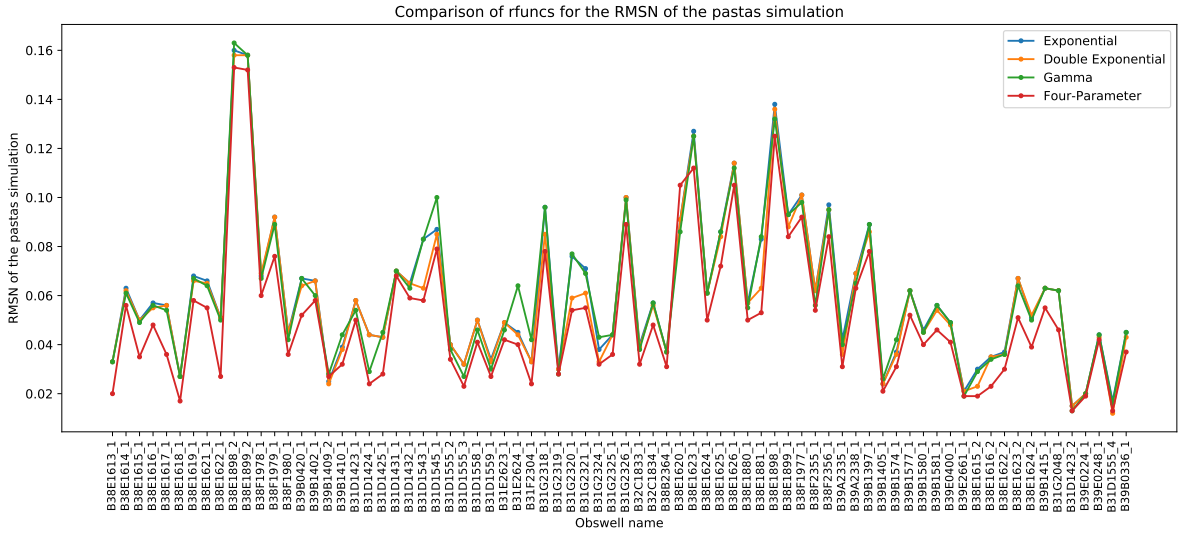

Figure 2.12: RMSN comparison for different response functions

3

Synthetic study

In this chapter the synthetic study is explained. The synthetic study is used to test the method in a synthetic environment where all parameters are known. First the general approach is briefly explained. Second, the first synthetic model, based on the Hantush Model, is presented. After this, the method for modelling different layouts is explained, together with the results for these models. Finally, some conclusions are drawn based on the results of the synthetic study.

3.1. Synthetic study approach

The first step of the synthetic study is to create a synthetic model. The synthetic model is created with Ttim. Ttim is an analytical groundwater modelling software (Bakker, 2013a,b). A simple canal layout is designed together with aquifer parameters. Using this the synthetic model is created. A stress is put on the synthetic model, this can be, for example, a recharge or an extraction. Using the synthetic Ttim model the groundwater head is modelled. A location in the synthetic model is selected as the location of the observation well (this is not a physical well in the groundwater system, just the location where the synthetic observations are simulated). At the location of this well the groundwater is simulated. This series is the synthetic groundwater observation series. The synthetic response of the system is simulated using a unit stress (unit stress can be for example 1 m/d of recharge or an extraction of 1 m^3).

The next step is to use the simulated synthetic observations for the time series analysis. These observations are simulated using Pastas. The stress series used in the time series analysis is the same series that is used in the synthetic model. With the time series analysis a response function is determined. The response function from the time series analysis is compared with the synthetic response function. This will verify if the time series analysis is able to determine the actual response function of the groundwater system.

To simulate the groundwater levels spatially a conceptual groundwater model is made using Ttim. The conceptual model is calibrated using the response function obtained with the time series analysis. This is done by adding a unit recharge stress to the conceptual model of 1 m/d (this is the stress used to simulate the step response function). The step response function of the conceptual model is fitted on the step response function from time series analysis. The aquifer parameters are optimized using the least squares method. The response function of the calibrated conceptual model is compared to the response function of the synthetic model and the time series analysis. Once the conceptual model is calibrated it can be used to simulate the groundwater in the area. First the groundwater head at the location of the observation well is simulated, the resulting series is compared with the synthetic observations of the synthetic model. Next, the simulated groundwater head can be compared between the conceptual and synthetic model at any location in the system. With this it can be verified if the conceptual model is able to simulate the groundwater head spatially. An overview of the method used in the synthetic study can be seen in Figure 3.1.

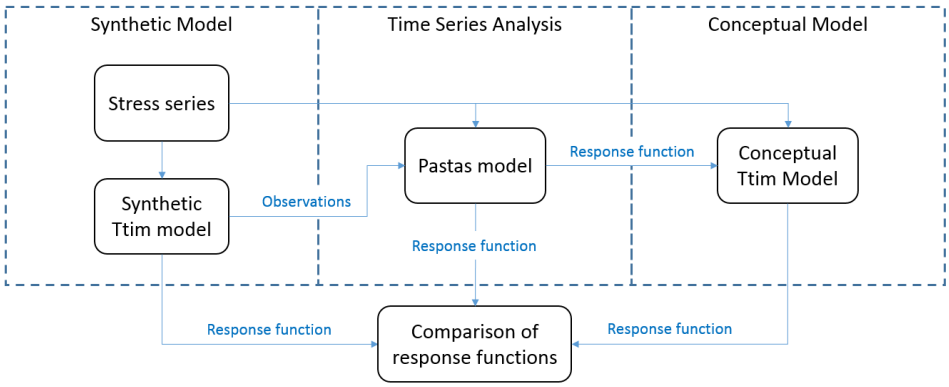

Figure 3.1: Model approach to verify response functions

3.2. Synthetic Hantush model

The first synthetic model is derived from the standard Hantush situation (Hantush, 1956; Hantush and Jacob, 1955). This situation has been extensively studied and is thus useful to verify the approach of this research. In Figure 3.2 the layout of the synthetic model is shown. This situation consists of a homogeneous infinite aquifer which is confined by a leaky layer with a constant groundwater head above the leaky layer. In this situation an extraction well fully penetrates the aquifer and extracts groundwater with a known rate (the extraction well is shown as the green dot in the figure).

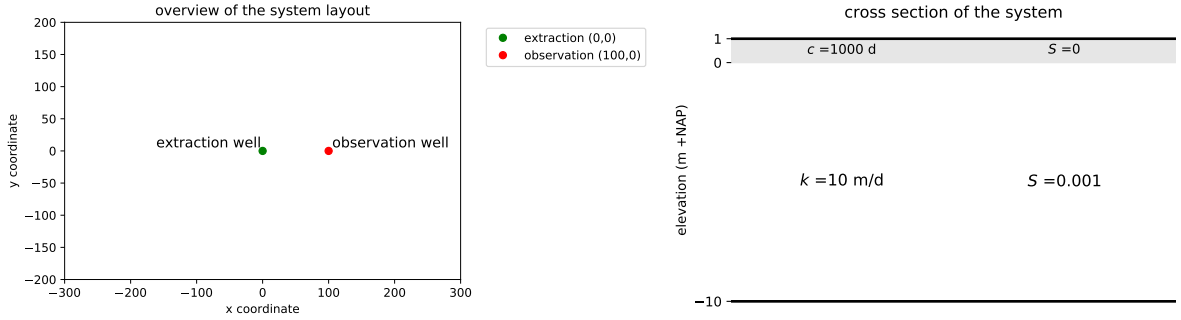

Figure 3.2: On the left the overview of the Hantush model and on the right the cross section of the ground in the model

For this synthetic model the only stress on the system is the extraction from the well; no precipitation or evaporation are present. An observation well is placed 100 m from the extraction well, as can be seen in Figure 3.2 (because of the layout of the system the groundwater will be radially symmetric, and only the distance from the observation well to the extraction well will affect the groundwater head). The pumping rate of the extraction well is presented in Figure 3.3, for this synthetic model a period of 10 years is chosen, between 1980 and 1990 (this series is an arbitrary series only used for validation purposes). In the second plot in Figure 3.3 the resulting head in the observation well is shown. This is the groundwater head as calculated by the synthetic Ttim model (this series is the synthetic data, or synthetic observations series in the monitoring well). No noise is added to the observations or stress in the model. Several attempts where made to add noise to the data used in the time series analysis. However, Pastas was not able to filter out the noise in most cases using the noise model. Therefore not noise is added in the synthetic study.

These two time series serve as the input for the Pastas model. Since the only stress on the system is an extraction well, the Hantush response function is used in the time series analysis (see Chapter 2). For this situation an analytical solution for the response function is known. The response function from the time series analysis is compared with both the synthetic model (the actual response function of the system) and the analytical solution for the Hantush situation. The equation for the Hantush well is:

$$h(t,r) = -\frac{Q}{4\pi kD}\int_u^t \frac{e^{(-\tau - r^2)/(4\lambda^2\tau)}}{\tau} d\tau \text{ with: } u = \frac{r^2 \cdot S}{4kD \cdot t} \text{ and } \lambda = \sqrt{kD \cdot c} \tag{3.1}$$

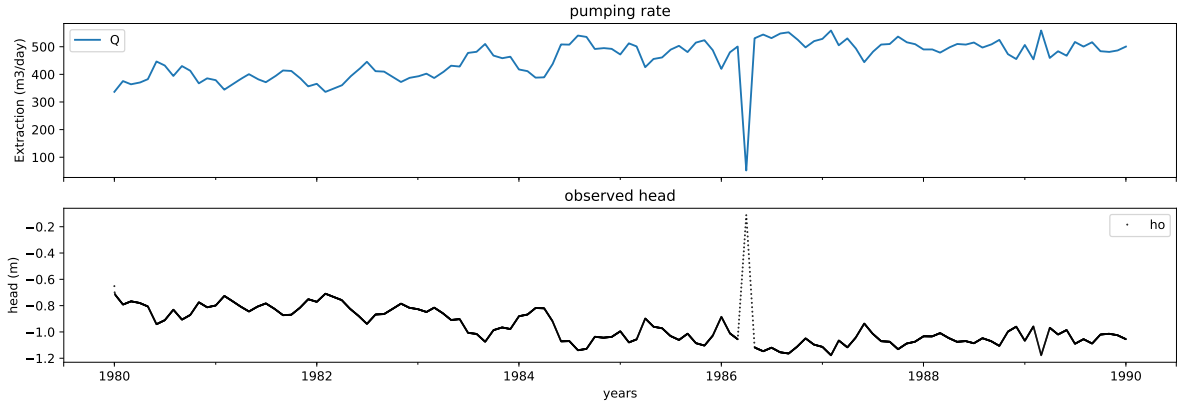

Figure 3.3: The pumping rate of the extraction well (top) and the resulting head in the observation well (bottom) for the Hantush model according to Ttim

where Q is the discharge of the well [L^3/T] (positive for extraction, negative for recharge), kD is the hydraulic conductivity [L/T] times the thickness of the aquifer [L] (also known as transmissivity, T,), r is the distance from the well [L], S is the storage in the aquifer [-], and c is the conductivity of the leaky layer [T] (Hantush and Jacob, 1955; Hantush, 1956).

The response function determined with time series analysis is used to calibrate a Ttim model. This Ttim model has the same aquifer characteristics as the synthetic model (see Figure 3.2). The aquifer parameters for this Ttim model are calibrated. The calibrated Ttim model is used to simulate a response function which is compared to the synthetic and Pastas response function.

3.2.1. Hantush model results

The time series analysis is performed using the data that can be seen in Figure 3.3. The result of the Pastas simulation is shown in Figure 3.4. The black dots represent the observed groundwater series and the blue line represents the result of the simulation.

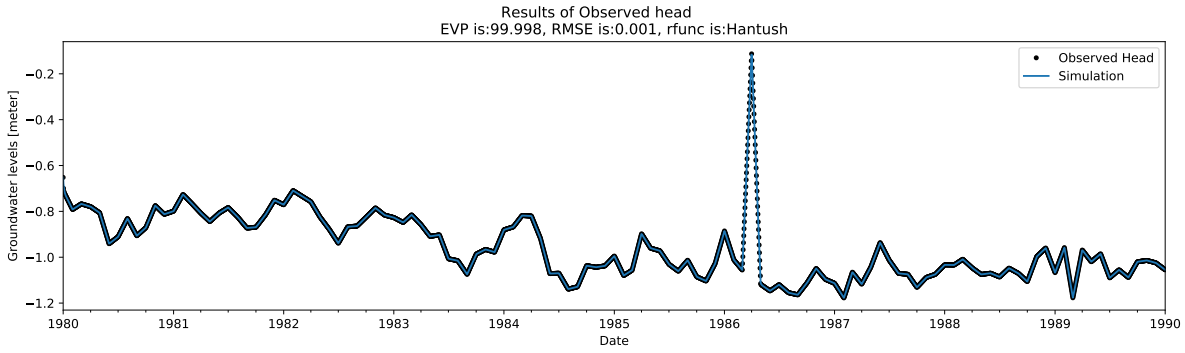

Figure 3.4: The Pastas simulation on the Hantush model

The EVP of the simulation is 99.998% and the RMSE is 0.001 m (Figure 3.4). This means the time series analysis yields near perfect results for this model. A step response function is obtained from the time series analysis. This is the result of a unit stress of 1 m^3/d from the extraction well, starting at time $t = 0$ and continuing with a constant rate. This response function is compared to the analytical solution for the Hantush situation, see Equation 3.1, and the synthetic response function from the Ttim model. All the response functions are shown in Figure 3.5. There are minimal difference between the three response functions. This means that the synthetic model follows the behaviour described by Hantush (Hantush and Jacob, 1955; Hantush, 1956) and the time series analysis is able to determine the correct response function of the system.

The resulting response function from the time series analysis is used to calibrate the Ttim model. This

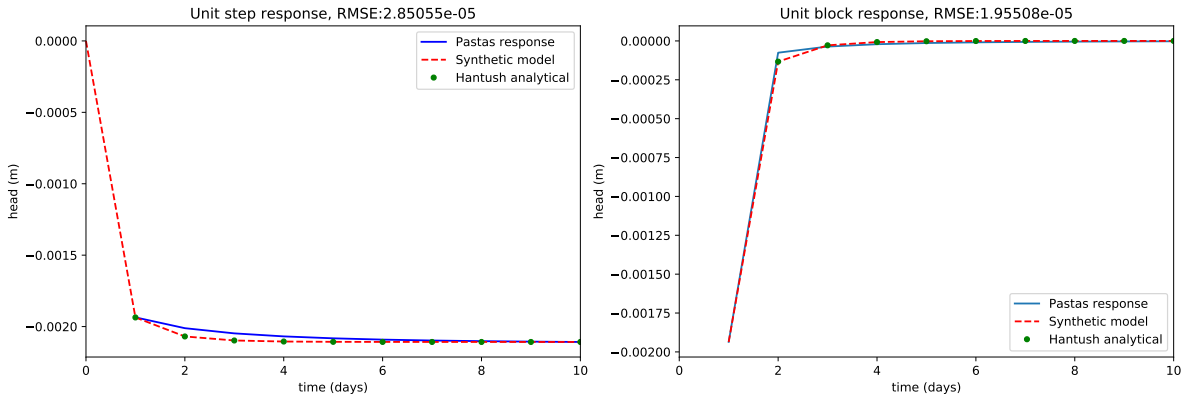

Figure 3.5: In the figures the response functions from the synthetic model, Pastas and the analytical solution

calibration results in a hydraulic conductivity, k, of 10.12 m/d and a storage coefficient, S, of $1.04 \cdot 10^{-3}$. These values are close to the original values as shown in Figure 3.2 of 10 m/d and $1 \cdot 10^{-3}$ respectively. From the calibrated Ttim model the response function is simulated, which is compared to the synthetic and time series response functions. In Figure 3.6 these response functions are shown. The differences between the response functions are very low. The RMSE between the conceptual and synthetic step responses is $1.85 \cdot 10^{-5}$ m.

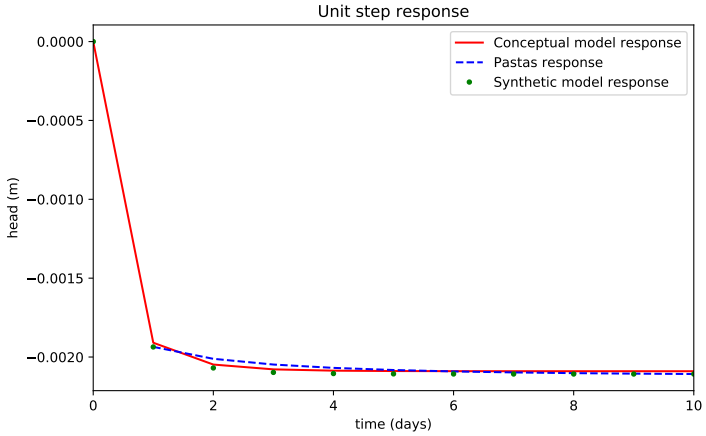

Figure 3.6: The conceptual model step response compared with the synthetic and time series responses

3.3. Multiple synthetic models

The next step in the synthetic study is to create groundwater models with different canal layouts and different aquifer parameters. First a synthetic Ttim model is created. This is used to simulate a synthetic observations series. The observations are used in Pastas to determine the response function of the system through time series analysis. Next, the response function from Pastas is used to calibrate the conceptual Ttim model. Finally, the groundwater is simulated using the conceptual Ttim model. These simulated groundwater series are compared to the synthetic groundwater series.

The stress on the synthetic model is the same for all models. The stress used for these models is a recharge, calculated as $P - E$, where P is the precipitation and E is the evaporation. The precipitation and the evaporation series are obtained from KNMI station 260 in De Bilt; the model period is 10 years, from 1980 until 1990. The recharge stress series is shown in Figure 3.7, in the figure the precipitation, evaporation and the resulting recharge series are displayed. This recharge series is used in the synthetic model to generate the synthetic observations, as well as in the Pastas simulation to perform the time series analysis and as a stress on the conceptual model.

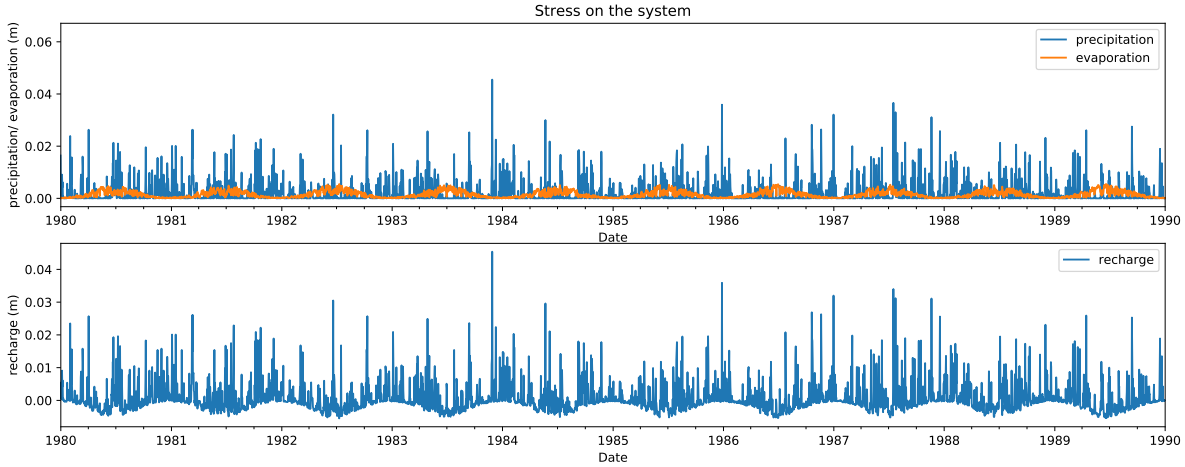

Figure 3.7: The recharge stress used in the synthetic models

Five canal layouts are designed. For each of the canal layouts three different sets of aquifer parameters are used. The first is a single layer with one k and one S value, the second is a multilayer system with three layers with different k and S values and finally a ground structure with two layers separated by a low permeable layer (or leaky layer). The five canal layouts and 3 sets of aquifer parameters create a total of 15 synthetic models. All canals in the synthetic models have a constant water level of 0 m +NAP. Each synthetic model has a square boundary where the groundwater level is fixed at 0 m +NAP. This boundary is 2000 by 2000 meter with the (0,0) coordinate as the center point. This is added to the synthetic models to ensure the groundwater can not rise infinitely. The recharge is added to the synthetic model in a circular area with a radius of 1500 m and the center at the (0,0) coordinate.

The synthetic groundwater series is simulated at the location of the observation well using the synthetic model. This synthetic series is simulated in the bottom aquifer of the synthetic model. These synthetic observation are used in the time series analysis. A response function is selected in the time series analysis. Since the stress on the system is a recharge stress, the Exponential, Gamma, Double Exponential and Four-Parameter functions can be used.

After the time series analysis performed using Pastas, the resulting response function is used to calibrate the conceptual Ttim model. Two parameters are calibrated: the hydraulic conductivity k [T/L] and the storage coefficient S [-]. The conceptual model has the same canal layout as the synthetic model and the location of the observation well in the system is known. The conceptual model consists of a single aquifer with a thickness of 10 m and an unknown k and S value. The cross-section for the calibration model is shown in Figure 3.8. This cross-section is the same for all synthetic models regardless of the aquifer composition of the synthetic model.

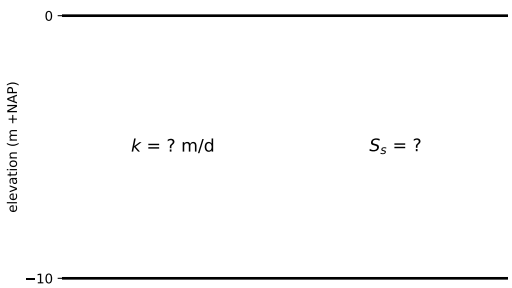

Figure 3.8: The cross-section of the conceptual model

The calibration of the conceptual model is done using a least squares minimization. The calibration optimizes the k and S values using the step response of the time series analysis. Using the calibrated parameters the conceptual model is set up in Ttim. From the conceptual model the response function can be determined and compared with the synthetic response function and the Pastas response function. The conceptual model us used to simulate the groundwater series in the observation well. This series is compared to the original synthetic observation series. This comparison is done by calculating the EVP and RMSE between the two series. The same is done for the validation points. The groundwater head in the conceptual model is compared to the synthetic model for these 9 points. This is done to see if the conceptual model is not only able to predict the head in the observation well but also at different locations in the system. The validation points are spread out over the system. In several cases some validation points will have identical observed head series because the system is symmetrical, for modelling purposes these points are still validated with the model.

3.3.1. Example: Rectangle canal layout with a single aquifer layer

As an example, the first model is considered, which is the rectangle canal layout with a single layer, the layout is shown in Figure 3.9. In the figure the location of the observation well (obswell) is shown, together with several validation points which are used to compare the groundwater head of the conceptual model with that of the synthetic model. The hydraulic conductivity of the system is 10 m/d and the storage coefficient is 0.2 (this is the phreatic storage).

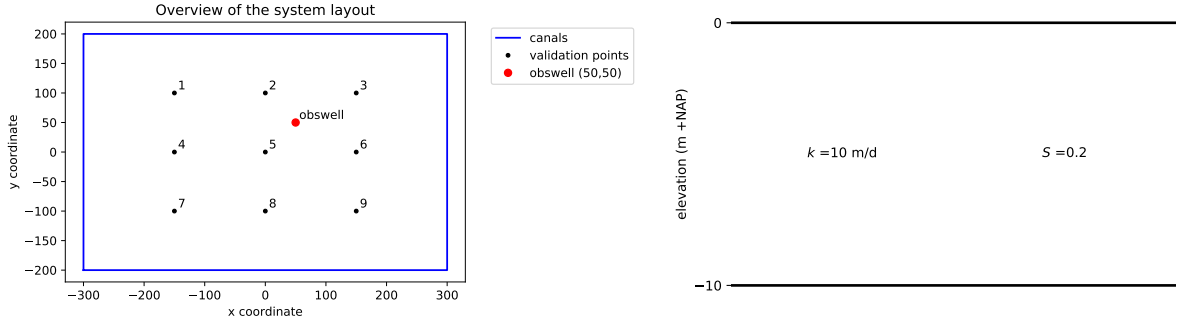

Figure 3.9: On the left the overview of the system and on the right the cross section of the system

Using this layout and the recharge presented in Figure 3.7, the synthetic model is run to simulate the synthetic groundwater observations. These can be seen in Figure 3.10. These observations are used in the time series analysis, together with the recharge stress (shown in Figure 3.7. For this synthetic model the Gamma response function is used. The time series analysis simulation has an EVP of 99.966%, this is an almost perfect match with the synthetic observations. The response function is determined with the time series analysis.

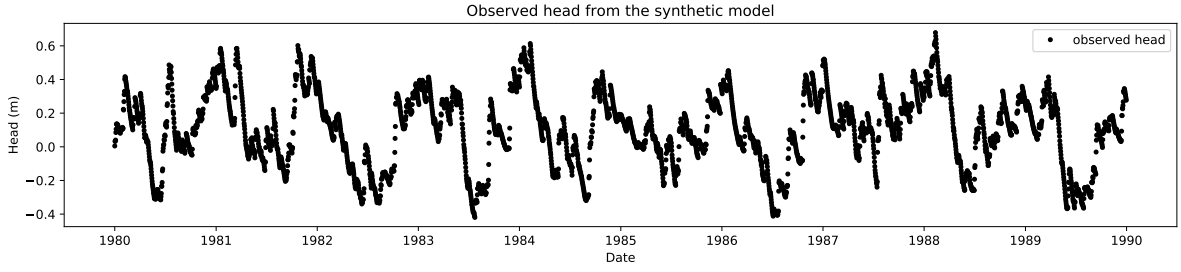

Figure 3.10: The observed head from the synthetic Ttim model, with the rectangle layout

The Pastas response function is compared to the response function of the synthetic model. In Figure 3.11 the response function example synthetic model and the response function of the time series analysis are shown. The RMSE between both functions is 0.49 m for the step response and 0.07 m for the block response, the highest deviation from the synthetic response is in the first part of the response function.

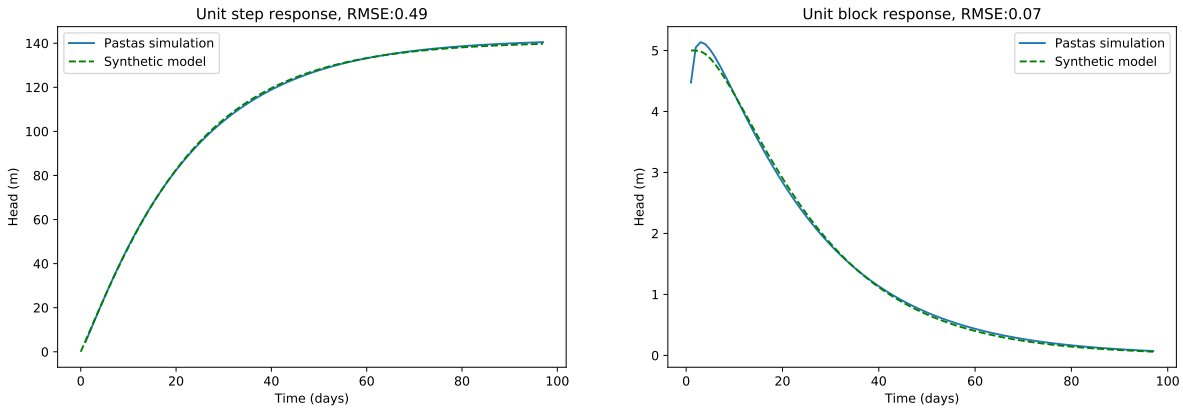

Figure 3.11: The step and block response of the synthetic model and from the time series analysis

The conceptual model is calibrated using the Pastas response function. The result of the calibration is shown in Figure 3.12. In the figure the step responses of the synthetic, time series analysis and the calibrated conceptual model are plotted. The response functions match very well. The calibrated hydraulic conductivity, k, is 9.966 m/d and the storage coefficient, S, is 0.202. The k and S value for the synthetic model are 10 m/d and 0.1 respectively as shown in Figure 3.9. The calibrated parameters are very close to the original values.

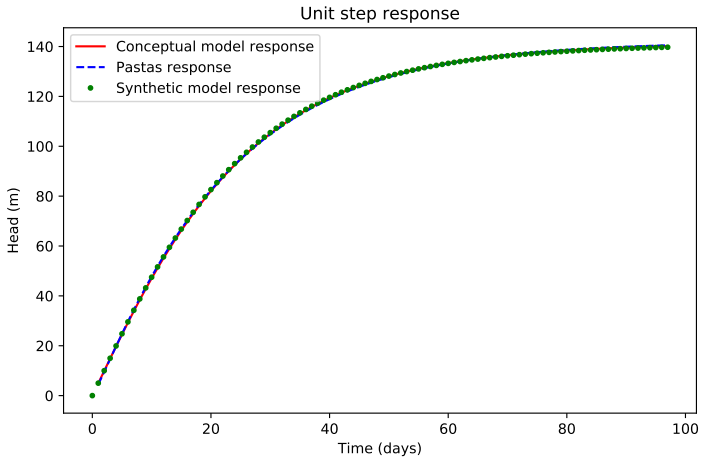

Figure 3.12: The step response of the synthetic, Pastas and the conceptual model are plotted.

The conceptual model is created with the same canal layout as seen in Figure 3.9. The aquifer parameters from the calibration are used. Using this model the groundwater head at the location of the observation well is simulated and compared with the original synthetic observations (as seen in Figure 3.10). The simulated head in the observation well can be seen in Figure 3.13, below that the difference between the simulated head and the synthetic head is shown. It can be seen that the differences between these two series are small, the highest deviation in the 10 year simulation period is less than 0.006 m.

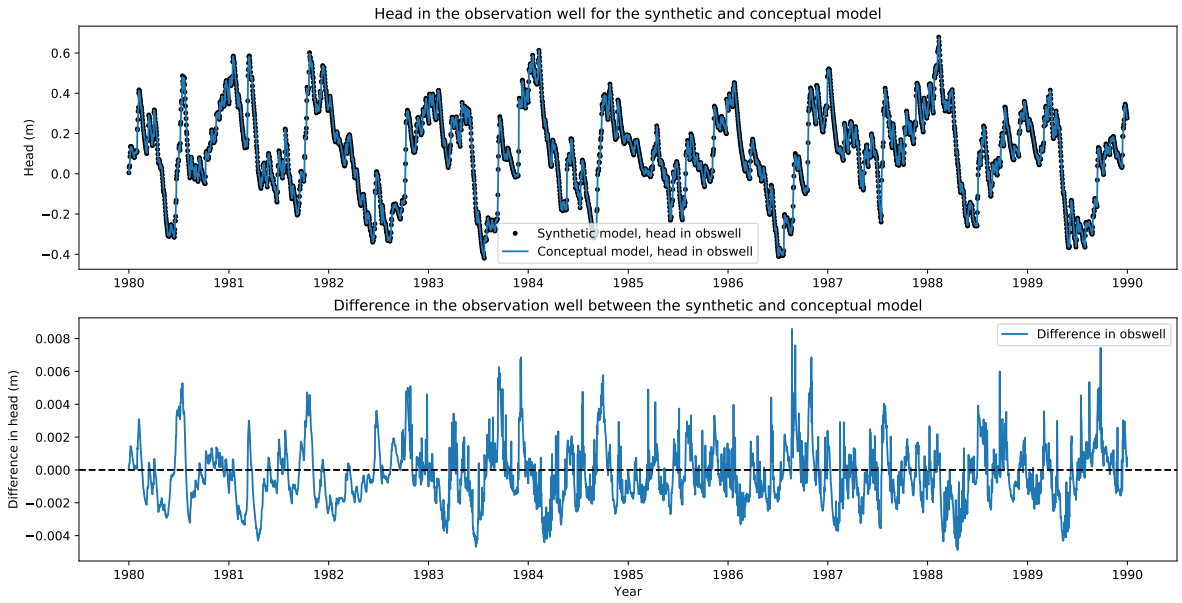

Figure 3.13: The observed head from the synthetic model and the conceptual model in the observation well (top) and the difference between the two models (bottom)

The next step is to verify if the conceptual model is able to simulate the head at different locations in the system. This is done by simulating the groundwater head in the checkpoints (the 9 points that can be seen in Figure 3.9) and compare this to the groundwater levels in synthetic. For this example model the head difference between the two models at each location is shown in Figure 3.14. At each location the EVP and RMSE of the series is calculated in comparison to the groundwater series of the synthetic model at that location. The average EVP of the conceptual model compared to the synthetic model for the validation points is 99.904% with an average RMSE of 0.004 m, the EVP of each individual validation point can be seen in Appendix B. The maximum difference between both model is less than 0.10 m for the 10 year simulation. This means the conceptual model is able to simulate the groundwater head at several points in the system.

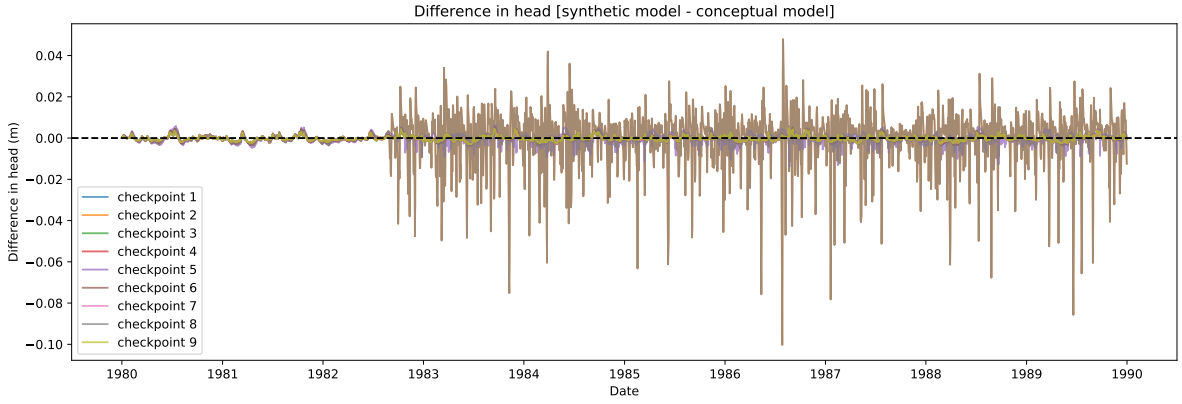

Figure 3.14: The difference in head between the synthetic and conceptual model at the checkpoints

3.3.2. Multiple synthetic model results

The method as described in the previous section is applied to multiple synthetic models. For each synthetic model the canal layout and aquifer parameters are shown in Appendix A. For each model the synthetic observations are simulated, these are shown in Appendix A. These observations, together with the recharge series shown in Figure 3.7, are used in the time series analysis.

The response function determined with the time series analysis is compared to the response function of the synthetic model. These response functions are shown in Appendix B. The response functions from the time series analysis are very close to the synthetic response functions for the single layer synthetic models. The response function comparison for the multi layer models show slightly higher deviations. The response functions for the leaky layer models show high deviations. The response function from the time series analysis is used to calibrate the conceptual model parameters. The head in the observation well is simulated using the conceptual model. The results for this simulation are shown in Appendix B for each model. The head at the location of the verification points is simulated. These series are compared to the head simulated with the synthetic model at those locations. The results of these simulations for each synthetic model are shown in Appendix B. The EVP values for each synthetic model at each individual validation point are shown in Appendix B.2.

An overview of the results for all synthetic models is shown in Table 3.1. The name of each model is derived from the canal layout, the addition _ml to the name is for the multilayer models and the _ll addition is for the models with a leaky layer. The k and S values that are calibrated for each conceptual model are shown in the table. The calibrated k and S values for conceptual models are very close to the k and S values of the synthetics single layer models. The response function that is used in the time series analysis is shown for each model. For the time series analysis in Pastas the EVP of the simulation is shown. The EVP and RMSE of the groundwater head simulation in the observation well of the conceptual model compared to the synthetic observations are shown in the table. For the checkpoints the average EVP and RMSE are shown.

For all models the EVP of the time series analysis simulation is very high (>98%), this means that the observed head series is simulated almost perfectly. The EVP of the simulation in the observation well in all the models is >98% with low RMSE values. The conceptual model for all different synthetic models is able to simulate the groundwater observations accurately. The average EVP values at the validation points is highest for the single layer models. The results for the individual validation points show that for the single layer aquifers models have EVP values of > 99%. The average EVP values are slightly lower for the simulation of the multi layer models. The EVP values of the multilayer models are generally higher than 95%. Point 1 in the triangle_ml has an EVP of 1.178%. The average EVP values are the lowest for the synthetic models with the leaky layer. The triangle_ll model has the lowest EVP value of all synthetic models. Point 1 for this conceptual model has an EVP of 0%.

Model name	**k value [m/d]**	**S value [-]**	**Response function**	**Pastas EVP [%]**	**EVP obswell [%]**	**RMSE obswell [m]**	**avg EVP points [%]**	**avg RMSE points [m]**
rectangle	9.966	0.202	Gamma	99.962	99.993	0.002	99.904	0.004
branched	9.788	0.202	Gamma	99.595	99.574	0.011	99.968	0.003
parrallel	9.903	0.201	Gamma	99.623	99.994	0.002	99.994	0.002
lshape	9.82	0.191	Gamma	99.148	99.865	0.013	99.867	0.013
triangle	9.858	0.201	Gamma	99.917	99.982	0.002	99.984	0.002
rectangle_ml	7.221	0.239	Gamma	99.939	99.838	0.01	99.702	0.011
branched_ml	6.9	0.22	Gamma	99.543	99.938	0.005	99.608	0.011
parrallel_ml	7.03	0.203	Gamma	99.559	99.952	0.008	99.963	0.007
lshape_ml	7.257	0.186	Gamma	99.121	99.642	0.024	99.541	0.028
triangle_ml	6.882	0.224	Gamma	99.763	99.848	0.007	88.025	0.021
rectangle_ll	7.508	0.252	Gamma	99.913	99.706	0.014	99.315	0.022
branched_ll	6.278	0.278	Gamma	99.178	99.405	0.014	95.271	0.039
parrallel_ll	6.571	0.235	Gamma	99.483	99.764	0.016	99.689	0.02
lshape_ll	6.89	0.203	Gamma	99.307	99.623	0.025	98.997	0.044
triangle_ll	6.05	0.308	Gamma	98.862	98.069	0.025	81.937	0.067

Table 3.1: Table with the results of the different synthetic models

3.4. Synthetic study conclusions

Two synthetic studies are performed. The first synthetic study was the Hantush model. This model was used to verify the approach of the research and test the method. After this several synthetic models are created. The synthetic models are used to simulate synthetic observations. These observations are used with time series analysis. A conceptual model is calibrated on the time series response function. Using this conceptual model the groundwater levels can be simulated. These simulated groundwater levels are compared to the groundwater levels in the synthetic model to see if the conceptual is correctly able to simulate the synthetic groundwater levels.

The synthetic Hantush model shows good results. The time series analysis was able to produce the same the response function as the synthetic model and as calculated using the analytical Hantush equation. This response function was used to calibrate the aquifer parameters of the conceptual model. The resulting parameters k and S of the calibration were close to the original parameters of the synthetic Hantush model. The response function of the conceptual model was the same as the response function of the synthetic model, the time series analysis response and the analytical response. The conceptual model was able to simulate the groundwater head of the original synthetic model.

For the different synthetic models the time series analysis was able to simulate the observed groundwater series with high accuracy. The simulation in Pastas resulted in EVP values of >98% for all models. The time series analysis was able to simulate the observed head series nearly perfect for all synthetic models. The EVP is >98% for all conceptual model simulations compared to the synthetic observations at the observation well. The RMSE of these simulations is low. This shows that the conceptual model simulates the observed head excellent at the location of the observation well for all synthetic models. The EVP at the different validation points is generally very high. This means that the conceptual model was able to accurately simulate the groundwater head at different locations in the system. As can be seen in Appendix B.2 this was not true for all validation points in all models. The simulation at point 1 in the triangle multi layer and leaky layer models have an EVP of 1.1% and 0%. This could be caused by the proximity to the canal of this point (see Appendix A for the model layout) which causes the conceptual model to be inaccurate.

The synthetic study shows the conceptual model is able to spatially determine the groundwater levels in a system. The EVP and RMSE values for the simulation at different locations in the systems show that the conceptual model can simulate the groundwater head spatially. Only when the groundwater head is simulated close to canals, the conceptual model is not able to simulate the synthetic observations, this results in a low EVP for these points. The results show that the conceptual model is better able to simulate the groundwater for the single layer models than for the multi layer and leaky layer models.

4

Case study

In this chapter the case study is explained and the results of the case study are presented. The method presented in Chapter 2 and 3 is applied to the case study. First the study area for the case study is briefly described. After which some additional methods are explained. Next, the results for the case study are presented. Finally, some conclusions about the case study are drawn.

4.1. Study area Pannenhoef

The Pannenhoef is an area in the province of Noord Brabant in The Netherlands. It is situated between the cities of Roosendaal and Breda. The Pannenhoef is a nature reserve and is maintained by Brabants Landschap, an organisation that manages several nature reserves in Noord Brabant. The area is a mix of agriculture and forest. The area has two main canals, the Bijloop and the Turfvaart, which have several smaller tributaries in the study area, these are shown in Figure 4.1. The area contains multiple smaller canals and rivers. The groundwater level in the area is monitored by several observation wells, these are shown in Figure 4.1.

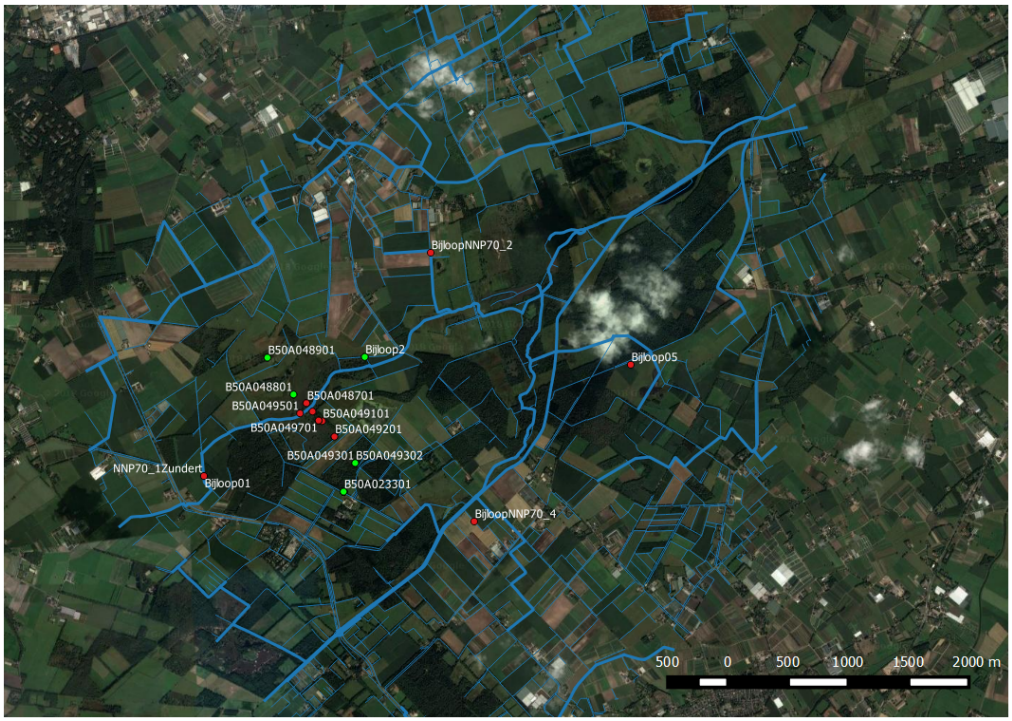

Figure 4.1: Map of the study area the Pannenhoef, with the different groundwater observation wells in the area.

The water management in the area is the responsibility of the water board Brabantse Delta. In 2009 the water board implemented measures in order to raise the groundwater levels in the area. This was done to accommodate more diversity in flora and fauna. The measures that were taken were closing several weirs and elevating the bottom of several canals. Because of the mix between agricultural and nature areas the groundwater level is important. For this area it is important to understand groundwater fluctuations both in time and space.

4.2. Case study methods

The method used in the case study is similar to the methods described in Chapter 2 and 3. Instead of the synthetic observations used in the previous chapter, the model in this chapter uses the observations from the different groundwater monitoring wells that are shown in Figure 4.1. The observations are simulated with time series analysis using precipitation and evaporation data. This data is obtained from the KNMI station closest to the study area, station Gilze-Rijen. In this case study no additional stress series are used. For each of the observation wells the time series analysis is performed using Pastas. The simulation period that is used is from 2010 until 2016. This period is after the waterboard implemented measures to raise the groundwater table in the area. This period is chosen to avoid a possible step trend in the observations. Only the wells which can be simulated with time series analysis with an EVP $\geq$ 65% are used for this research. The observation wells that satisfy this condition are B50A0488001, B50A0489001, B50A0493001, B50A0493002, B50A0497001, B50A0497002, B50A0233001 and Bijloop2. These wells are marked with a green dot in Figure 4.1, the wells that are not taken into account are red.

A single layer conceptual model is created for one of the observation wells in the study area. The cross-section of this model is the same as shown in Figure 3.8. To create the canal layout of the conceptual model, a boundary is created around the observation well. This boundary is a fixed head boundary for the conceptual model. The boundary is 2000 by 2000 m with the well at the center. Only the canals within this boundary are taken into account, this is done to reduce calculation time of the model. As an example, the conceptual model layout for the calibration well B50A0233001 can be seen in Figure 4.2. The precipitation and evaporation are used as the stress on the conceptual model. They are added as a recharge in a circular area with a diameter of 2500 m, with the center at the observation well. The recharge is calculated using Equation 2.12, where f is calculated with time series analysis.

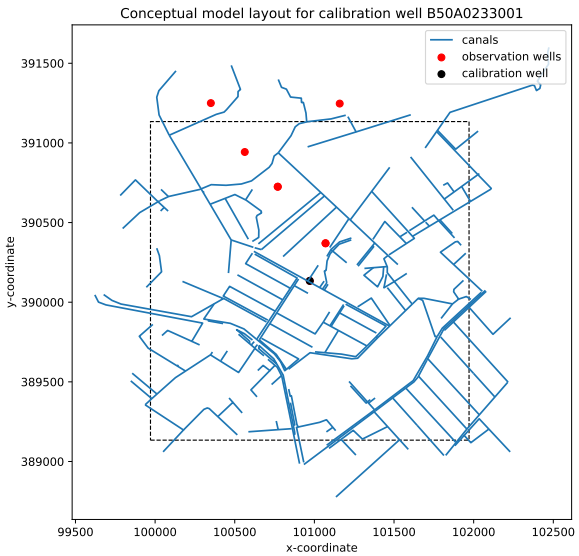

Figure 4.2: Conceptual model layout for calibration well B50A0233001

The response function obtained from time series analysis is used to calibrate this conceptual Ttim model. This is done by adding a unit recharge to the conceptual model of 1 m/d. The aquifer parameters k and S are then calibrated by fitting the response of the conceptual model to the time series analysis step response. The drainage (or base level) of a groundwater system is the groundwater level when no stresses are affecting the groundwater. The conceptual Ttim model has a drainage level of 0 m +NAP, in the study area this is not the case. The drainage level needs to be determined for the conceptual model. Using the time series analysis a drainage level can be determined. This drainage level is added to the conceptual model results. The next step is to simulate groundwater levels at the other observation wells using the conceptual model. The resulting series are then compared with the groundwater levels in the other observations wells. This method is repeated for all observation wells in the study area.

4.3. Example: Observation well B50A0233001

In this section the results of well B50A0233001 are presented, this observation well is used as an example. The groundwater observations in this well are simulated using time series analysis. The results from Pastas for well B50A0233001 are shown in Figure 4.3. The time series analysis is able to simulate the observed head with an EVP of 83.61%. The observed groundwater series is simulated reasonably well.

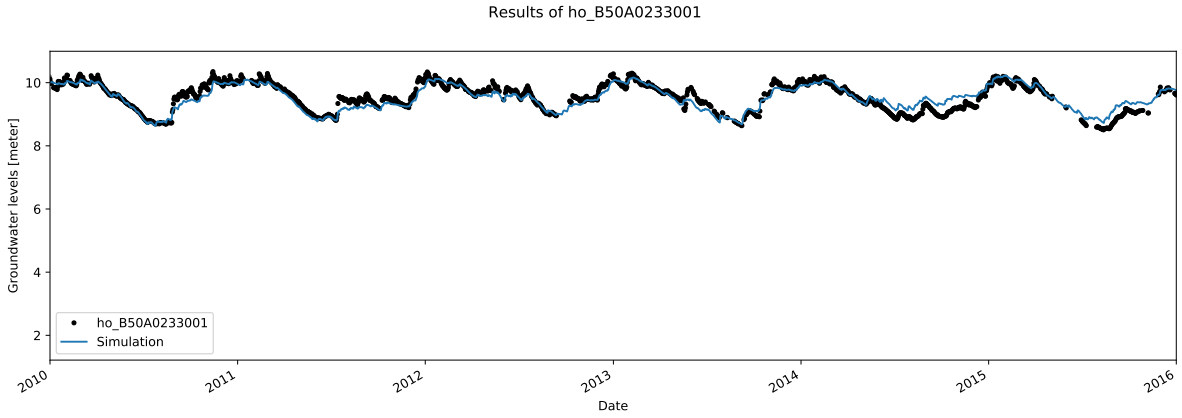

Figure 4.3: Results for the time series analysis for well B50A0233001.

A Ttim model is constructed using the canal layout shown in Figure 4.2, and the hydraulic conductivity k and the storage coefficient S are estimated by fitting the response of the conceptual model to the response function from Pastas. The estimated k and S values are 24.86 m/d and 0.2098 respectively. The response function from Pastas and of the calibrated conceptual model are shown in Figure 4.4.

Using the conceptual model the head in observation well B50A0233001 can be simulated. The results for this simulation are shown in Figure 4.5. The observations in the well are plotted together with the time series analysis simulation and the simulation of the conceptual model. In the bottom plot the differences between the time series analysis and the conceptual model simulation are plotted. It can be seen that the differences between these are small. This indicates that the conceptual model is able to replicate the groundwater levels from the time series analysis simulation at the observation well reasonably well.

Using the calibrated conceptual model the groundwater head is simulated at the other observation wells in the area. The results for the simulation at all well locations can be seen in Figure 4.6. In the figure the observations, the time series analysis simulation and the conceptual model simulation (this is the conceptual model calibrated on well B50A0233001) are shown for each individual observation well. The results show that the conceptual model is not able to simulate the observed head in the other observation wells. There are large deviations between the modelled and observed groundwater head at the other observation wells. A consistent shift is observed between the simulated and observed groundwater levels.

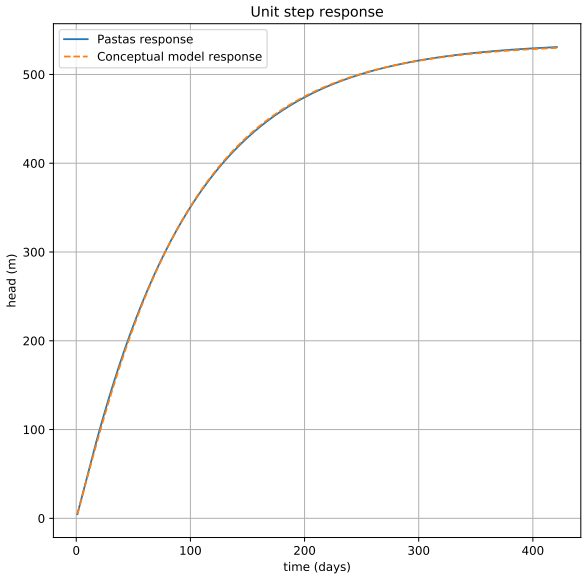

Figure 4.4: The calibration result of the conceptual model to the Pastas step response

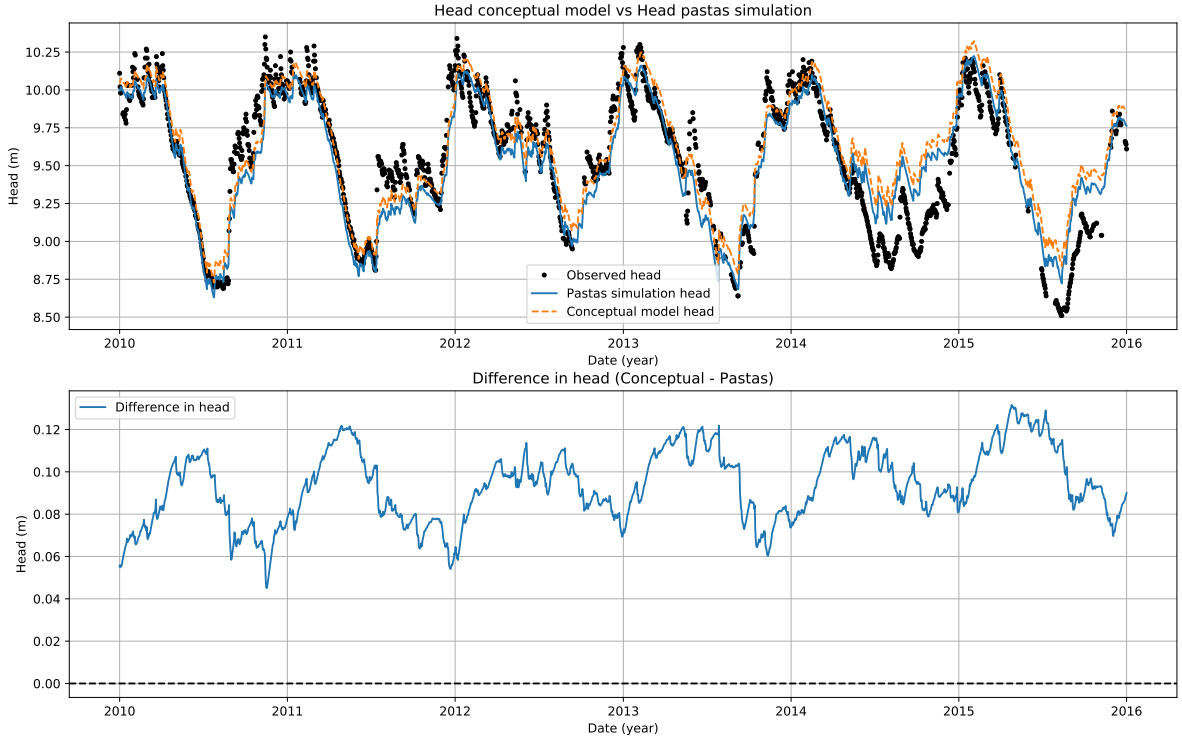

Figure 4.5: Simulated head inside the observation well, compared with the observations and the time series simulation

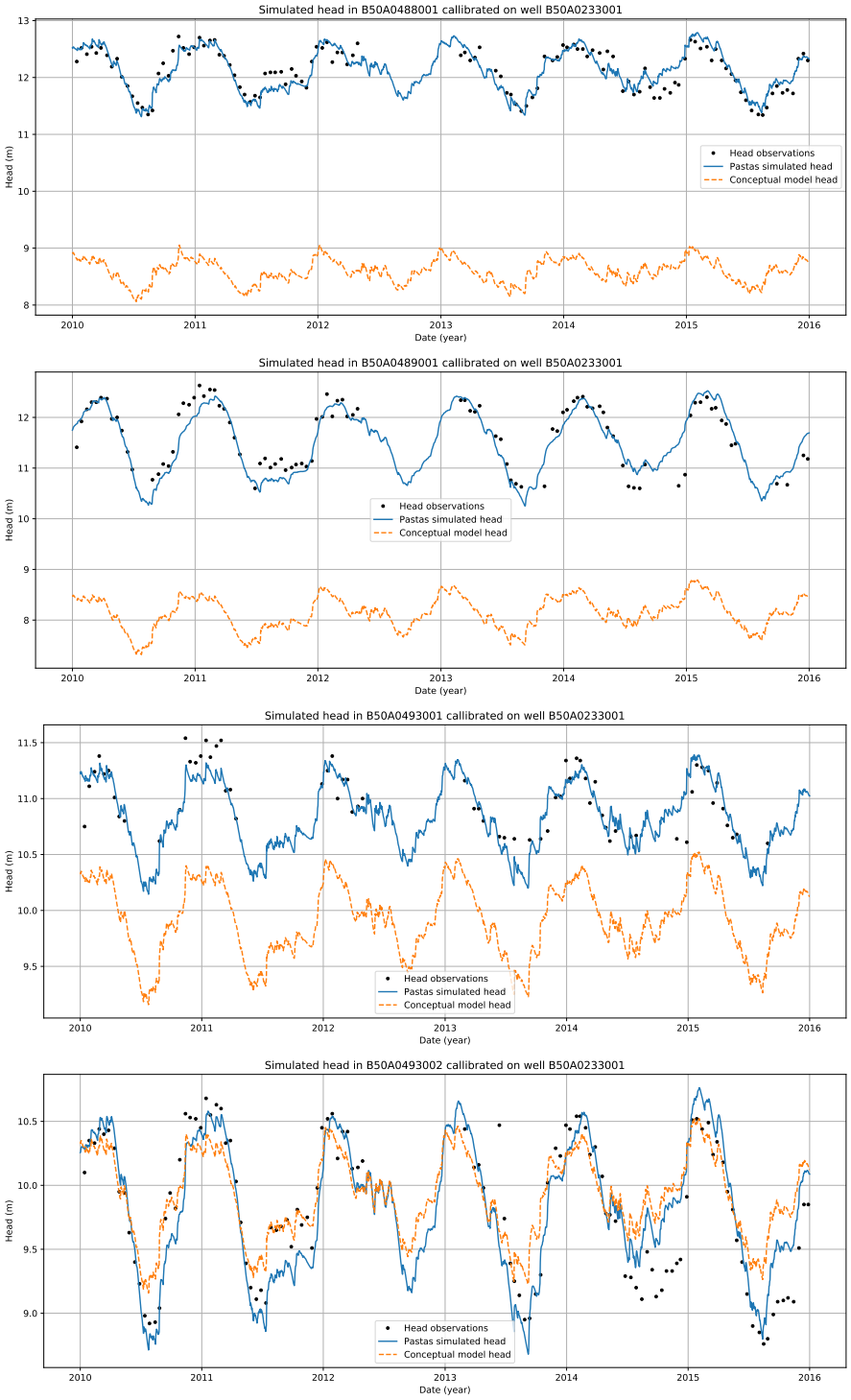

Figure 4.6: The conceptual model simulation at the observations wells

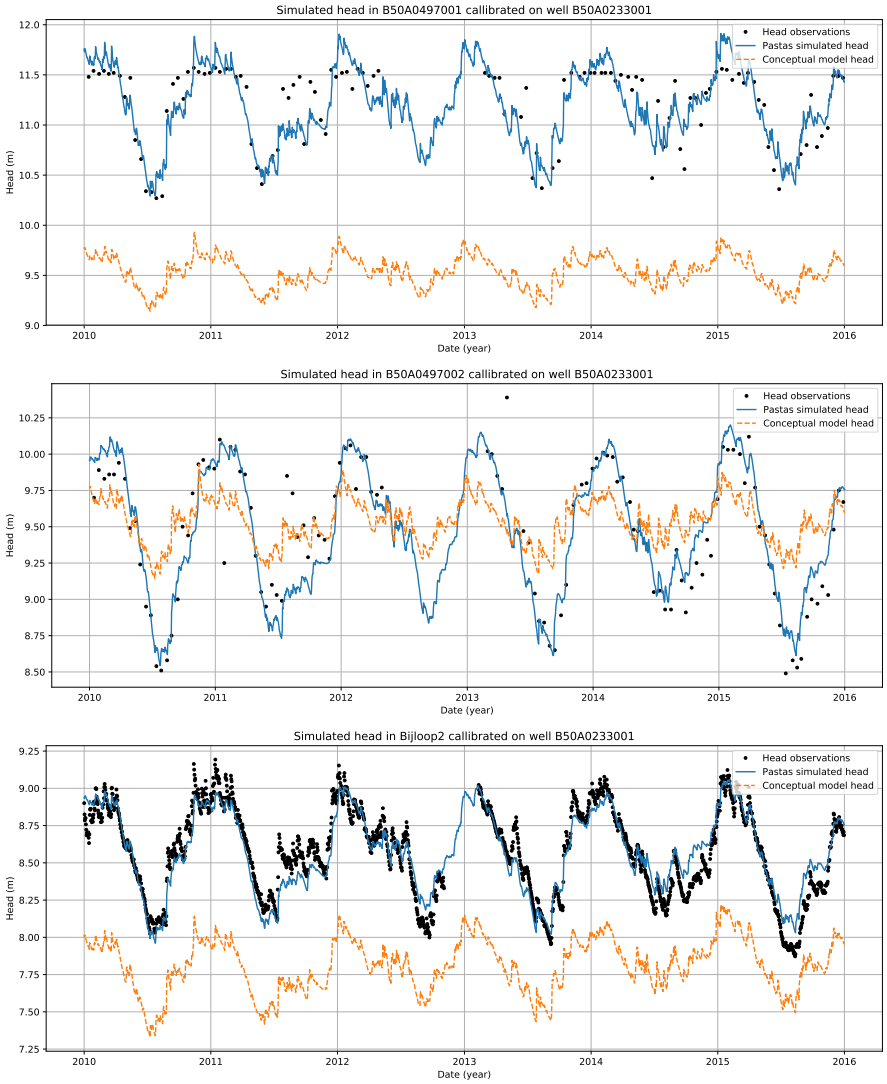

Figure 4.6: Continued: The conceptual model simulation at the observations wells

The fluctuations of the series shown in Figure 4.6 are compared. The fluctuations are defined as the variations in groundwater head around the mean of the series. The fluctuations are calculated for the observations, time series analysis simulation and conceptual model simulation. In Figure 4.7 the fluctuations are shown at the location of each observation well. As can be seen Figure 4.7 the conceptual model is able to simulate the fluctuations of the groundwater head in some observation wells reasonably well.

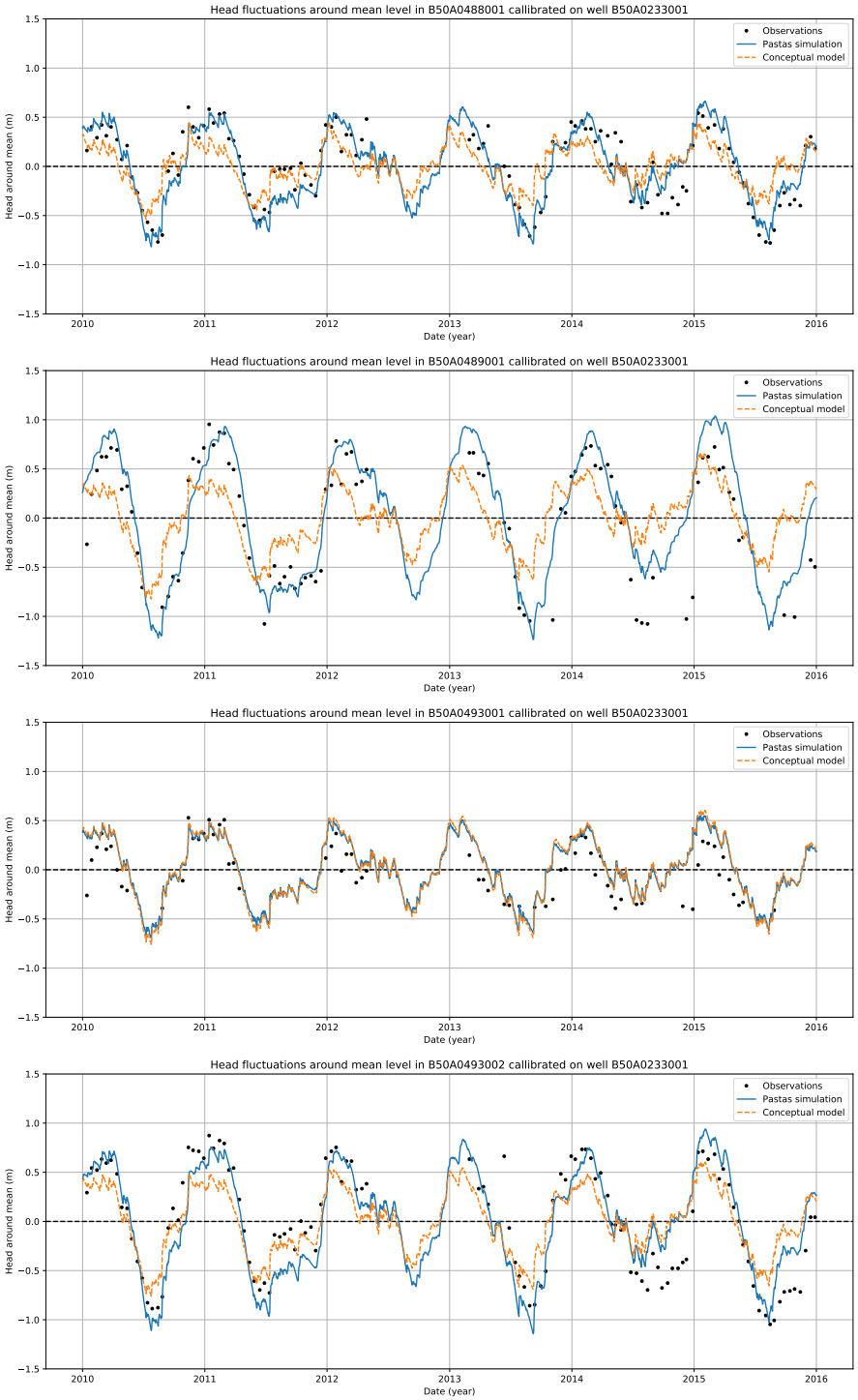

Figure 4.7: Fluctuations of the observation wells for the observations, Pastas simulation and conceptual model simulation

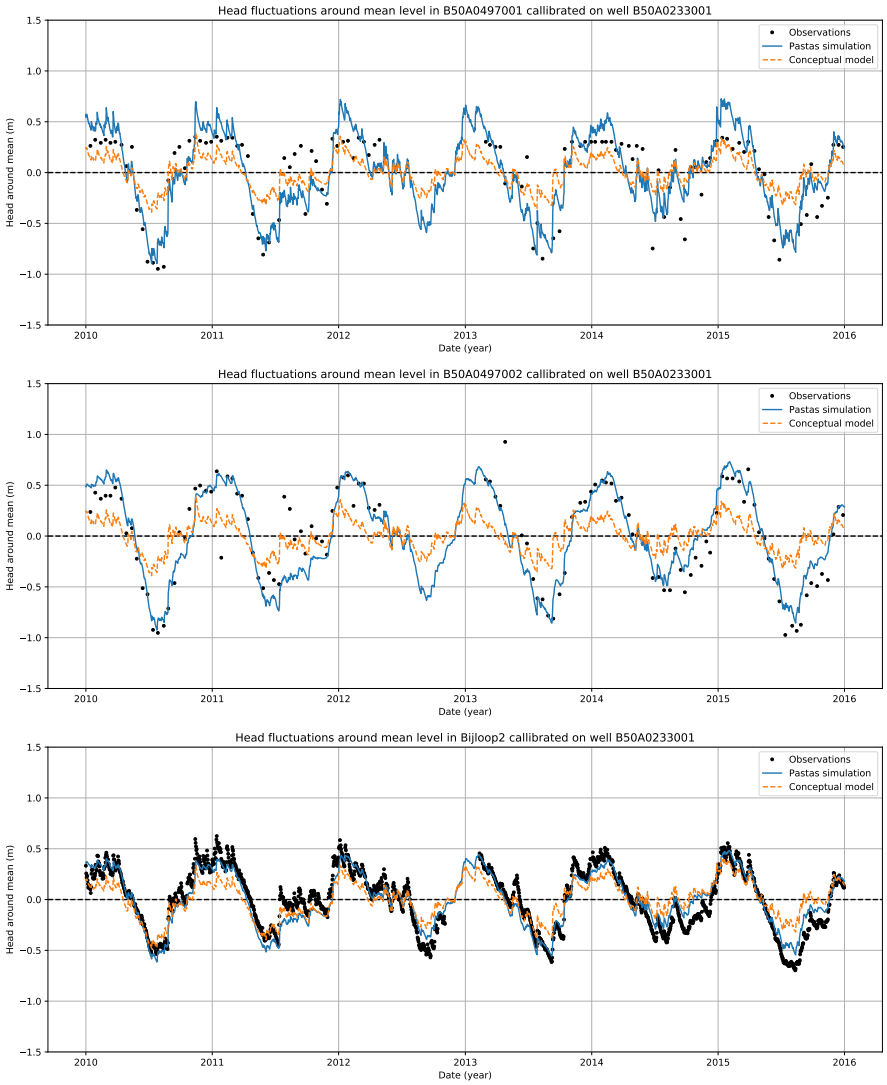

Figure 4.7: Continued: Fluctuations of the observation wells for the observations, Pastas simulation and conceptual model simulation

The RMSE and EVP are calculated for the fluctuations of the conceptual model simulation with respect to the groundwater observations and to the time series analysis simulation. An overview of the results for the simulation of the fluctuations calibrated on well B50A0233001 can be seen in Table 4.1. In each column the results of the fluctuation conceptual model at the location of each observation well are shown. The distance is the distance in meters between the well used for calibration (well B50A0233001) and each observation well. The mean amplitude is the amplitude of the conceptual model at the location of the observation well. The mean amplitude is calculated as the mean of the difference between the highest and lowest groundwater head for each year. The EVP values of the fluctuation simulated with the conceptual model with respect to the fluctuations of the Pastas simulation are higher than those with respect to the observations. This is a result of the conceptual model being calibrated on the step response from the time series analysis and not directly on the observations. The EVP is highest for the simulation at the calibration well itself (see Figure 4.5).

	B50A0488001	B50A0489001	B50A0493001	B50A0493002	B50A0497001	B50A0497002	B50A0233001	Bijloop2
EVP w.r.t. Pastas [%]	67.51	54.72	99.17	82.19	61.65	49.26	99.81	83.1
RMSE w.r.t. Pastas [m]	0.18	0.37	0.02	0.19	0.2	0.26	0.01	0.09
EVP w.r.t. observations [%]	53.77	40.98	66.51	67.4	47.85	37.67	82.42	68.04
RMSE w.r.t. observations [m]	0.21	0.39	0.19	0.26	0.23	0.31	0.14	0.14
Distance [m]	906.06	1277.14	255.92	255.92	624.25	624.25	0	1128.77
Mean amplitude [m]	1.71	1.68	1.15	1.88	2.92	2.89	1.3	1.69

Table 4.1: Results of well B50A0233001

4.4. Conceptual model results

For each observation well a single layer conceptual model is created to estimate the groundwater head at the location of the other observation wells. The results for the time series analysis and the calibration of the conceptual model are shown in Table 4.2. For each well the EVP for the time series analysis and the drainage level determined with the time series analysis are shown (this is the drainage level used in the conceptual model). The estimated k and S values are shown in the table. There is a large spread in the values for the hydraulic conductivity ranging from 6.06 to 24.86 m/d. Additional information about the location of the well and the average observed head can be seen in the table. The time series analysis simulation and the calibrated step response function for each observation well can be seen in Appendix C.

Calibration well	**Pastas EVP [%]**	**Drainage level [m NAP]**	**k value [m/d]**	**S value [-]**	**x coordinate well**	**y coordinate well**	**Avg observed head [m]**
B50A0233001	83.61	9.33	24.857	0.2098	100971	390134	8.808
B50A0488001	80.88	11.91	6.909	0.1658	100563	390943	12.027
B50A0489001	80.68	11.83	9.76	0.2042	100350	391250	11.887
B50A0493001	68.35	10.66	22.324	0.26	101070	390370	10.962
B50A0493002	78.91	9.17	9.13	0.1491	101070	390370	9.754
B50A0497001	71.74	11.01	6.497	0.0928	100770	390725	11.231
B50A0497002	79.86	9.55	6.057	0.1186	100770	390725	9.462
Bijloop2	87.02	8.41	6.101	0.1655	101159	391247	8.589

Table 4.2: Overview of the calibration using the different observation wells

The conceptual models are each used to simulate the groundwater levels at the observation wells. The results for the simulations can be seen in Appendix C. Similar to the results of well B50A0233001 presented in the previous section, the conceptual models simulations show high deviations from the observed groundwater levels. There is generally a consistent shift between the simulated and observed groundwater series. For each conceptual model the fluctuations can be seen in Appendix C. In Table 4.3 the EVP values for the fluctuations simulated with the conceptual models compared to the time series analysis simulations are shown. In Table 4.4 the RMSE between these series are shown. On the left axis the well used to calibrate the conceptual model is shown and the top axis shows the well used for validation. On the diagonal of the tables the EVP val-

ues are high and the RMSE values are low, these results show that the conceptual models are able to simulate the groundwater fluctuations at the location of the well used for calibration very well. The results are mixed at the locations of the other observation wells. 63% of the fluctuation simulations have an EVP ≥ 70%. It can be seen that the table is not symmetrical around the diagonal, this means that using well A for calibration to determine the head in well B yields different results than when well B is used for calibration to determine the head in well A.

	B50A0488001	B50A0489001	B50A0493001	B50A0493002	B50A0497001	B50A0497002	B50A0233001	Bijloop2
B50A0488001	97.22	96.67	45.51	96.92	91.58	79.33	42.27	96.17
B50A0489001	97.7	99.24	27.55	96.29	92.7	84.15	56.3	97.71
B50A0493001	70.06	65.3	99.51	79.79	58.61	47.82	97.25	68.33
B50A0493002	89.84	83.54	53.29	98.63	86.67	70.87	71.85	91.46
B50A0497001	68.85	59.21	0	74.77	96.75	81.13	0	77.12
B50A0497002	66.45	69.51	0	67.02	98.5	91.02	0	78.48
B50A0233001	67.51	54.72	99.17	82.19	61.65	49.26	99.81	83.1
Bijloop2	97.48	95.9	41.82	96.58	92.83	80.89	51.09	96.9

Table 4.3: Overview of the EVP [%] of the fluctuations between the conceptual model and the time series analysis simulation, on the left axis are the wells used for calibration and on the top axis are the well used in the validation.

	B50A0488001	B50A0489001	B50A0493001	B50A0493002	B50A0497001	B50A0497002	B50A0233001	Bijloop2
B50A0488001	0.05	0.1	0.18	0.07	0.09	0.17	0.24	0.04
B50A0489001	0.04	0.05	0.22	0.08	0.08	0.15	0.21	0.03
B50A0493001	0.17	0.33	0.02	0.2	0.2	0.27	0.05	0.13
B50A0493002	0.1	0.21	0.17	0.05	0.12	0.2	0.17	0.06
B50A0497001	0.17	0.33	0.39	0.21	0.06	0.16	0.44	0.1
B50A0497002	0.17	0.29	0.45	0.26	0.04	0.11	0.49	0.1
B50A0233001	0.18	0.37	0.02	0.19	0.2	0.26	0.01	0.09
Bijloop2	0.05	0.11	0.19	0.08	0.09	0.16	0.22	0.04

Table 4.4: Overview of the RMSE [m] of the fluctuations between the conceptual model and the time series analysis simulation, on the left axis are the wells used for calibration and on the top axis are the well used in the validation.

In Table 4.5 the mean amplitude of the simulated groundwater head is displayed. This value is calculated as the mean of the difference between the highest and lowest simulated fluctuation for each year at the location of the observation well. This value is used as an indication of how much high fluctuation around the mean is of the simulated groundwater level at the location of each observation well. In Table 4.6 the distances in meters between the observation wells is shown. This table is, of course, symmetrical over the diagonal (distance between well A and B is the same as distance between well B and A). On the diagonal the distance between wells is 0 m.

	B50A0488001	B50A0489001	B50A0493001	B50A0493002	B50A0497001	B50A0497002	B50A0233001	Bijloop2
B50A0488001	1.29	1.31	0.72	1.3	1.9	1.93	0.81	1.31
B50A0489001	1.8	1.97	1.07	1.81	3.01	3	1.08	1.76
B50A0493001	1.57	1.66	1	1.68	2.56	2.62	1.12	1.58
B50A0493002	1.57	1.66	1	1.68	2.56	2.62	1.12	1.58
B50A0497001	1.05	1.03	0.57	1.05	1.49	1.51	0.64	1.08
B50A0497002	1.05	1.03	0.57	1.05	1.49	1.51	0.64	1.08
B50A0233001	1.71	1.68	1.15	1.88	2.92	2.89	1.3	1.69
Bijloop2	0.96	0.93	0.52	0.94	1.37	1.4	0.68	0.98

Table 4.5: Overview of the mean amplitude in meters of the conceptual model, on the left axis are the wells used for calibration and on the top axis are the well used in the validation.

	B50A0488001	B50A0489001	B50A0493001	B50A0493002	B50A0497001	B50A0497002	B50A0233001	Bijloop2
B50A0488001	0	373.65	765.1	765.1	300.62	300.62	906.06	669.05
B50A0489001	373.65	0	1,137.01	1,137.01	672.33	672.33	1,277.14	809.01
B50A0493001	765.1	1,137.01	0	0	464.78	464.78	255.92	881.5
B50A0493002	765.1	1,137.01	0	0	464.78	464.78	255.92	881.5
B50A0497001	300.62	672.33	464.78	464.78	0	0	624.25	651
B50A0497002	300.62	672.33	464.78	464.78	0	0	624.25	651
B50A0233001	906.06	1,277.14	255.92	255.92	624.25	624.25	0	1,128.77
Bijloop2	669.05	809.01	881.5	881.5	651	651	1,128.77	0

Table 4.6: Overview of the distance in meter between the different wells.

The EVP values shown in Table 4.3 are compared to the EVP of the time series analysis of the calibration well. The comparison is shown in Figure 4.8. No correlation can be observed between the EVP of the time series analysis and the EVP of the simulation conceptual model.

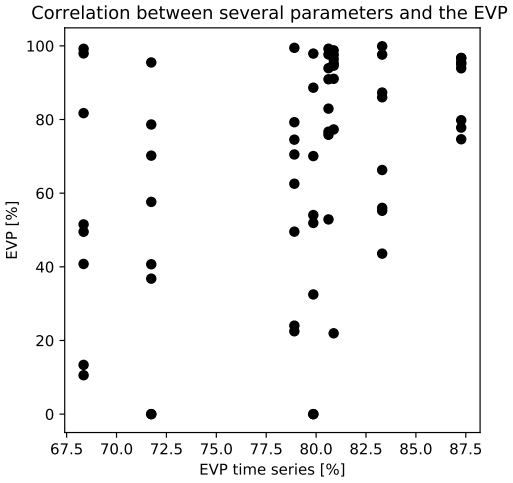

Figure 4.8: EVP at the observation wells compared to the EVP of the calibration well

Different parameters are compared with the EVP values of the fluctuation series to see if a correlation exists. The results of this comparison can be seen in Figure 4.9. The first parameter that is compared to the EVP of the fluctuations simulation, is the absolute difference in the calibrated hydraulic conductivity, k, between two conceptual models. For example, the EVP for the fluctuations simulation is 99.17% for the conceptual model calibrated on well B50A0233001 at the location of well B50A0493001, and the hydraulic conductivity difference is $24.857 - 22.324 = 2.533$ m/d for these observation wells. Second, the EVP of the fluctuations simulation is compared to the absolute difference in the storage coefficient, S. This is calculated in the same manner as the difference in k. In the bottom two plots the mean amplitude and distance results are plotted versus the EVP of the fluctuations simulation. All four plots show little correlation between the parameters and the EVP values.

4.5. Base groundwater levels

There is a consistent shift between the simulated groundwater levels at the observation well and the observed groundwater levels. This implies that the base groundwater level in the conceptual model is not correct. Data is obtained of the water levels in the canals in the Pannenhoef study area from the waterboard Brabantse Delta. In Figure 4.10 the average water level for each canal section is shown, together with the average observed groundwater head in each observation well. The average water levels in some observation wells is lower than the water level of the surrounding water bodies.

Using the canal data a stationary groundwater model can be made to determine the base groundwater level for the conceptual model. This stationary model is created using TimML, an analytic groundwater modelling software for steady flow. The model is created with the same cross section and layout as the Ttim model presented in the previous section (see Figure 3.8 and 4.2). To calibrate this steady flow model a constant unit recharge of 1 mm/d is added as a stress on the model. The model is calibrated on the different observation wells. The head in the wells used for calibration is calculated as:

$$h = N \cdot A + d \tag{4.1}$$

Where h is the structural head in the well, N is the recharge on the system, A is the parameter calculated with time series analysis in Pastas and d is the drainage level calculated with time series analysis. The structural groundwater levels for each well are shown in Table 4.7. The model is calibrated to these structural levels.

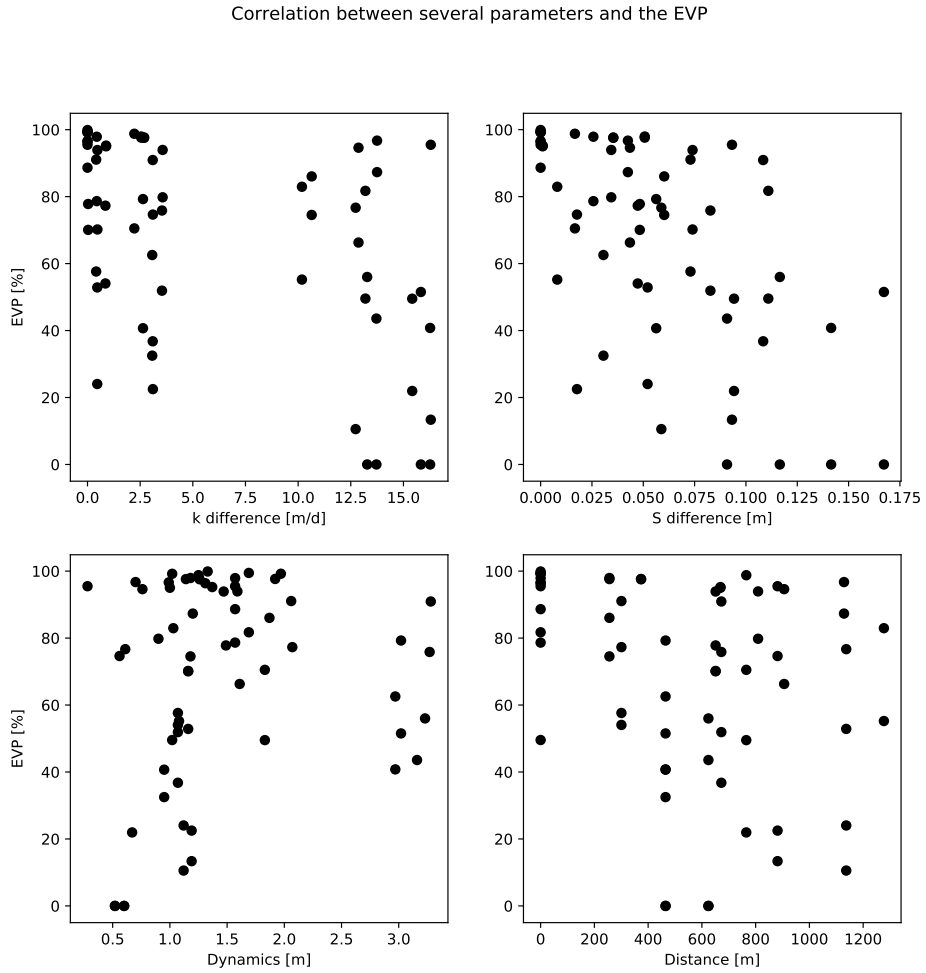

Figure 4.9: EVP at the observation wells compared to different parameters

The calibrated hydraulic conductivity is 0.75 m/d. The residuals for the calibrated model in each well can be seen in Table 4.7. The residuals show two outliers in well B50A049302 and B50A049702 both of these are the second filter of an observation well. A second calibration is done without these wells to see if the results improve. The residuals of the second calibration can be seen in Table 4.7. These results show that there is no significant improvement in the residuals of the steady state model when the two wells are excluded.

Well	Structural head [m]	Residuals [m]	Residuals 2nd calibration [m]
B50A048801	12.47	-0.57	0.47
B50A048901	12.80	-0.13	1.11
B50A049301	11.06	0.29	0.75
B50A049302	10.13	1.22	
B50A049701	11.44	-0.23	0.41
B50A049702	9.99	1.23	
B50A023301	9.74	0.53	1.06
Bijloop2	8.74	-0.09	0.23

Table 4.7: Structural head for each observation well

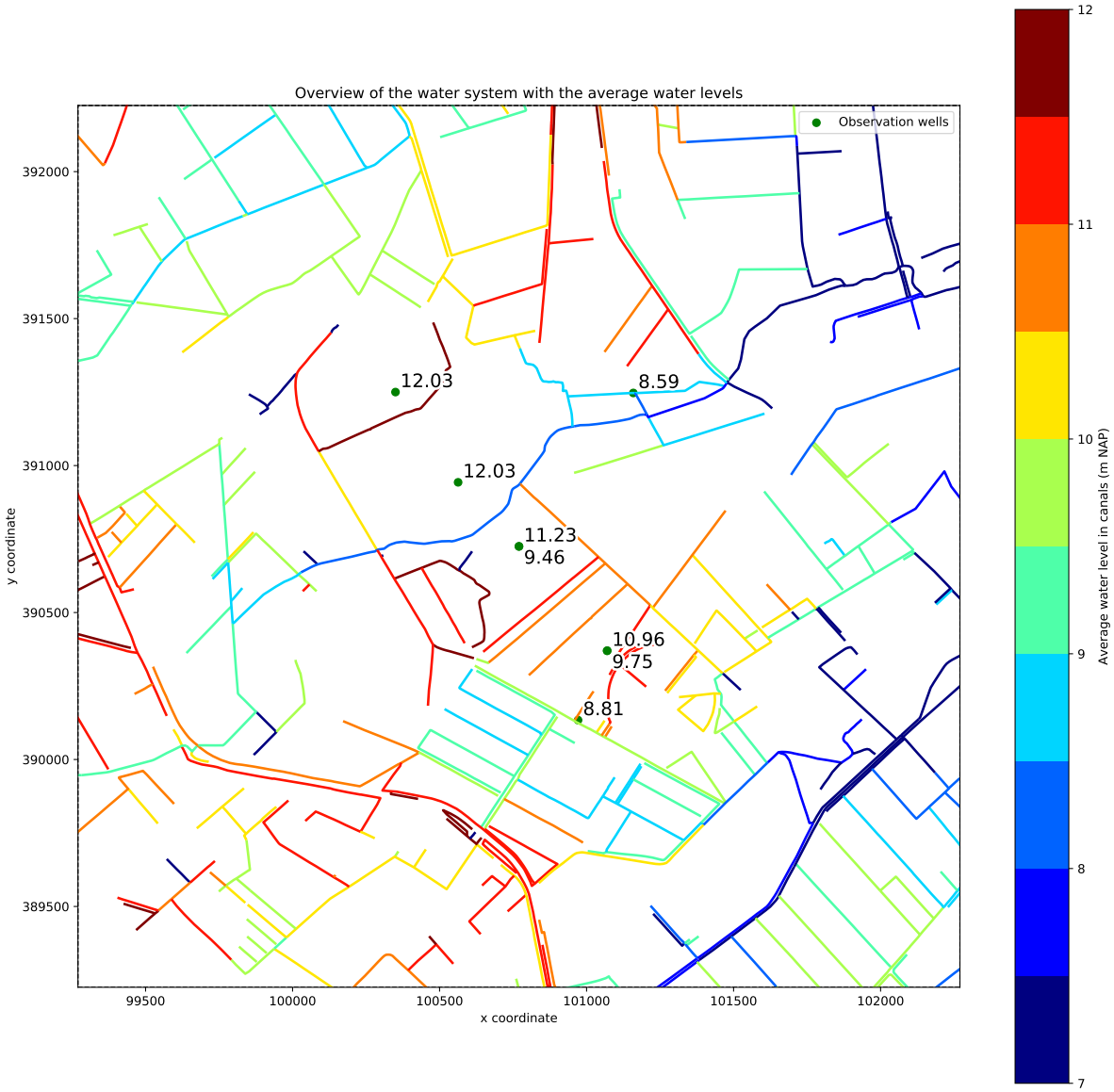

Figure 4.10: Average water levels in the canal and observation wells in m NAP

The resulting structural groundwater levels are shown in Figure 4.11. The contour levels of the groundwater head are plotted with 0.5 m intervals. Additionally, the calculated structural head in the wells is shown in the figure for a recharge of 1 mm/d . In the figure the deviation between the groundwater head of the simulation and the head calculated in the wells can be seen. No steady state model could be made using the available data of the water levels in the canals and the observed groundwater levels which gives a reasonable fit.

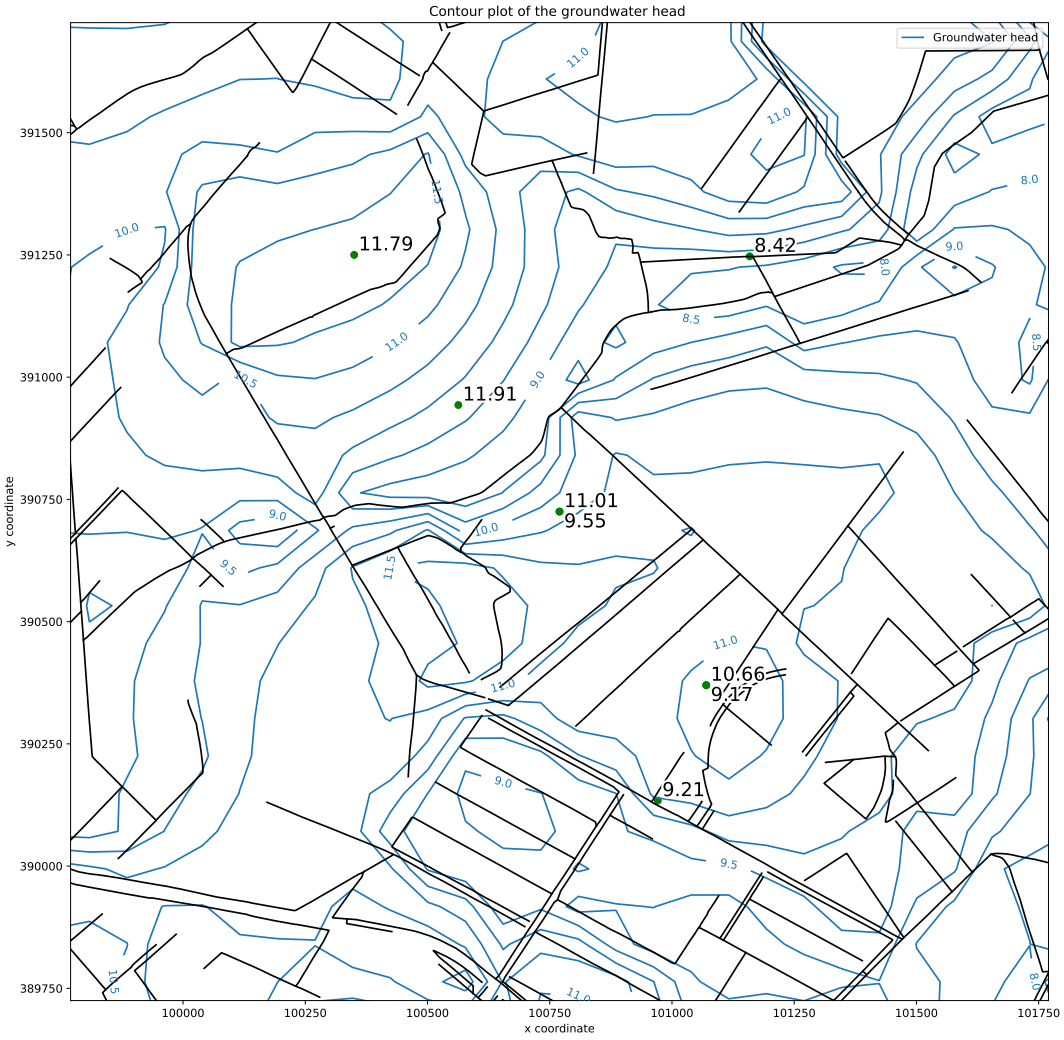

Figure 4.11: Calibrated steady flow model with the contour lines of the groundwater head.

4.6. Case study conclusions

The proposed method is tested on a case study in The Netherlands. In the study area several observation wells monitor the groundwater levels. Time series analysis is performed on the groundwater series from one of the observation wells. The resulting response function is used to calibrate a single layer conceptual groundwater model. Using this conceptual model the groundwater level at the location of the observation well is simulated. This simulation is compared to the observed groundwater levels. Next, the conceptual model is used to simulate the groundwater levels at the location of the other observations wells in the area. The simulated groundwater levels are compared to the observed groundwater levels at the other observation wells.

The conceptual model is able to simulate the observed groundwater levels at the observation well used for calibration with mixed accuracy. The conceptual model is able to simulate the time series simulation reasonably well. The EVP values for the simulated head in the observation well compared to the Pastas simulation are larger than 98%. The conceptual model is not able to simulate the groundwater head at other observation wells, this can be seen in Figure 4.6 and Appendix C. There is a high consistent shift between the simulated groundwater levels and the observed groundwater levels. This implies that the base groundwater level of the conceptual model is incorrect.

The fluctuations simulated by the conceptual model are compared to the observed fluctuation and the fluctuation simulated with time series analysis. The fluctuations of the conceptual model are compared to the fluctuations of the Pastas simulation at each well. For more than 63% of the simulations the conceptual model is able to simulate the Pastas fluctuations with an EVP greater than 70%. For the majority of the wells the conceptual model is able to simulate the fluctuations of the groundwater head fairly well. The EVP values for the fluctuations are compared with several parameters, but no correlation is observed.

The results shown in Figure 4.10 show a discrepancy between the data from the observation wells and the water levels in the canals. It can be seen that the average observed groundwater level in some wells is lower than the surrounding water levels. This would only be possible if the average net recharge is negative. When the structural groundwater levels in the observations wells are fitted with a steady state groundwater model no reasonable fit is found. It is impossible to create an accurate spatial conceptual model for the base level in the area which satisfies the observed groundwater levels.

5

Conclusions

The objective of this study was to extend the results of time series analysis at an observation well to determine the spatial variation and dynamics of the groundwater head. The proposed method is to use time series analysis to determine the response function at an observation well and to use this response to calibrate a relatively simple conceptual groundwater model. This method was first tested in a synthetic environment. A variety of synthetic models was tested to evaluate the method. Next, the method was evaluated using a case study in The Netherlands. In this case study the method was tested on several observations wells. The main research question was answered using the different research questions mentioned in Chapter 1.

5.1. Can the response function at an observation well be determined with time series analysis?

The ability of time series analysis to predict the response function of an observation well was tested in a synthetic study. A variety of synthetic groundwater models was created. From these models a response function and synthetic groundwater observations were simulated (these are the synthetic observations). Time series analysis was performed on these observation series and a response function was determined. The results show that the synthetic response functions for each model can be estimated using time series analysis. Small deviations exist between the simulated and synthetic response functions.

Time series analysis is better able to simulate the response function for the simple canal layouts. The synthetic models with more complex canal layouts show a higher deviation from the actual (synthetic) response function. The response function was most accurate for the single layer synthetic models. The response functions for the multi and leaky layer models show higher deviations from the actual response function. From the results of the synthetic study it is concluded that time series analysis is able to determine the response function of a system with reasonable accuracy. However, the results also show that with more complex synthetic models, the determined response function is less accurate. In the case study, the response function determined with time series analysis can, of course, not be compared to the actual response function of the system because this is not known.

5.2. Can a single layer conceptual model be used to reproduce the response function at an observation well obtained with time series analysis?

The response function at an observation well determined with time series analysis, was used to calibrate a single layer conceptual groundwater model. The conceptual groundwater model uses a single aquifer and the same canal system. The results from the synthetic study show that for the single layer synthetic models the calibration is able to accurately estimate the soil parameters of the synthetic model. For the different synthetic models the conceptual groundwater model was calibrated on the response function from time series analysis. For all synthetic models the conceptual model was able to simulate the observed head in the calibration well with EVP values largetr than 98%. The simulated groundwater head in the observation well

shows slightly higher deviations for the multi layer and leaky layer synthetic models. The high EVP values show that the single layer conceptual model is able to reproduce the response function at the observation well for the tested synthetic models.

In the case study the response function determined with time series analysis was used to calibrate the single layer conceptual model. A conceptual model was created for each observation well. Each conceptual model was used to simulate the groundwater head in the observation well that was used for calibration. For each observation well the simulation of the conceptual model has an EVP larger than 88%. This shows that a conceptual single aquifer model can simulate the groundwater head in the calibration well reasonably well. This suggests that the response at the observation well is reasonably reproduced. However, there are deviations between the groundwater head obtained with the conceptual model simulation and the observed head in the observation well.

5.3. Can a calibrated single layer conceptual model be used to estimate the response at other observation wells?

The response function determined with time series analysis was used to calibrate a single layer conceptual groundwater model. Using this model the groundwater head was simulated at the locations of the verification points in the synthetic model. For the synthetic study, the conceptual model is able to simulate the groundwater head at multiple locations in the system. For the tested single layer models the average EVP is larger than 99% at all verification points. For the multi layer synthetic models the average EVP at these points is larger than 88%, and for leaky layer system larger than 81%. The results show that the conceptual model gives results that are less accurate at locations very close to a canal, especially in the multi and leaky layer models. From the synthetic study it is concluded that the single layer conceptual model can determine groundwater levels at locations of other observation wells . However, at some locations the conceptual model is not able to simulate the synthetic head very accurate.

The same approach is applied to the case study. A single layer conceptual model is calibrated for each observation well and this model is used to simulate the groundwater at the locations of the other observation wells in the study area. The conceptual models are not able to simulate the groundwater head at the locations of the other observation wells. The results show a consistent shift between the conceptual model and the observed groundwater head. This suggests that the base level of the conceptual model is incorrect. A steady state groundwater model was made to determine the base level of the groundwater using the water levels of the canals in the case study area. This model was compared with the observed mean groundwater head which showed large deviations. No base model could be created using the available data which gives a reasonable match with the mean groundwater head in the observation wells. It is concluded that the conceptual model is not able to simulate the groundwater head spatially for this case study, because no logical spatial pattern is observed in the mean groundwater heads and the water levels in the area.

The fluctuations around the mean that are simulated with the conceptual model were compared with the observed groundwater fluctuations. At several locations in the study area the conceptual model was able to simulate the observed fluctuations in groundwater head reasonably well. At some locations in the study area the fluctuations were not simulated correct. No correlation was found between the ability to simulate the fluctuations well and several parameters of the system. From the results it is concluded that the conceptual model is able to simulate the groundwater fluctuations at many points in the system. No conclusion can be drawn on the cause of an inaccurate simulation of the fluctuations.

6

Recommendations

In Chapter 2, two new response functions were introduced and tested. The results show that the two response functions perform well and in most cases better than the original response functions. However, the response functions are not further investigated in this research. Only a limited number of wells are tested in this research. These wells are all in the same area in the Netherlands and have only a single stress series. By increasing the variety of observation wells, the performance of the new response functions can be investigated further researched. More research should be done on the observations series currently used in this research, to investigate why certain response functions perform better for certain series. Finally, the implementation of the response functions in the time series analysis software Pastas should be improved. The results show that the current version of Pastas is not always able to find the optimal solution of the time series analysis.

The synthetic study showed that the current version of Pastas software was not always able to filter out noise in the stresses or observations using the noise model. It is recommended to take a closer look at the noise model and identify why or when the noise model is not able to filter out the noise in the data. This could improve the results of the time series analysis and thus of this research.

Several synthetic models are tested in this research, but the variety of models is limited. Different model layouts should be tested to evaluate the performance of the conceptual model in other settings. More complex aquifer systems and canal layouts should be tested to evaluate the conceptual model. The canals in the current synthetic study have a constant homogeneous water level. The performance of the conceptual model is not tested using spatial or temporal variation of the water levels. Testing the conceptual model on a synthetic model where this is implemented could improve the base level of the conceptual model which is currently assumed constant. The results of the synthetic study show that the conceptual model is not able to simulate the groundwater head close to canals. The performance of the conceptual model should be investigated more to find the limits and improve the model. Finally, the current synthetic models only have a single stress on the system (recharge). For further research it would be beneficial to add multiple stresses to the system.

The results of the case study show that the conceptual model is not able to simulate the groundwater levels in the area. The results show a consistent shift between the conceptual model results and the observed groundwater head. This suggests that the base level of the conceptual model is incorrect. To improve the conceptual model, the base level should be improved. Several attempts at modelling the base groundwater level in the area were unsuccessful. More research is needed to try to model the base groundwater level using the available data. Alternatively, a different case study could be selected where the base level is known or can be modelled accurately. This could verify if the conceptual model is able to simulate the groundwater spatially. A different case study where more parameters regarding the groundwater level and the boundary conditions are known, could provide a better understanding on where or when the conceptual model is able to simulate the groundwater levels and could reveal where improvements on the method are needed.

The conceptual model is able to simulate the fluctuations around the mean at many locations in the system. It is recommended to try to identify why the conceptual model is not able to simulate the fluctuations at some locations in the area. Additionally, the conceptualization needs to be evaluated further. Currently the conceptual model consists of a single aquifer system in which canals are in direct contact with the aquifer. No additional conceptual models are tested. It is recommended to try different conceptual models, both in the synthetic and case study, to see if the simulation of the spatial groundwater levels can be improved. This can be done by adding additional layers to the conceptual model or adding additional boundary conditions, for example, adding resistance to the bottom of the canals in the conceptual model.

Bibliography

Bakker, M. (2013a). Analytic Modeling of Transient Multilayer Flow. In Mishra, P. K. and Kuhlman, K. L., editors, *Advances in Hydrogeology*, pages 95–114. Springer New York, New York, NY.

Bakker, M. (2013b). Semi-analytic modeling of transient multi-layer flow with TTim. *Hydrogeology Journal*, 21(4):935–943.

Bakker, M., Collenteur, R., Calje, R., and Schaars, F. (2018). Untangling groundwater head series using time series analysis and Pastas. volume 20, page 7194.

Bakker, M., Maas, K., and Von Asmuth, J. R. (2008). Calibration of transient groundwater models using time series analysis and moment matching. *Water Resources Research*, 44(4).

Box, G. E. P., Jenkins, G. M., Reinsel, G. C., and Ljung, G. M. (2015). *Time Series Analysis: Forecasting and Control*. John Wiley & Sons. Google-Books-ID: rNt5CgAAQBAJ.

Hantush, M. S. (1956). Analysis of data from pumping tests in leaky aquifers. *Transactions, American Geophysical Union*, 37(6):702.

Hantush, M. S. and Jacob, C. E. (1955). Non-steady radial flow in an infinite leaky aquifer. *Transactions, American Geophysical Union*, 36(1):95.

Hughes, J. D., Langevin, C. D., and Banta, E. R. (2017). Documentation for the MODFLOW 6 framework. USGS Numbered Series 6-A57, U.S. Geological Survey, Reston, VA. IP-081538.

Veling, E. J. M. and Maas, C. (2010). Hantush Well Function revisited. *Journal of Hydrology*, 393(3):381–388.

Von Asmuth, J. R. and Bierkens, M. F. P. (2005). Modeling irregularly spaced residual series as a continuous stochastic process: IRREGULARLY SPACED RESIDUAL SERIES. *Water Resources Research*, 41(12).

Von Asmuth, J. R., Bierkens, M. F. P., and Maas, K. (2002). Transfer function-noise modeling in continuous time using predefined impulse response functions. *Water Resources Research*, 38(12):23–1–23–12.

Von Asmuth, J. R., Maas, K., Bakker, M., and Petersen, J. (2008). Modeling Time Series of Ground Water Head Fluctuations Subjected to Multiple Stresses. *Groundwater*, 46(1):30–40.

Von Asmuth, J. R., Maas, K., Knotters, M., Bierkens, M. F. P., Bakker, M., Olsthoorn, T. N., Cirkel, D. G., Leunk, I., Schaars, F., and von Asmuth, D. C. (2012). Software for hydrogeologic time series analysis, interfacing data with physical insight. *Environmental Modelling & Software*, 38:178–190.

A

Synthetic models

In this section the synthetic model are displayed. The canal layout of each model can be seen together with the cross section. For each model the synthetic observations are displayed.

Rectangle layout

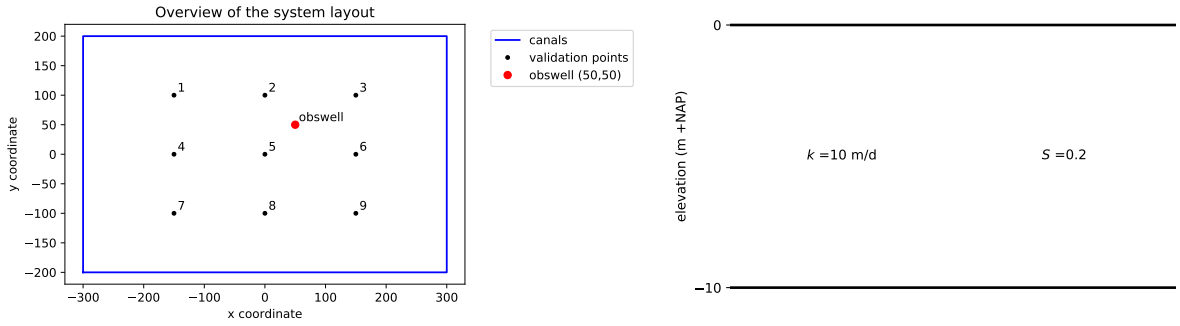

Figure A.1: On the left the overview of the system and on the right the cross section of the system for the rectangle layout

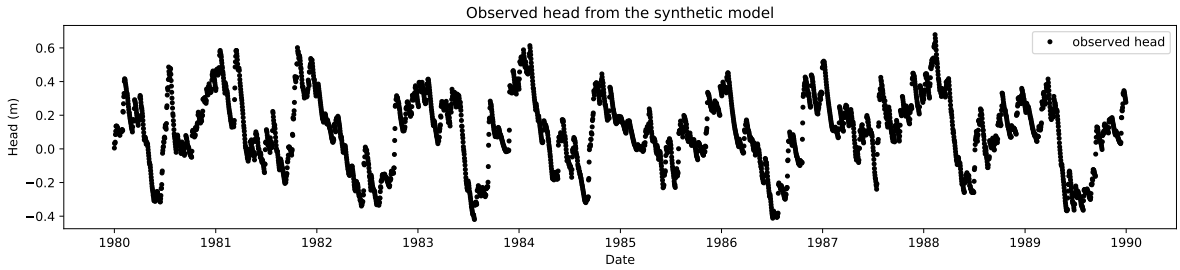

Figure A.2: The observed head for the rectangle layout

Parallel layout

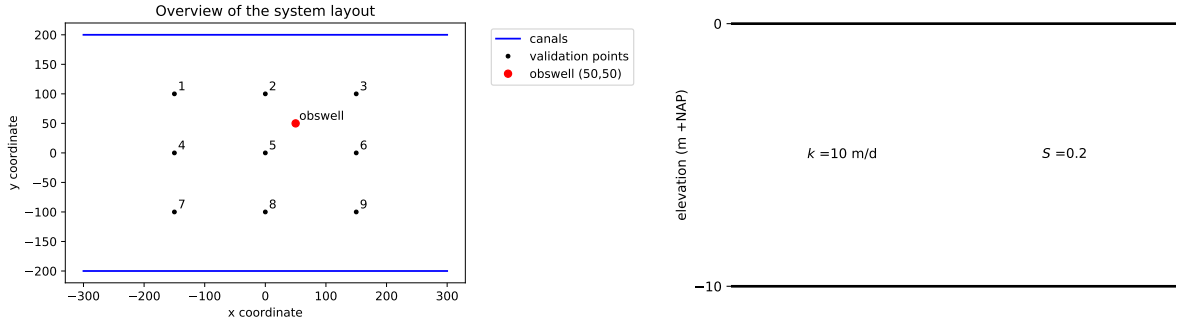

Figure A.3: On the left the overview of the system and on the right the cross section of the system for the parallel layout

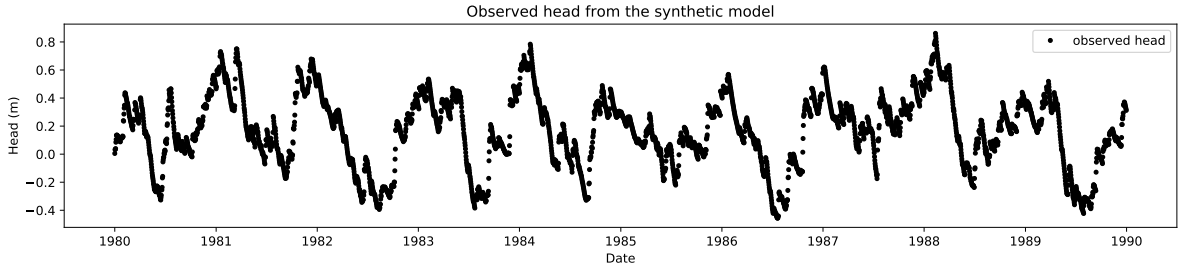

Figure A.4: The observed head for the parallel layout

L-shape layout

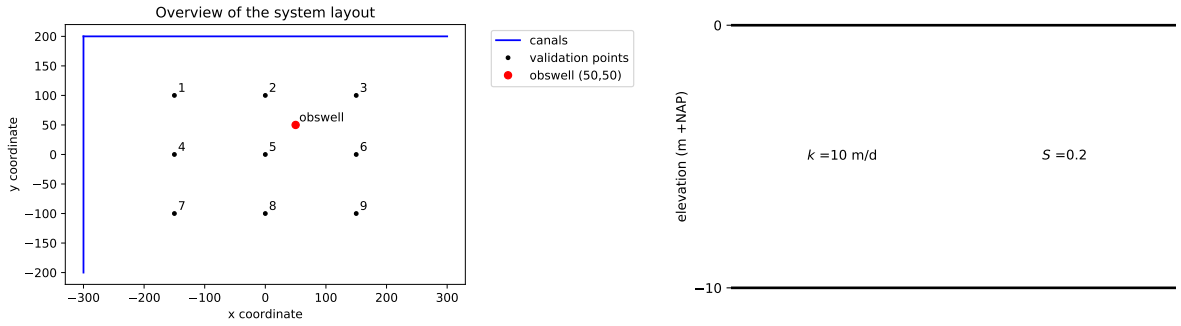

Figure A.5: On the left the overview of the system and on the right the cross section of the system for the L-shape layout

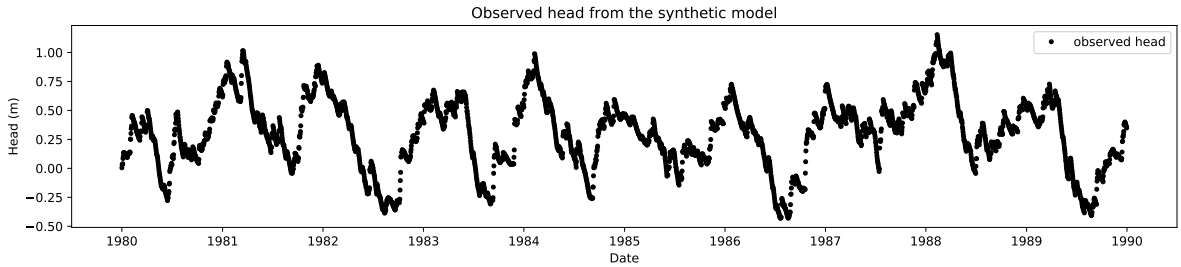

Figure A.6: The observed head for the L-shape layout

Branched layout

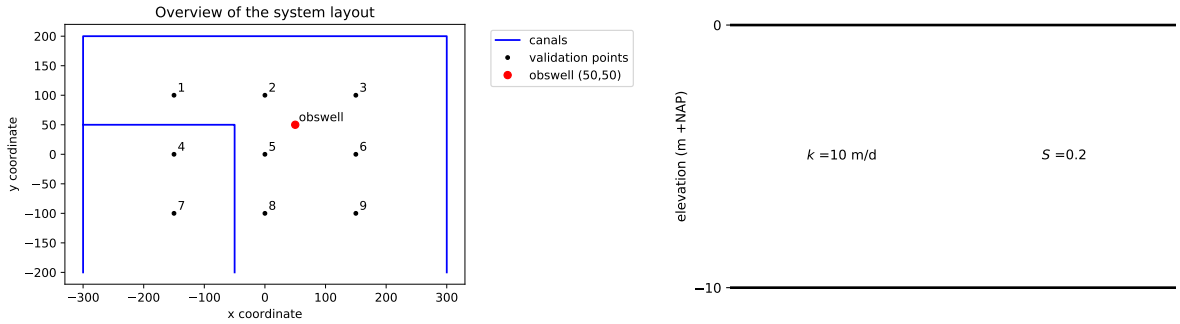

Figure A.7: On the left the overview of the system and on the right the cross section of the system for the branched layout

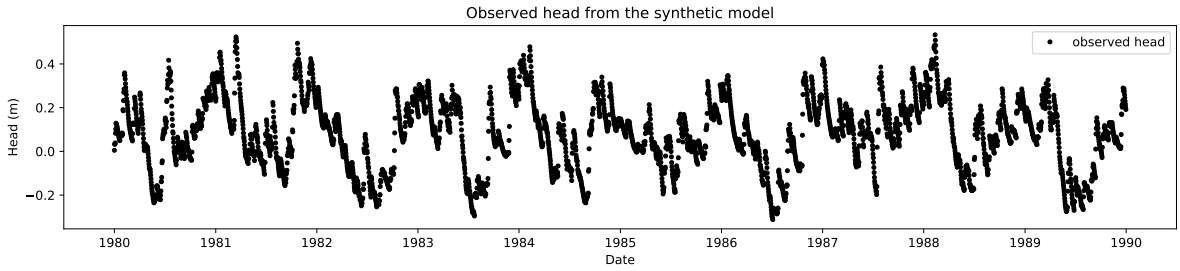

Figure A.8: The observed head for the branched layout

Triangle layout

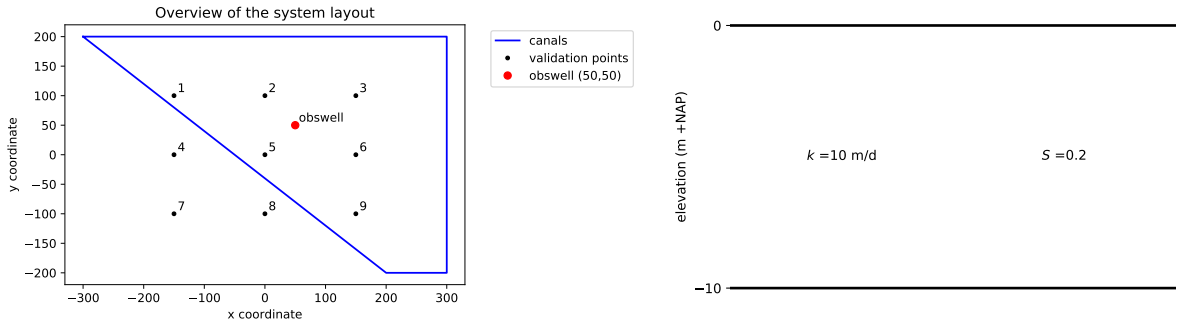

Figure A.9: On the left the overview of the system and on the right the cross section of the system for the triangle layout

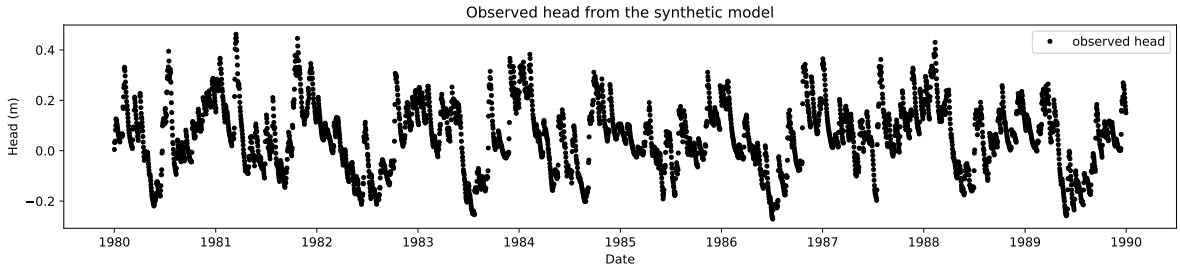

Figure A.10: The observed head for the triangle layout

Rectangle multi layer layout

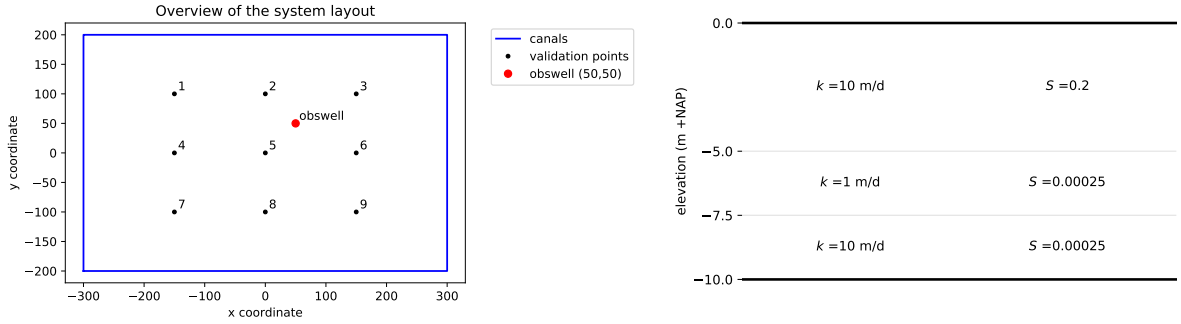

Figure A.11: On the left the overview of the system and on the right the cross section of the system for the rectangle multi layer layout

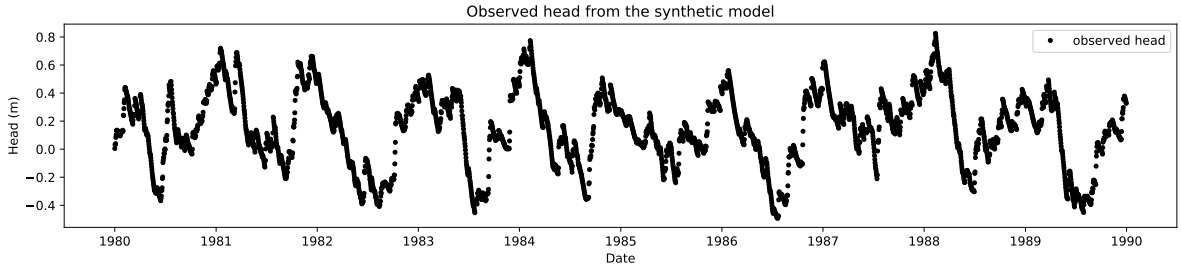

Figure A.12: The observed head for the rectangle multi layer layout

Parallel multi layer layout

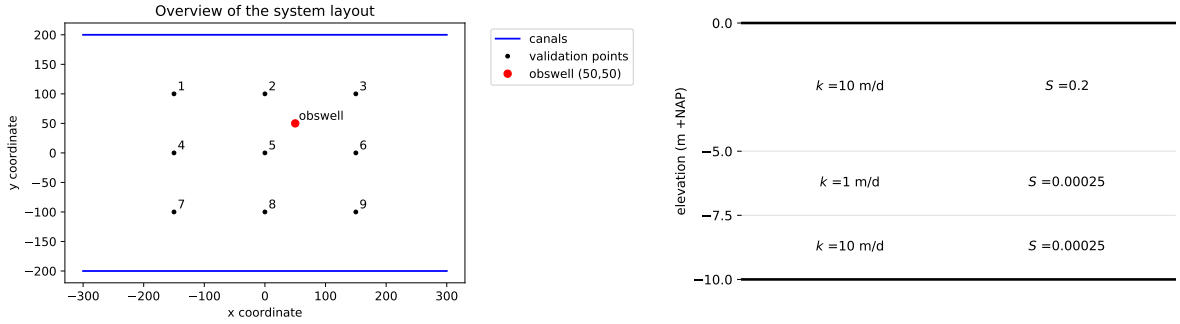

Figure A.13: On the left the overview of the system and on the right the cross section of the system for the parallel multi layer layout

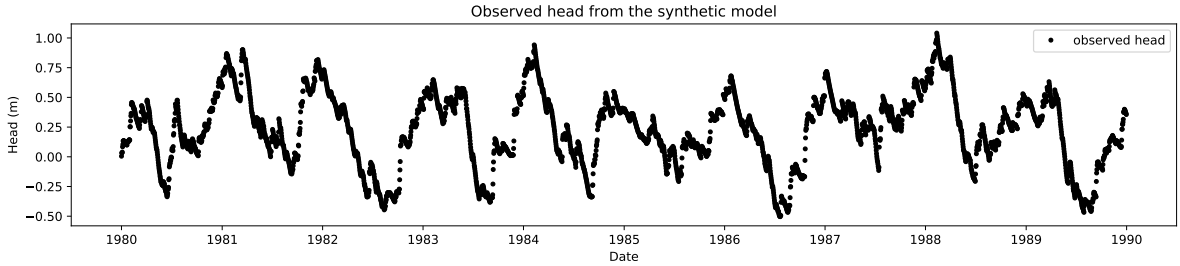

Figure A.14: The observed head for the parallel multi layer layout

L-shape multi layer layout

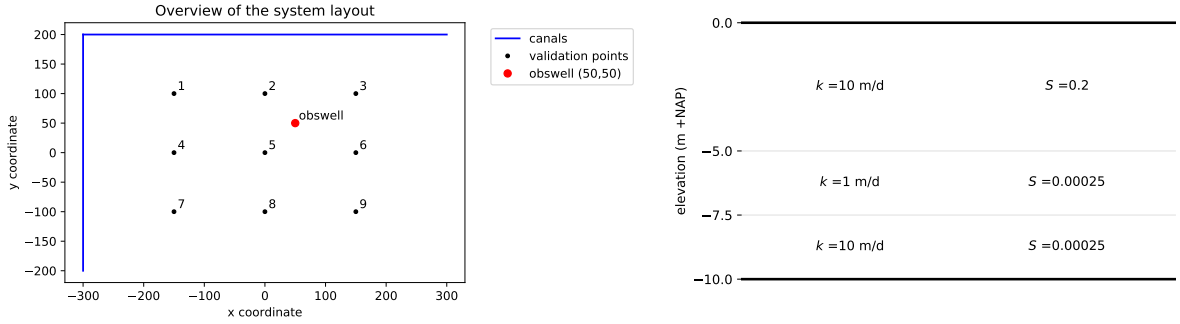

Figure A.15: On the left the overview of the system and on the right the cross section of the system for the L-shape multi layer layout

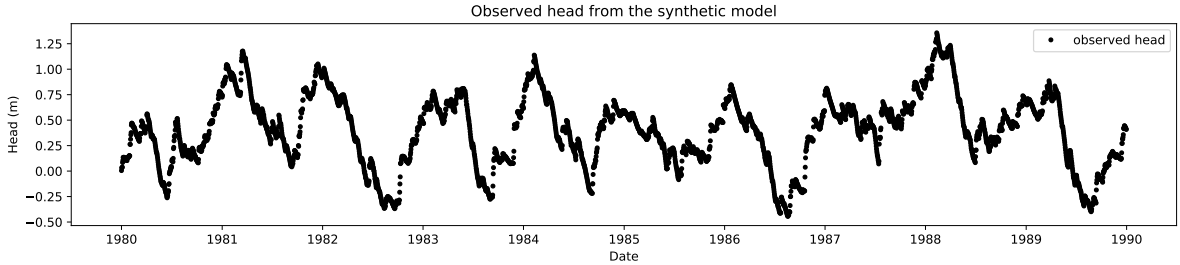

Figure A.16: The observed head for the L-shape multi layer layout

Branched multi layer layout

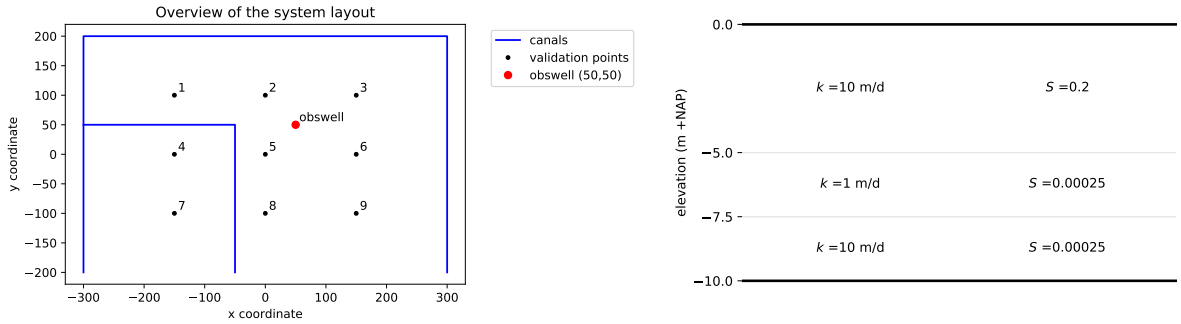

Figure A.17: On the left the overview of the system and on the right the cross section of the system for the branched multi layer layout

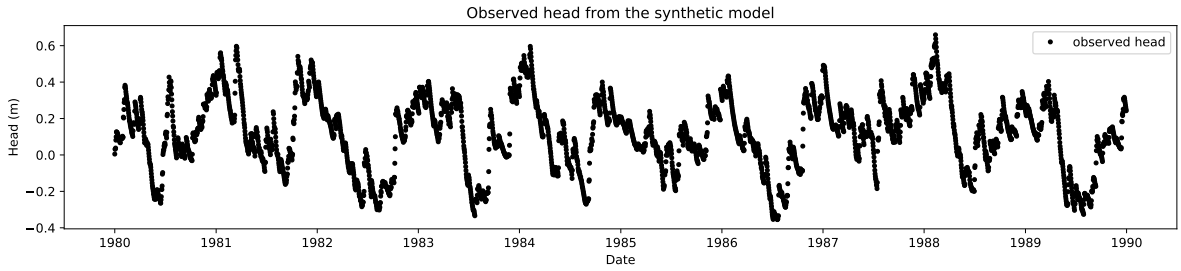

Figure A.18: The observed head for the branched multi layer layout

Triangle multi layer layout

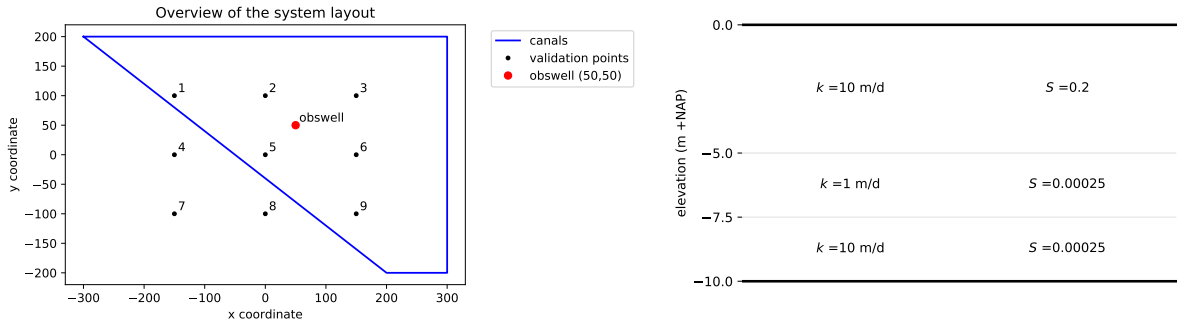

Figure A.19: On the left the overview of the system and on the right the cross section of the system for the triangle multi layer layout

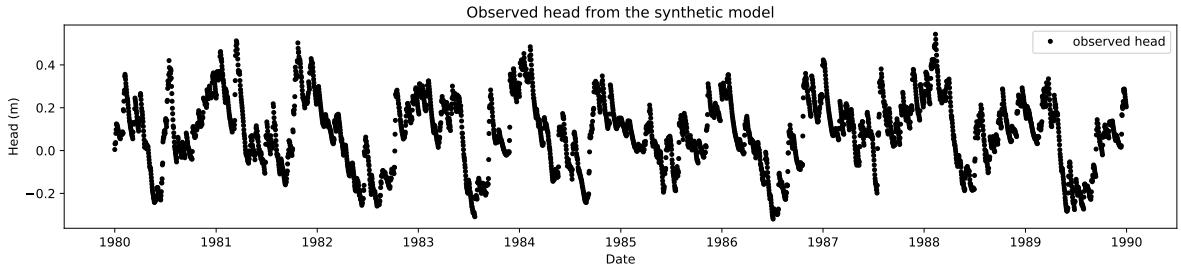

Figure A.20: The observed head for the triangle multi layer layout

Rectangle leaky layer layout

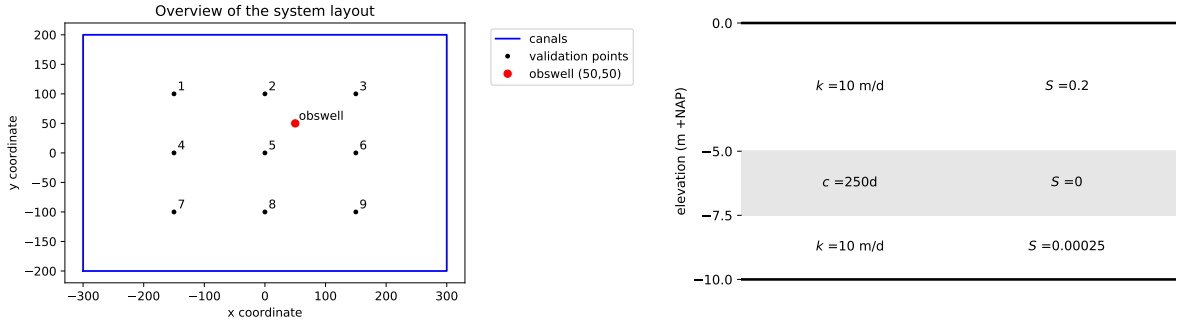

Figure A.21: On the left the overview of the system and on the right the cross section of the system for the rectangle leaky layer layout

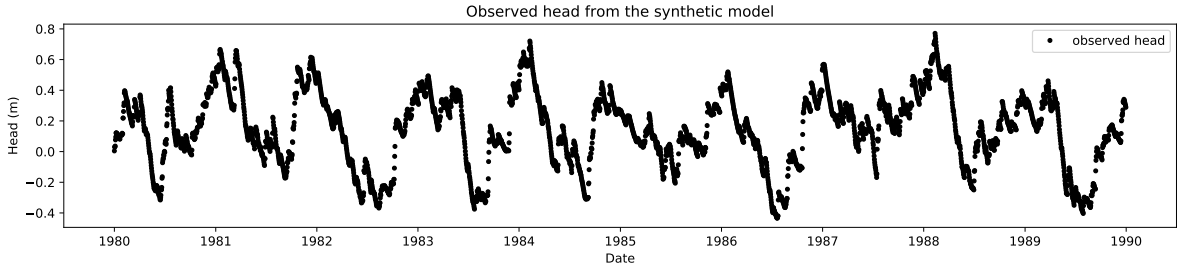

Figure A.22: The observed head for the rectangle leaky layer layout

Parallel leaky layer layout

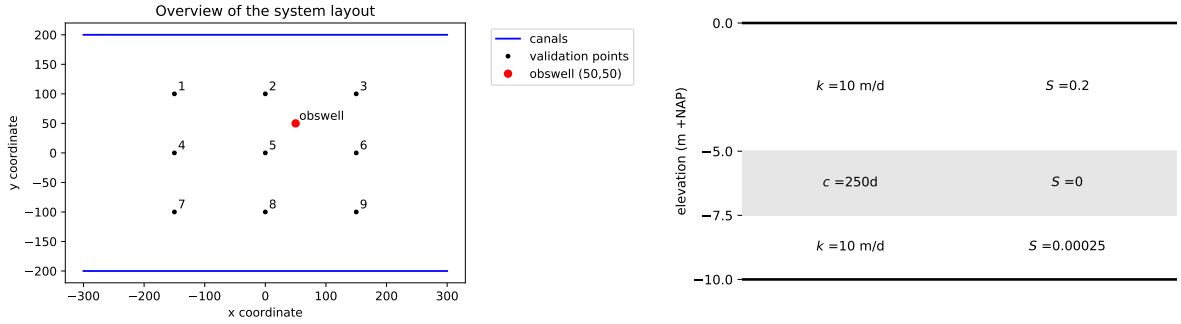

Figure A.23: On the left the overview of the system and on the right the cross section of the system for the parallel leaky layer layout

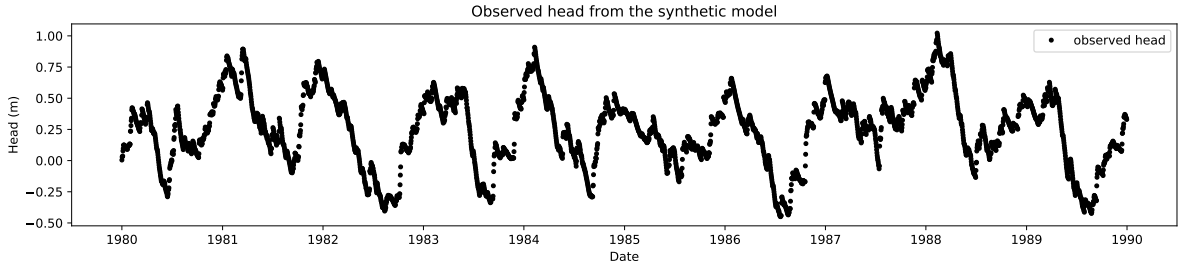

Figure A.24: The observed head for the parallel leaky layer layout

L-shape leaky layer layout

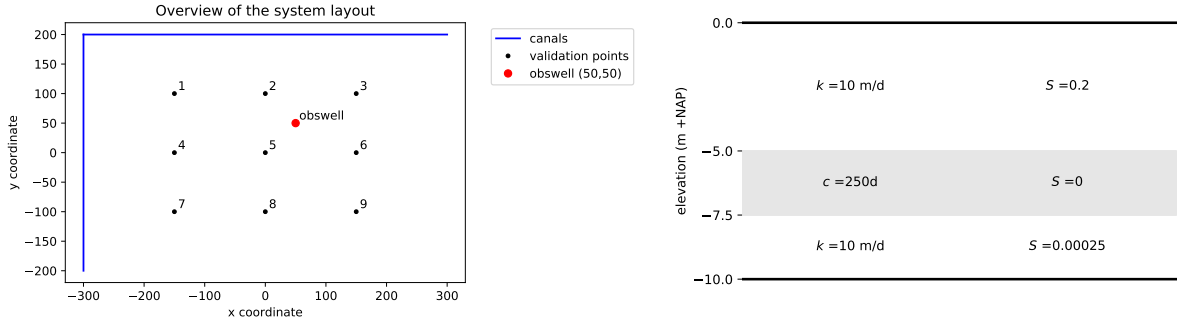

Figure A.25: On the left the overview of the system and on the right the cross section of the system for the L-shape leaky layer layout

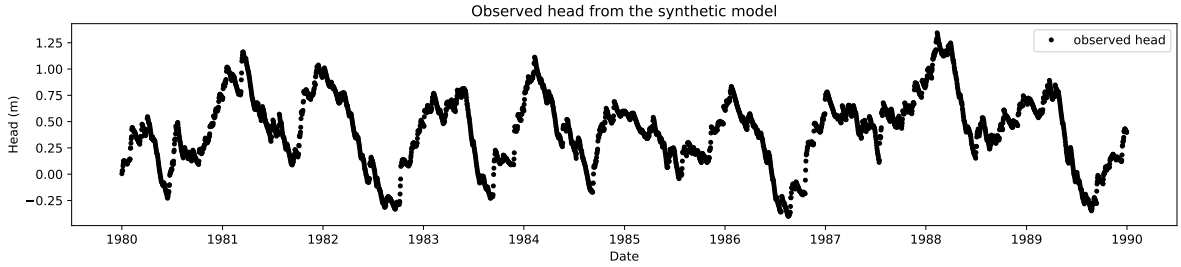

Figure A.26: The observed head for the L-shape leaky layer layout

Branched leaky layer layout

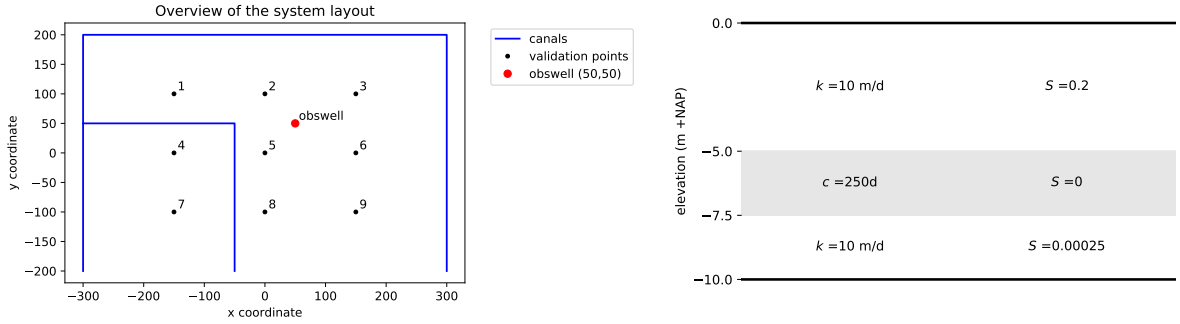

Figure A.27: On the left the overview of the system and on the right the cross section of the system for the branched leaky layer layout

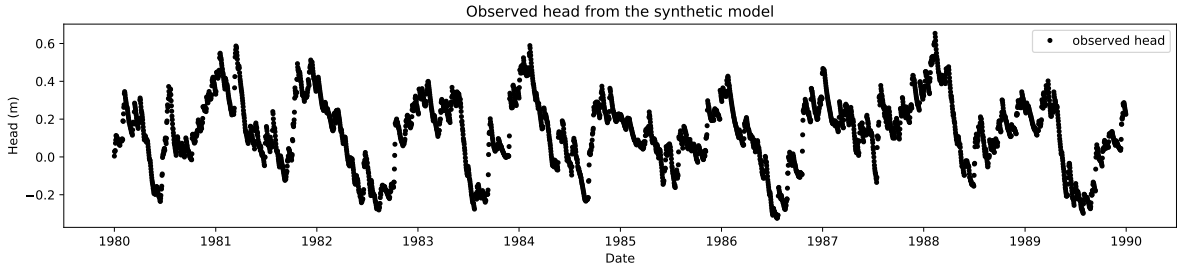

Figure A.28: The observed head for the branched leaky layer layout

Triangle leaky layer layout

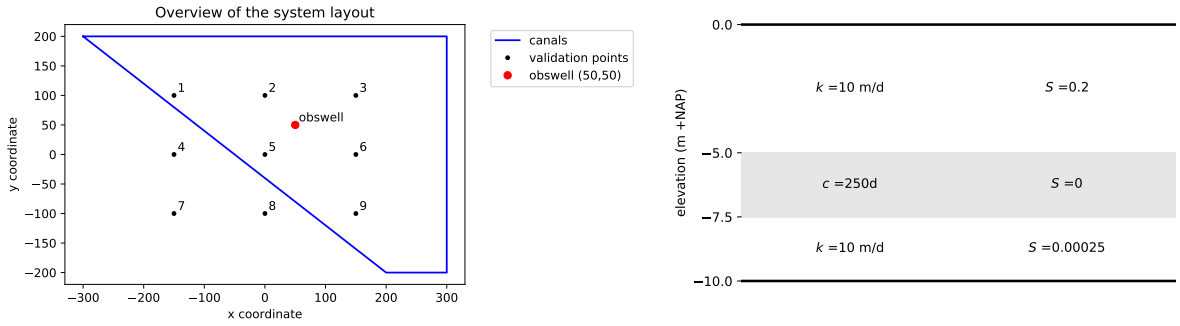

Figure A.29: On the left the overview of the system and on the right the cross section of the system for the triangle leaky layer layout

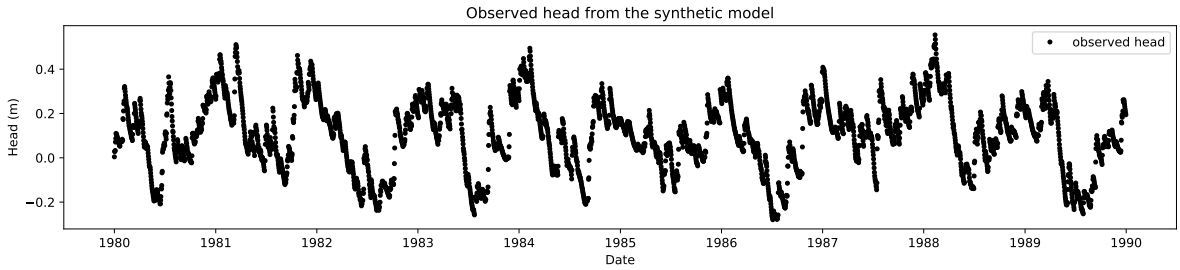

Figure A.30: The observed head for the triangle leaky layer layout

B

Synthetic model results

In this Appendix the results for the different synthetic model layouts can be seen. For all of the models the response functions of the synthetic model and the time series analysis are shown. For the observation well the observed synthetic head and the simulated head from the conceptual model are plotted, together with the difference between these models. For each of the checkpoints in the synthetic model (as can be seen in Appendix A) the difference in head is plotted between the synthetic and conceptual model. The statistics of the checkpoints can be seen in the second section of this chapter.

B.1. Model Results

Rectangle Model

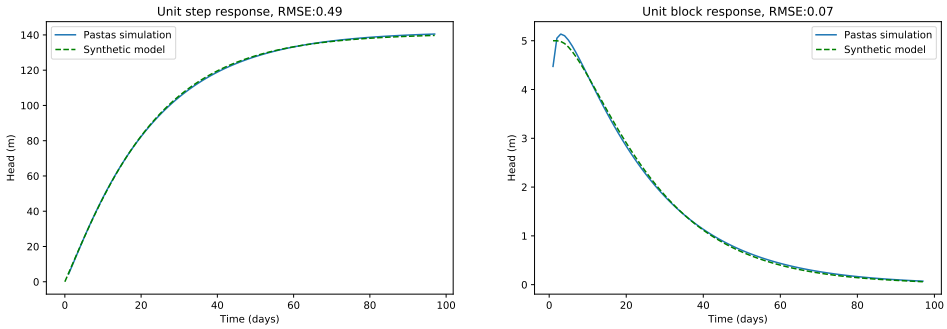

Figure B.1: The step and block response of the synthetic model and the time series analysis simulation

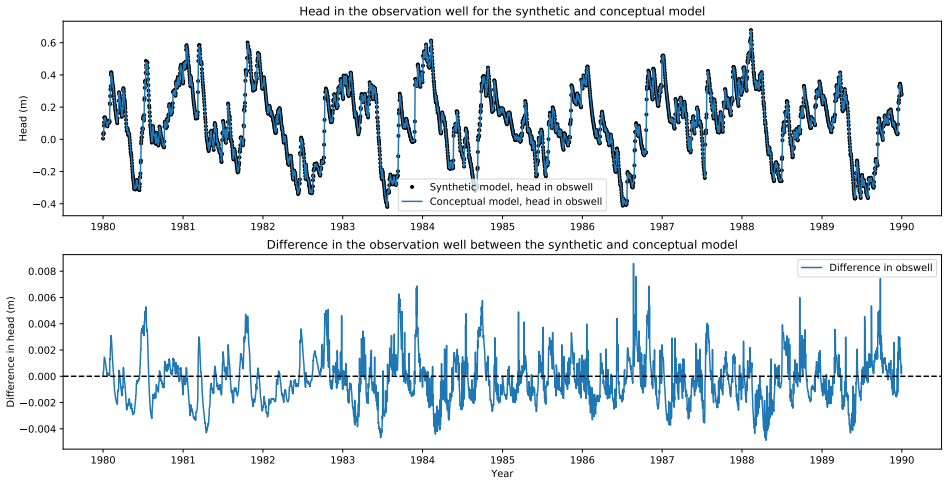

Figure B.2: The observed head from the synthetic model and the conceptual model in the observation well. On the bottom the difference between the two models

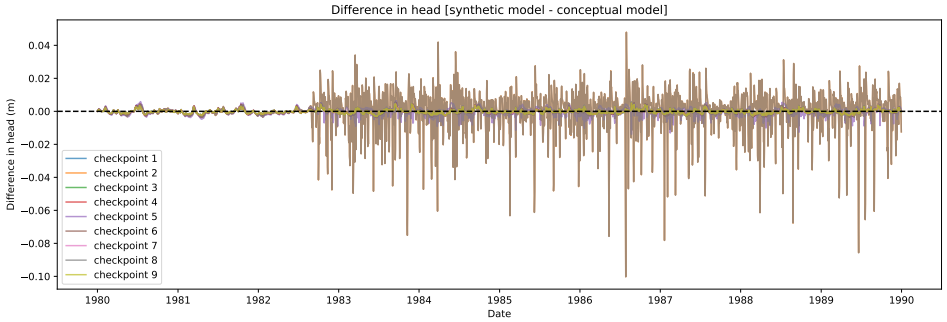

Figure B.3: The difference in head between the synthetic and conceptual model at the checkpoints

Parallel Model

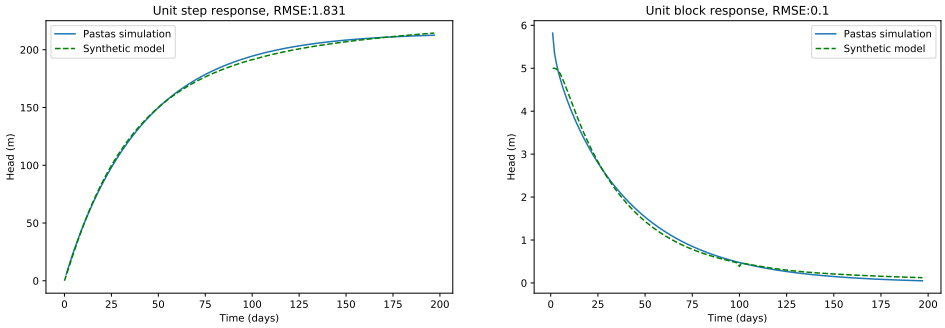

Figure B.4: The step and block response of the synthetic model and the time series analysis simulation

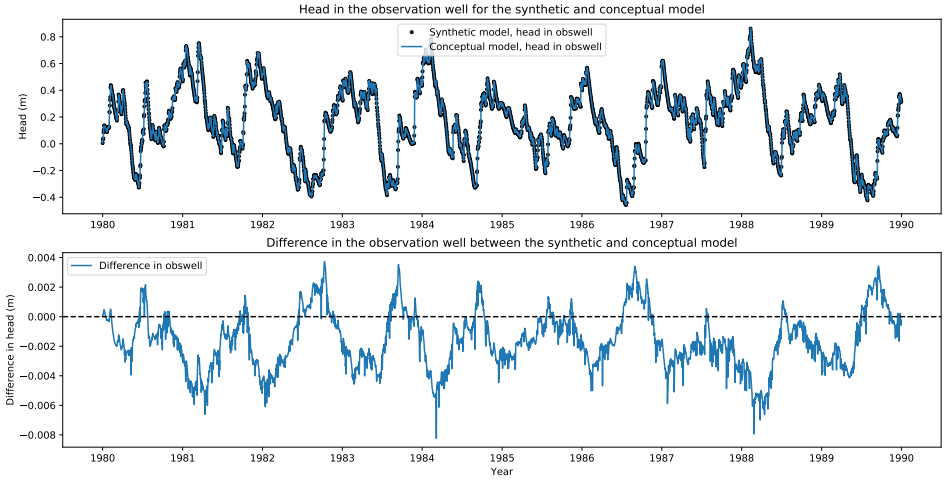

Figure B.5: The observed head from the synthetic model and the conceptual model in the observation well. On the bottom the difference between the two models

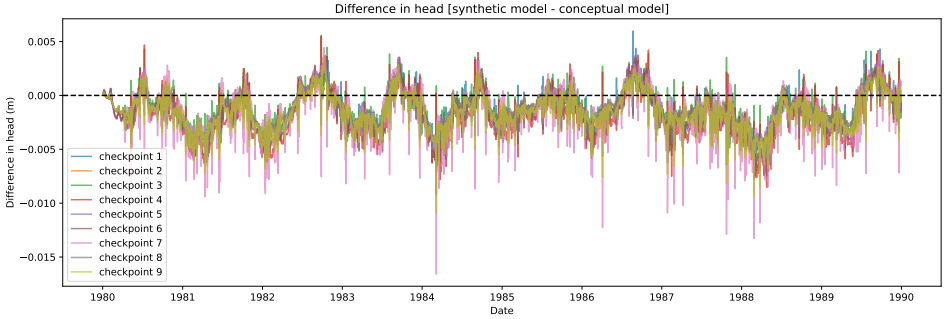

Figure B.6: The difference in head between the synthetic and conceptual model at the checkpoints

L-shape Model

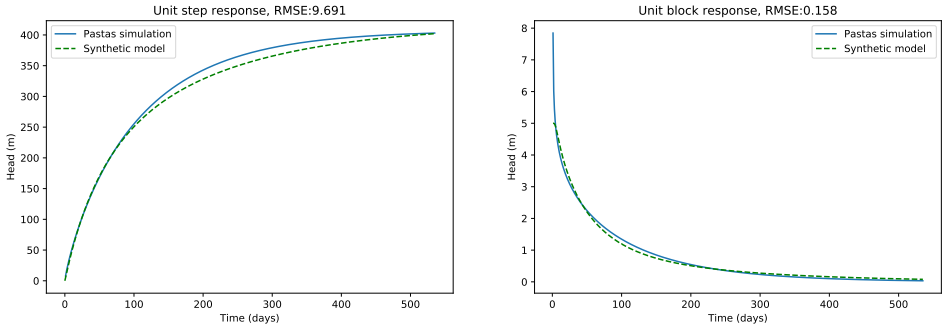

Figure B.7: The step and block response of the synthetic model and the time series analysis simulation

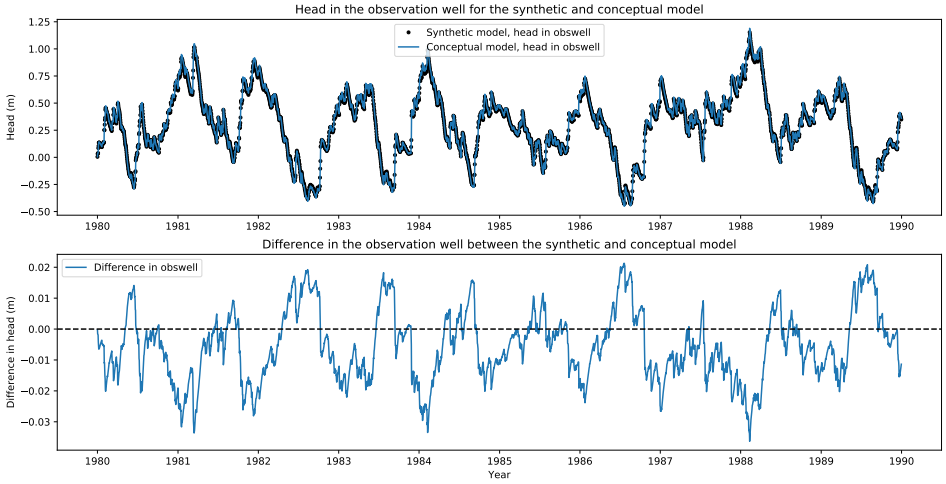

Figure B.8: The observed head from the synthetic model and the conceptual model in the observation well. On the bottom the difference between the two models

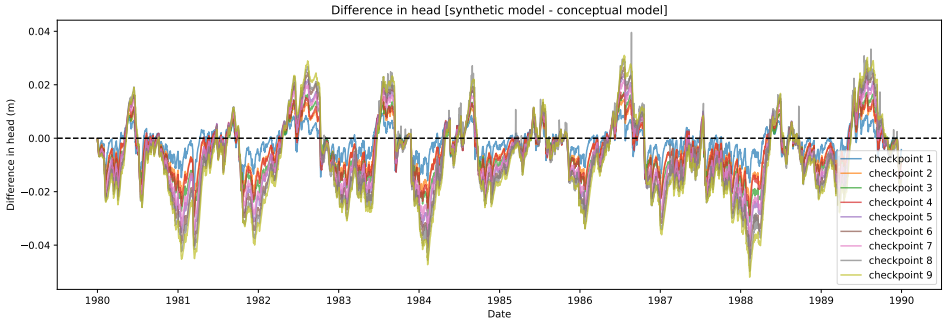

Figure B.9: The difference in head between the synthetic and conceptual model at the checkpoints

Branched Model

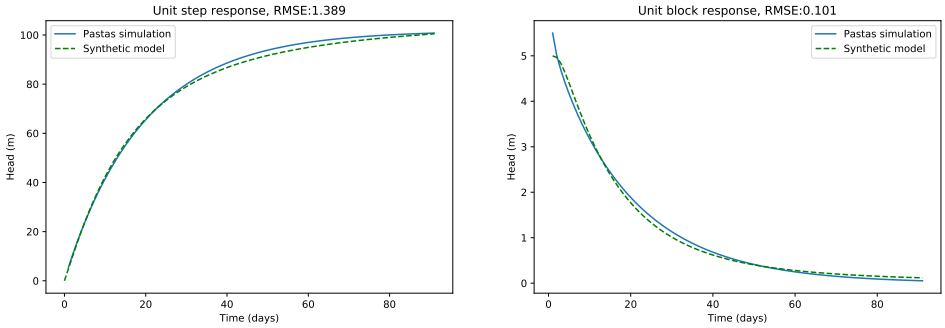

Figure B.10: The step and block response of the synthetic model and the time series analysis simulation

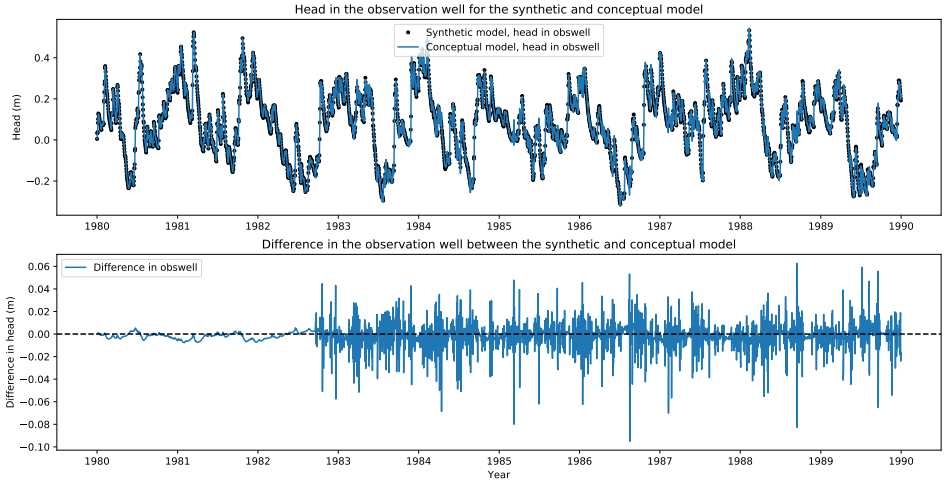

Figure B.11: The observed head from the synthetic model and the conceptual model in the observation well. On the bottom the difference between the two models

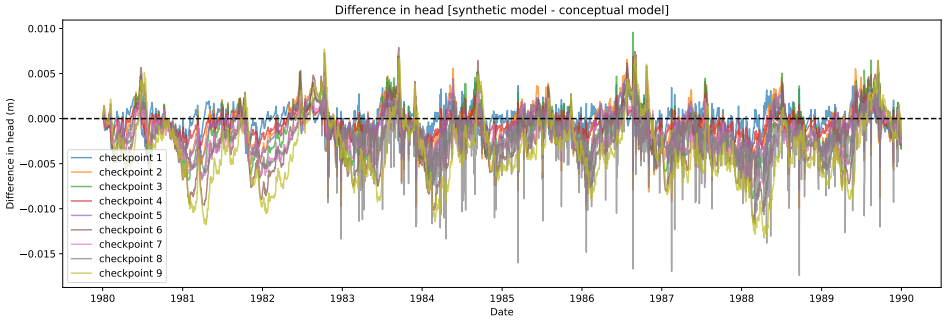

Figure B.12: The difference in head between the synthetic and conceptual model at the checkpoints

Triangle Model

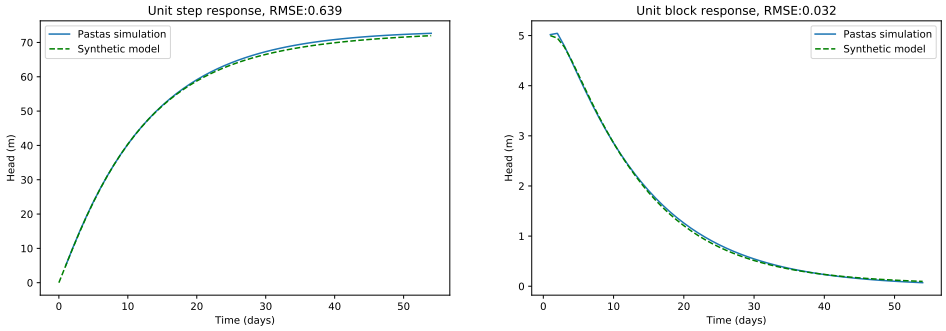

Figure B.13: The step and block response of the synthetic model and the time series analysis simulation

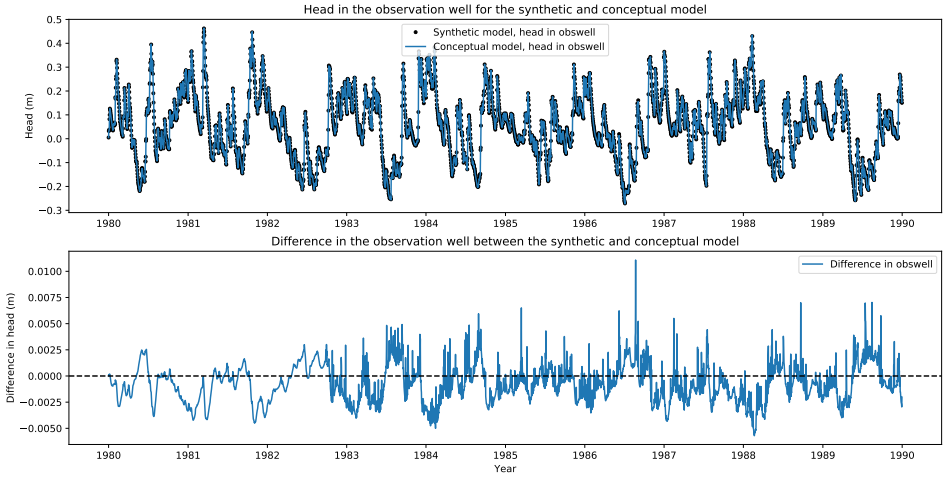

Figure B.14: The observed head from the synthetic model and the conceptual model in the observation well. On the bottom the difference between the two models

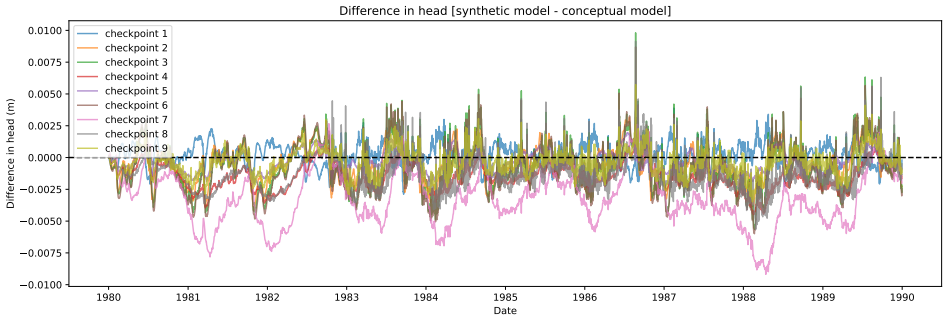

Figure B.15: The difference in head between the synthetic and conceptual model at the checkpoints

Rectangle multi layer Model

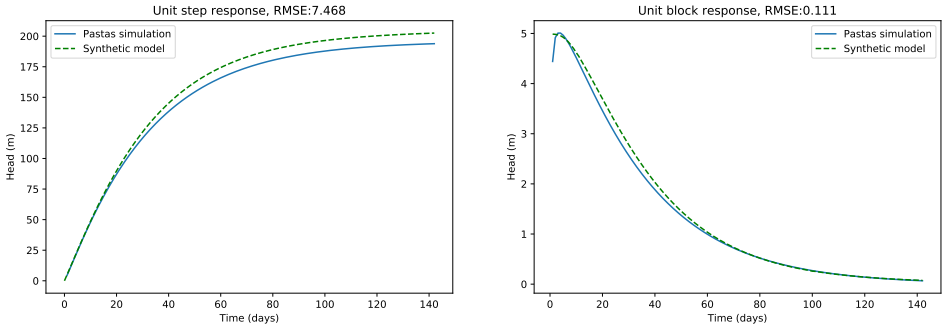

Figure B.16: The step and block response of the synthetic model and the time series analysis simulation

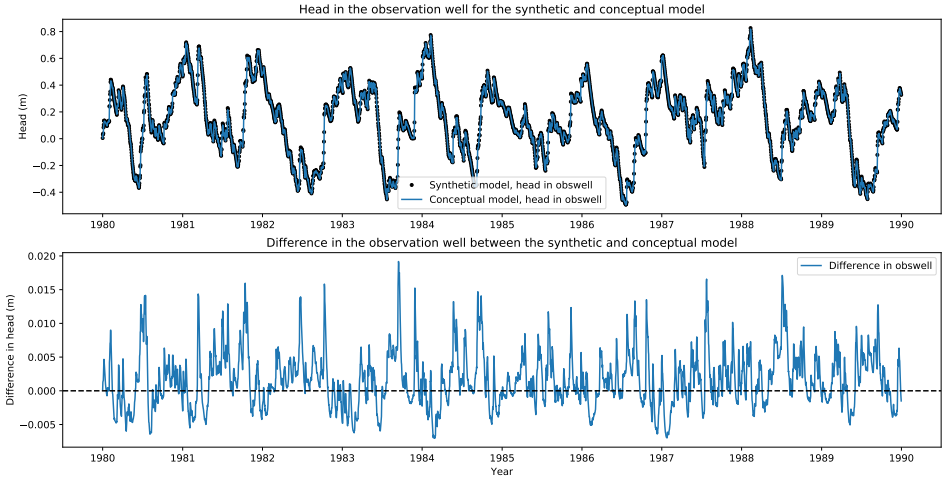

Figure B.17: The observed head from the synthetic model and the conceptual model in the observation well. On the bottom the difference between the two models

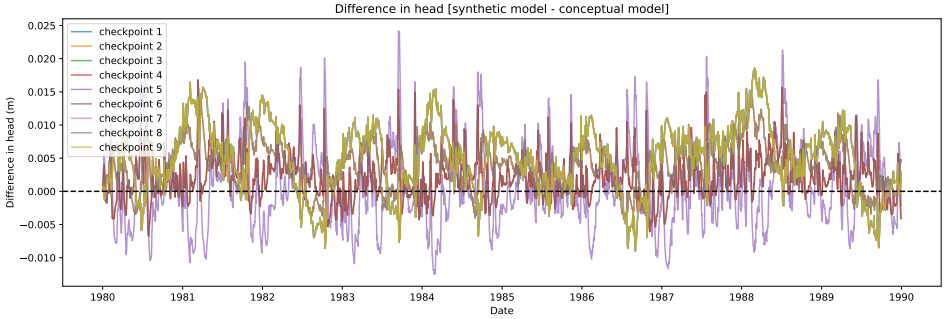

Figure B.18: The difference in head between the synthetic and conceptual model at the checkpoints

Parallel multi layer Model

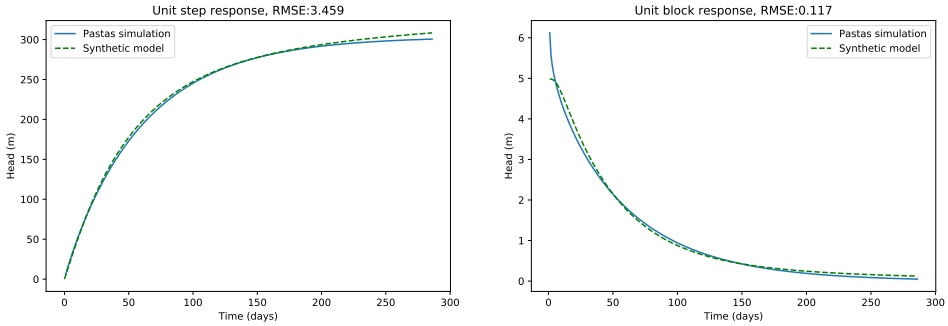

Figure B.19: The step and block response of the synthetic model and the time series analysis simulation

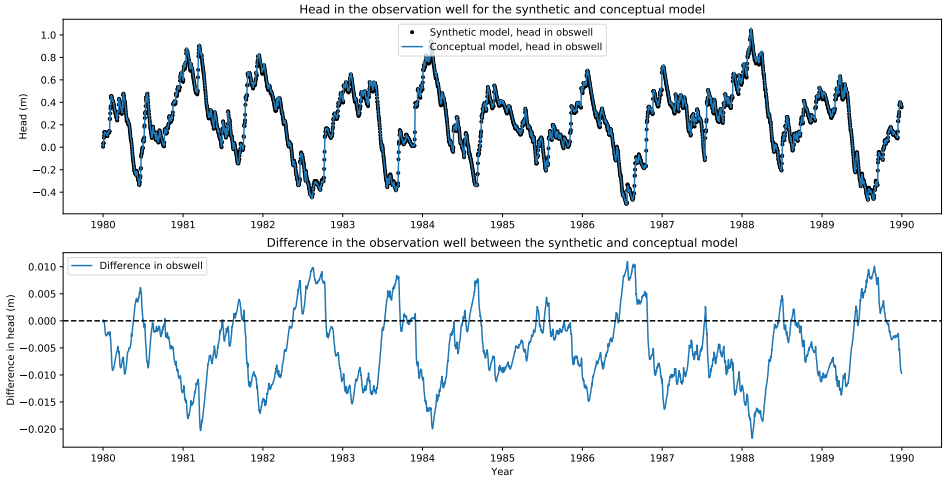

Figure B.20: The observed head from the synthetic model and the conceptual model in the observation well. On the bottom the difference between the two models

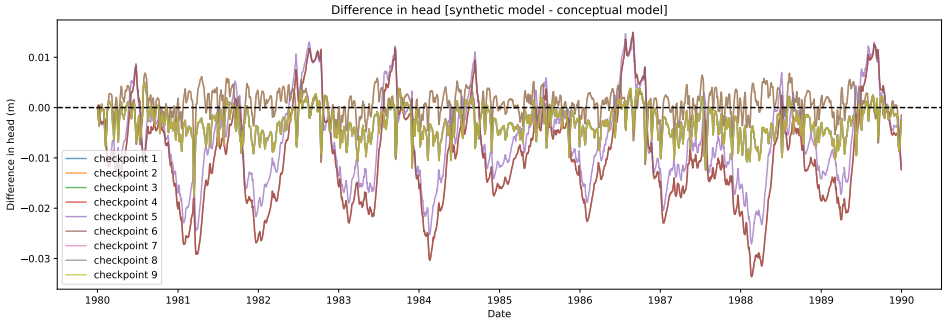

Figure B.21: The difference in head between the synthetic and conceptual model at the checkpoints

L-shape multi layer Model

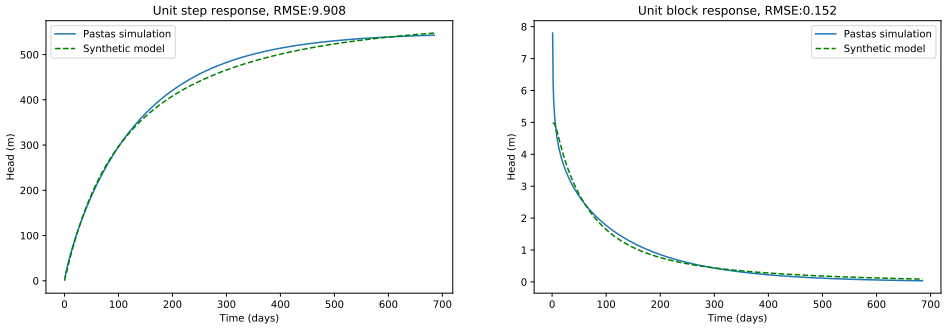

Figure B.22: The step and block response of the synthetic model and the time series analysis simulation

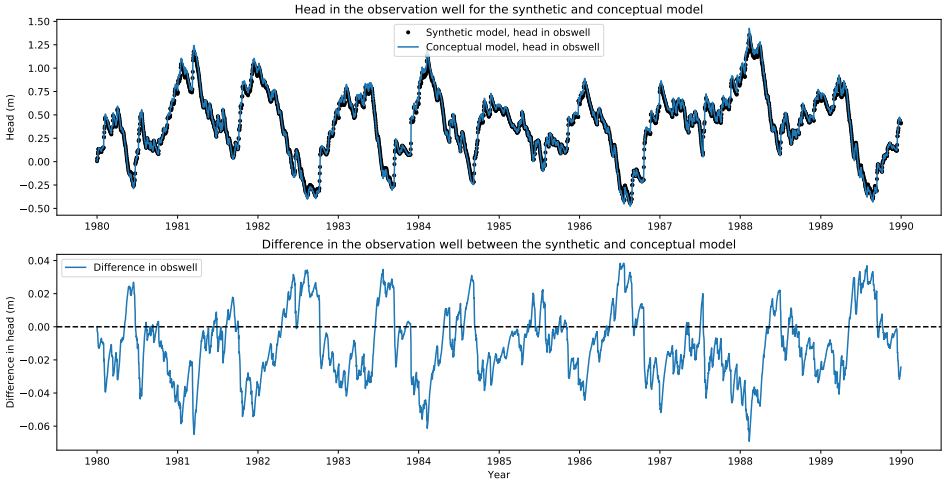

Figure B.23: The observed head from the synthetic model and the conceptual model in the observation well. On the bottom the difference between the two models

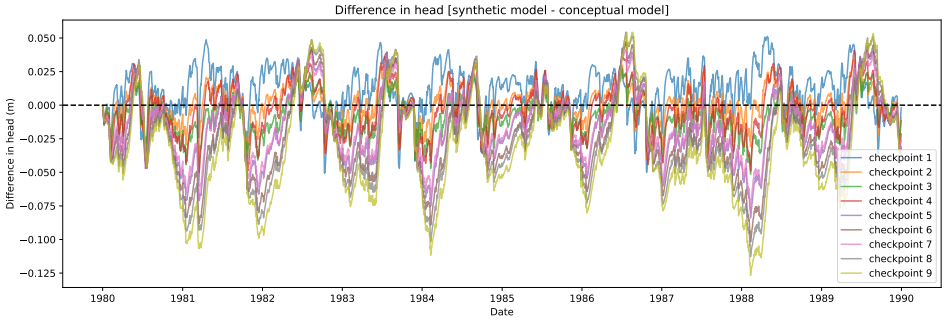

Figure B.24: The difference in head between the synthetic and conceptual model at the checkpoints

Branched multi layer Model

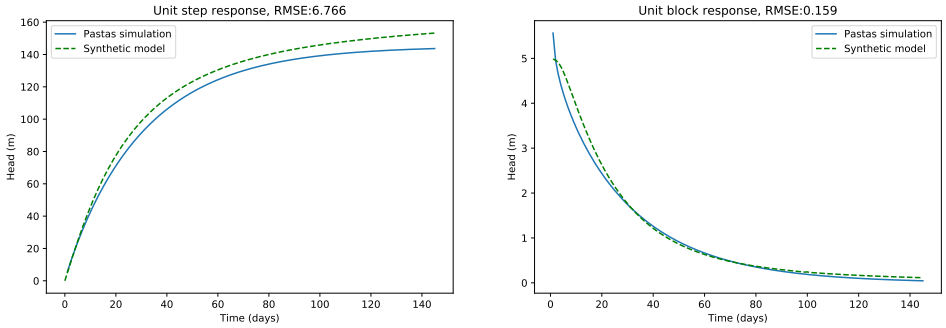

Figure B.25: The step and block response of the synthetic model and the time series analysis simulation

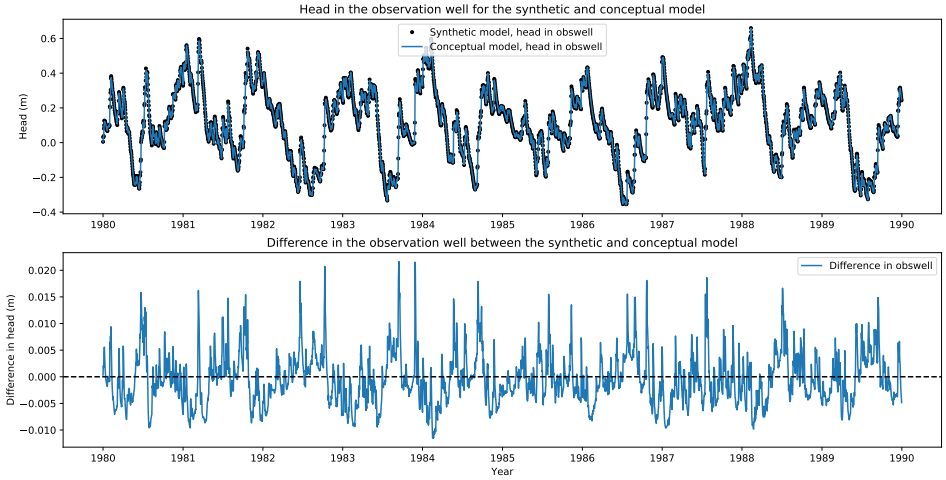

Figure B.26: The observed head from the synthetic model and the conceptual model in the observation well. On the bottom the difference between the two models

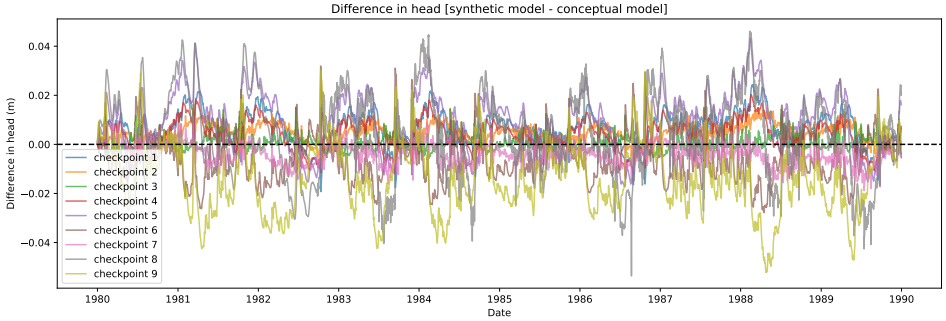

Figure B.27: The difference in head between the synthetic and conceptual model at the checkpoints

Triangle multi layer Model

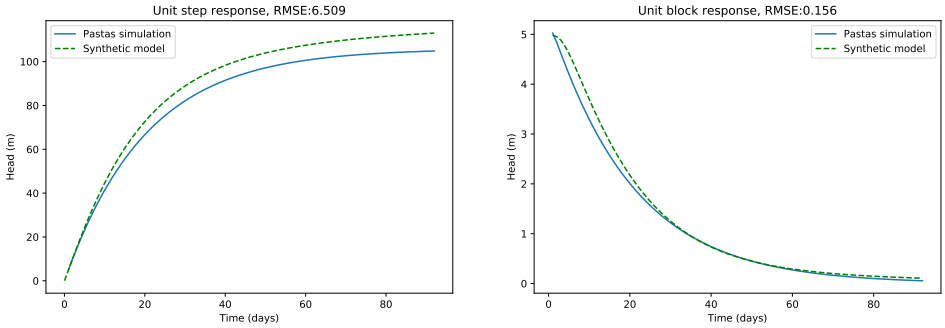

Figure B.28: The step and block response of the synthetic model and the time series analysis simulation

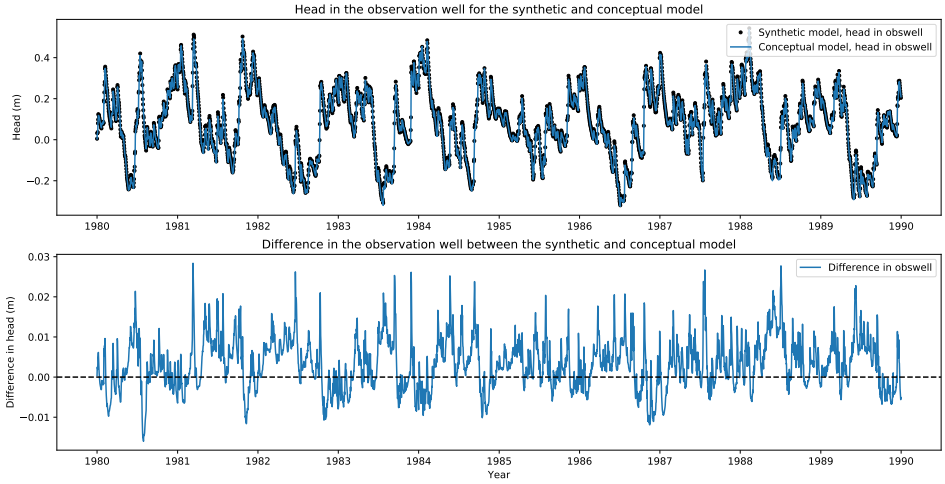

Figure B.29: The observed head from the synthetic model and the conceptual model in the observation well. On the bottom the difference between the two models

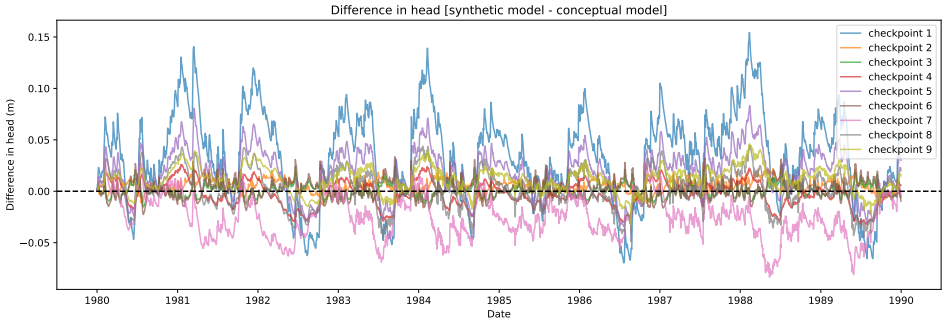

Figure B.30: The difference in head between the synthetic and conceptual model at the checkpoints

Rectangle leaky layer Model

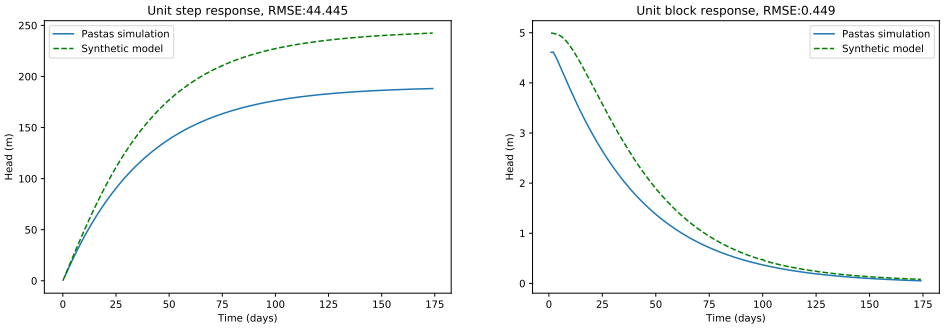

Figure B.31: The step and block response of the synthetic model and the time series analysis simulation

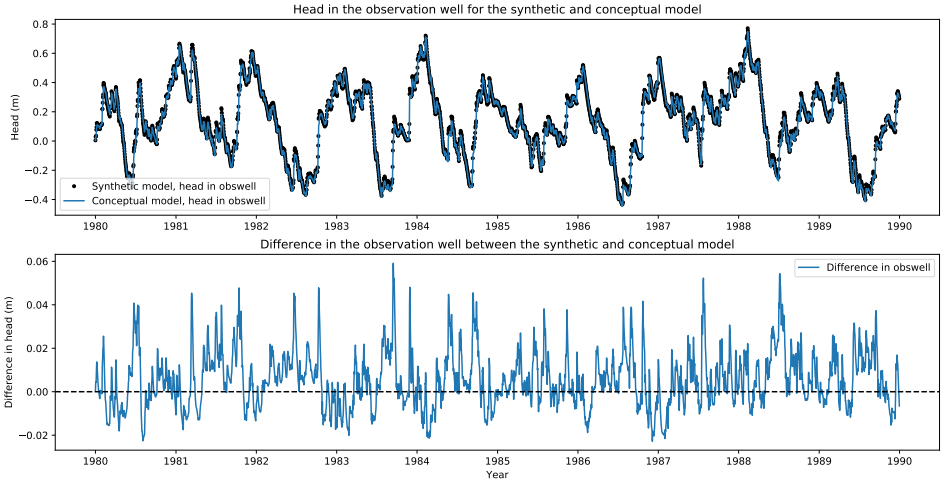

Figure B.32: The observed head from the synthetic model and the conceptual model in the observation well. On the bottom the difference between the two models

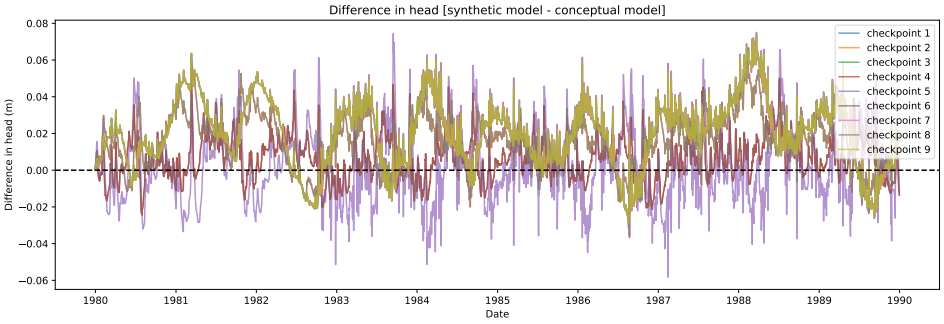

Figure B.33: The difference in head between the synthetic and conceptual model at the checkpoints

Parallel leaky layer Model

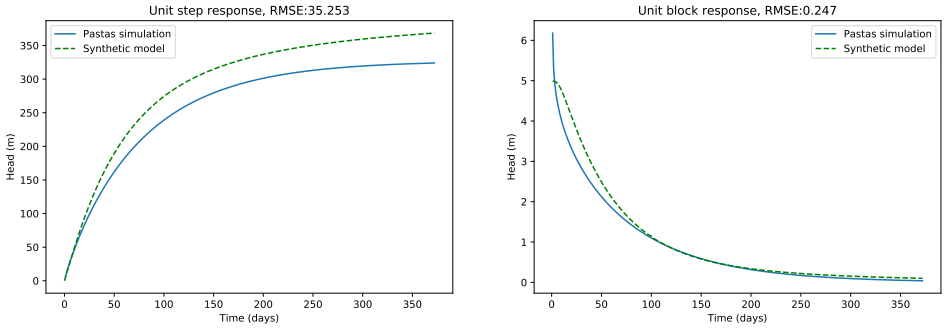

Figure B.34: The step and block response of the synthetic model and the time series analysis simulation

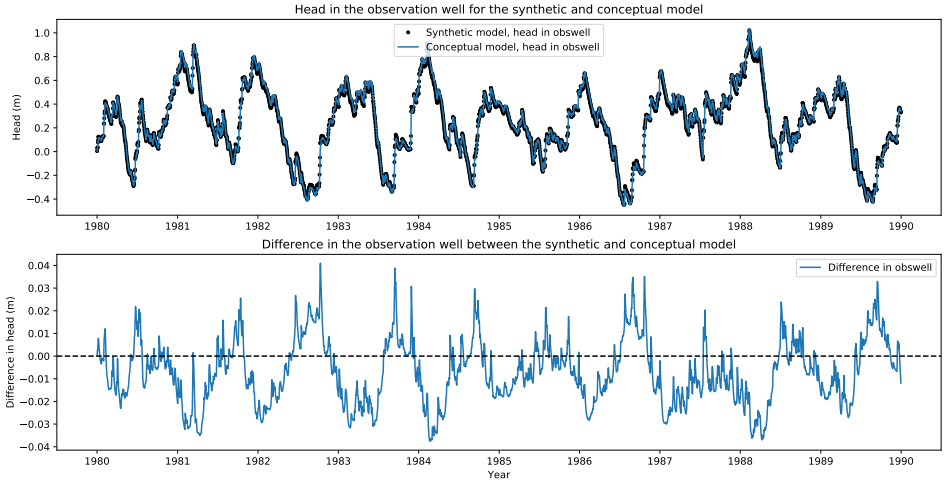

Figure B.35: The observed head from the synthetic model and the conceptual model in the observation well. On the bottom the difference between the two models

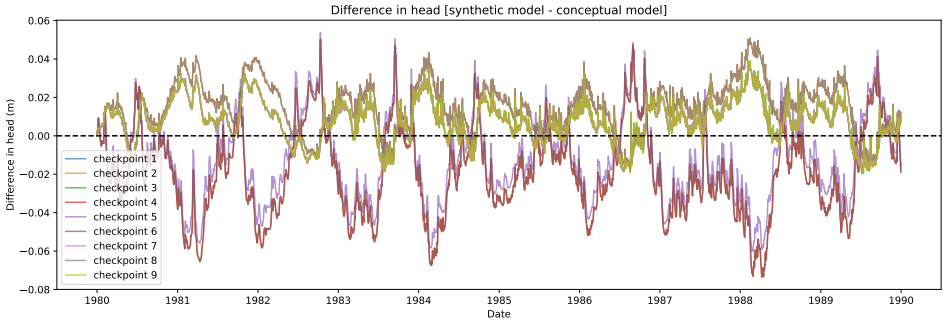

Figure B.36: The difference in head between the synthetic and conceptual model at the checkpoints

L-shape leaky layer Model

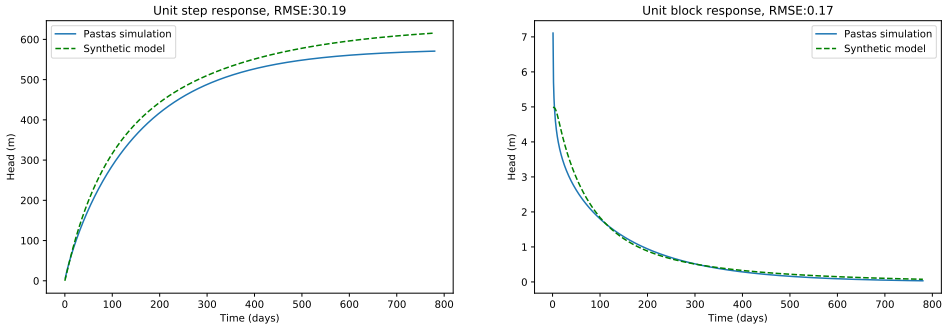

Figure B.37: The step and block response of the synthetic model and the time series analysis simulation

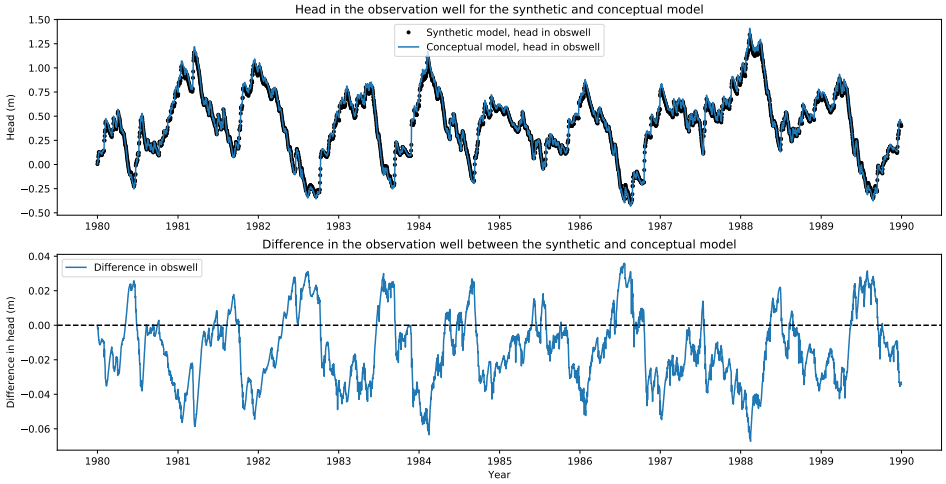

Figure B.38: The observed head from the synthetic model and the conceptual model in the observation well. On the bottom the difference between the two models

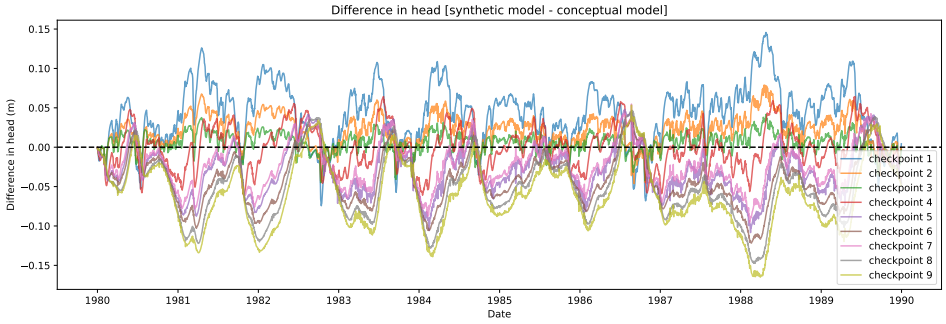

Figure B.39: The difference in head between the synthetic and conceptual model at the checkpoints

Branched leaky layer Model

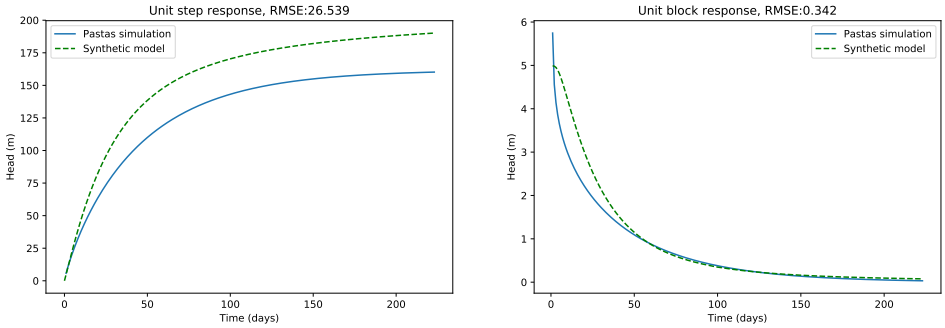

Figure B.40: The step and block response of the synthetic model and the time series analysis simulation

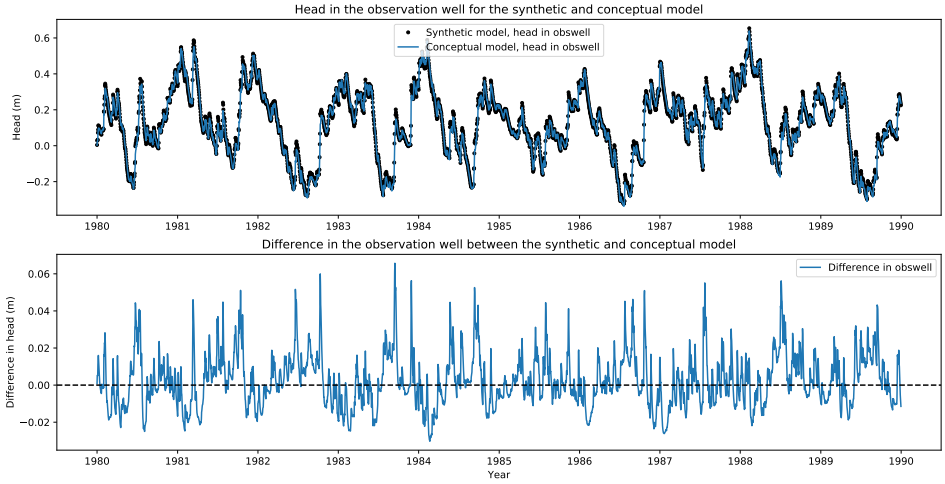

Figure B.41: The observed head from the synthetic model and the conceptual model in the observation well. On the bottom the difference between the two models

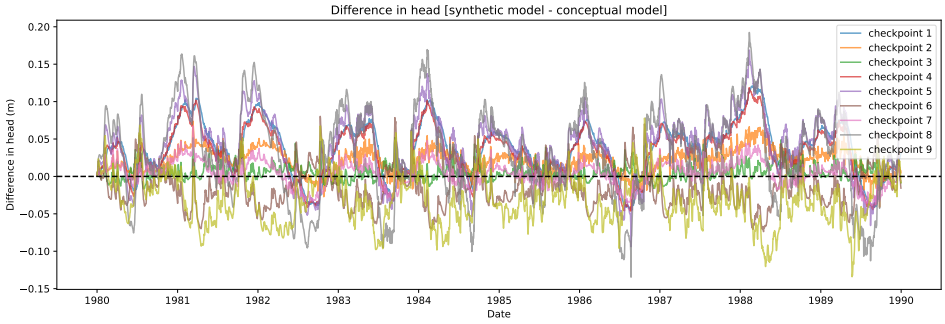

Figure B.42: The difference in head between the synthetic and conceptual model at the checkpoints

Triangle leaky layer Model

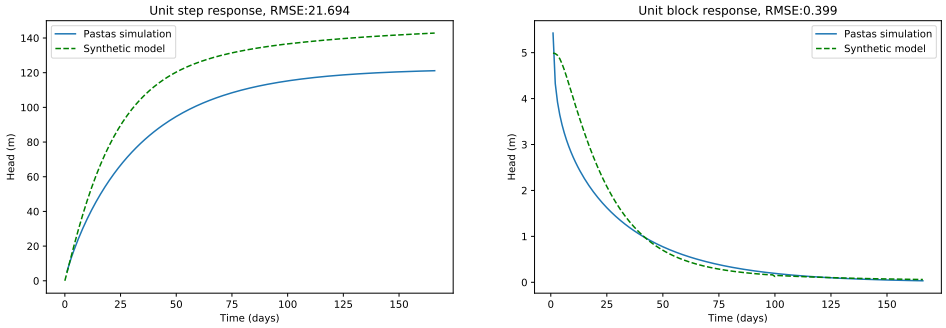

Figure B.43: The step and block response of the synthetic model and the time series analysis simulation

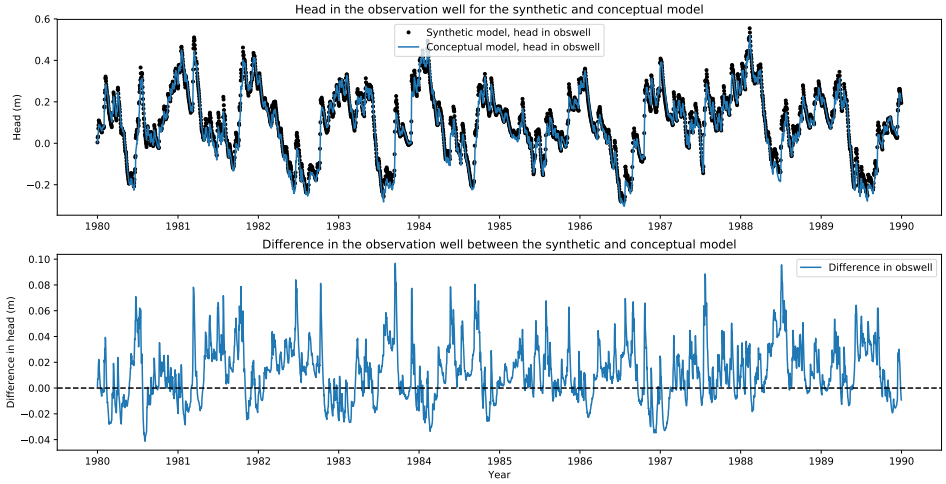

Figure B.44: The observed head from the synthetic model and the conceptual model in the observation well. On the bottom the difference between the two models

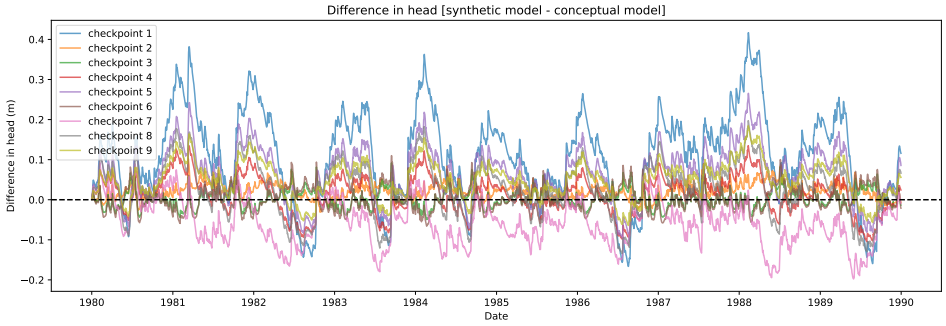

Figure B.45: The difference in head between the synthetic and conceptual model at the checkpoints

B.2. EVP at validation point

Model name	Point 1	Point 2	Point 3	Point 4	Point 5	Point 6	Point 7	Point 8	Point 9
square	99.994	99.59	99.994	99.994	99.99	99.994	99.994	99.589	99.994
branched	99.948	99.955	99.969	99.977	99.961	99.972	99.984	99.968	99.978
parrallel	99.994	99.995	99.994	99.995	99.995	99.995	99.991	99.994	99.994
lshape	99.897	99.877	99.862	99.879	99.864	99.856	99.865	99.855	99.849
triangle	99.957	99.984	99.983	99.994	99.985	99.984	99.993	99.989	99.984
square_ml	99.593	99.74	99.592	99.814	99.843	99.814	99.592	99.74	99.593
branched_ml	99.028	99.922	99.97	99.609	99.318	99.854	99.947	99.066	99.761
parrallel_ml	99.986	99.987	99.986	99.908	99.929	99.908	99.986	99.987	99.986
lshape_ml	99.283	99.738	99.755	99.626	99.564	99.5	99.574	99.445	99.382
triangle_ml	1.178	99.789	99.865	99.443	95.178	99.768	99.542	98.69	98.771
square_ll	98.982	99.543	98.965	99.703	99.446	99.703	98.965	99.542	98.982
branched_ll	85.424	98.835	99.656	91.872	93.365	98.731	99.223	91.823	98.514
parrallel_ll	99.83	99.746	99.824	99.443	99.511	99.446	99.83	99.746	99.824
lshape_ll	96.616	99.408	99.818	99.075	99.277	99.309	99.334	99.078	99.058
triangle_ll	0.0	98.077	97.851	93.529	78.081	96.75	96.21	88.005	88.928

Table B.1: EVP values of the different synthetic models at the location of the validation points in [%].

C

Case study results

In this appendix the results for the case study The Pannenhoef are shown. For each observation well the response function used for calibration is shown, next, the observed head in the well, the Pastas simulation and the conceptual model simulation for the well are shown. The simulated groundwater head of conceptual model at the location of each observation well is shown. For these locations the fluctuations of the simulations and observations are displayed.

Well B50A0488001

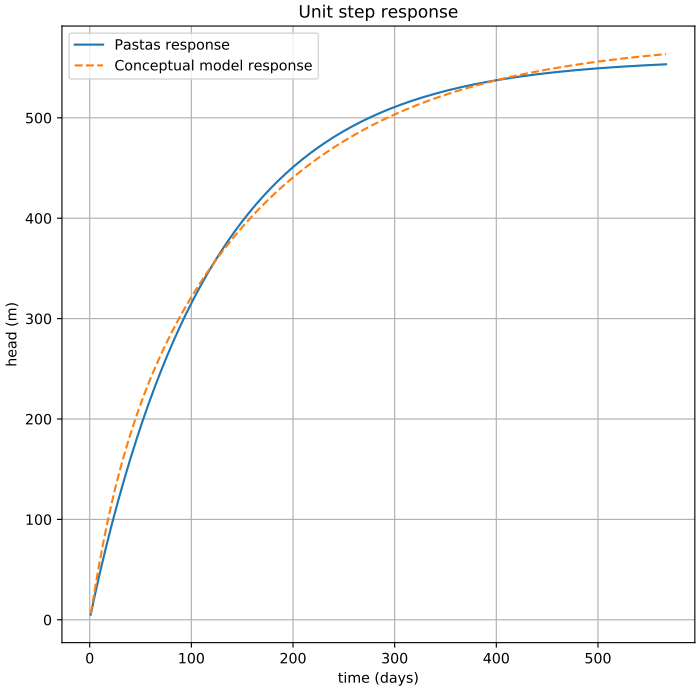

Figure C.1: The calibration result of the conceptual model to the Pastas step response of well B50A0488001

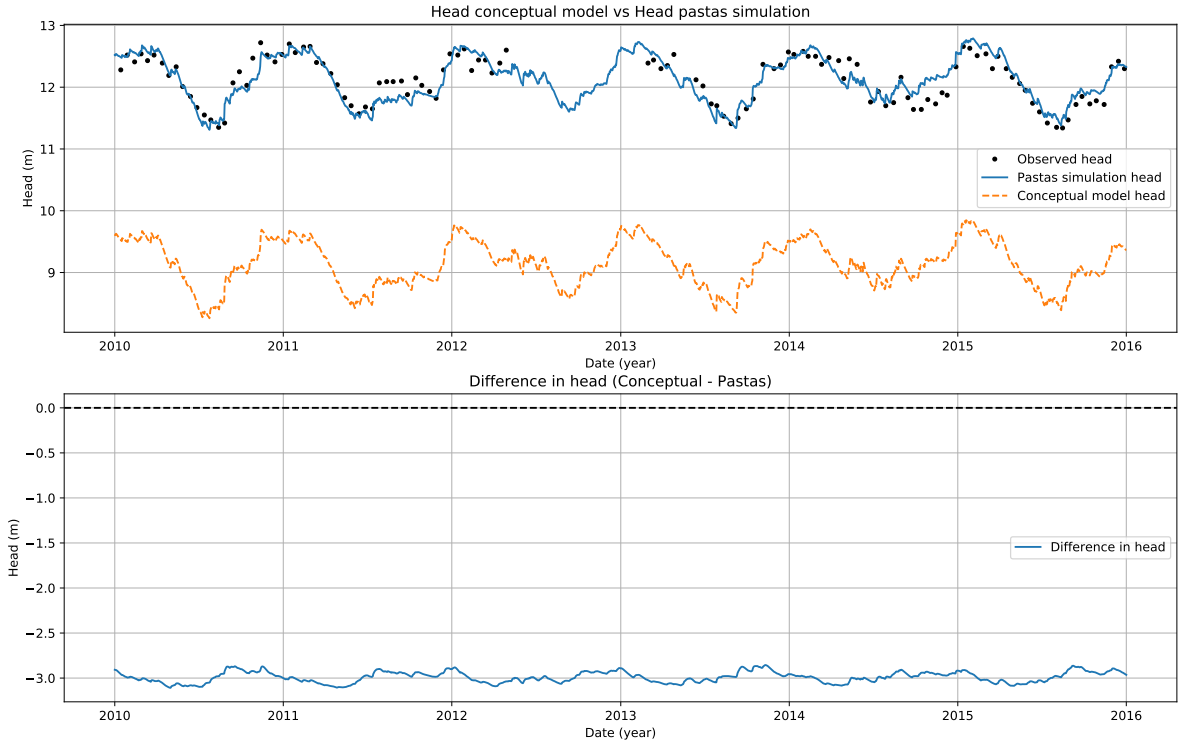

Figure C.2: Simulated head in well B50A0488001, compared with the observations and the time series simulation

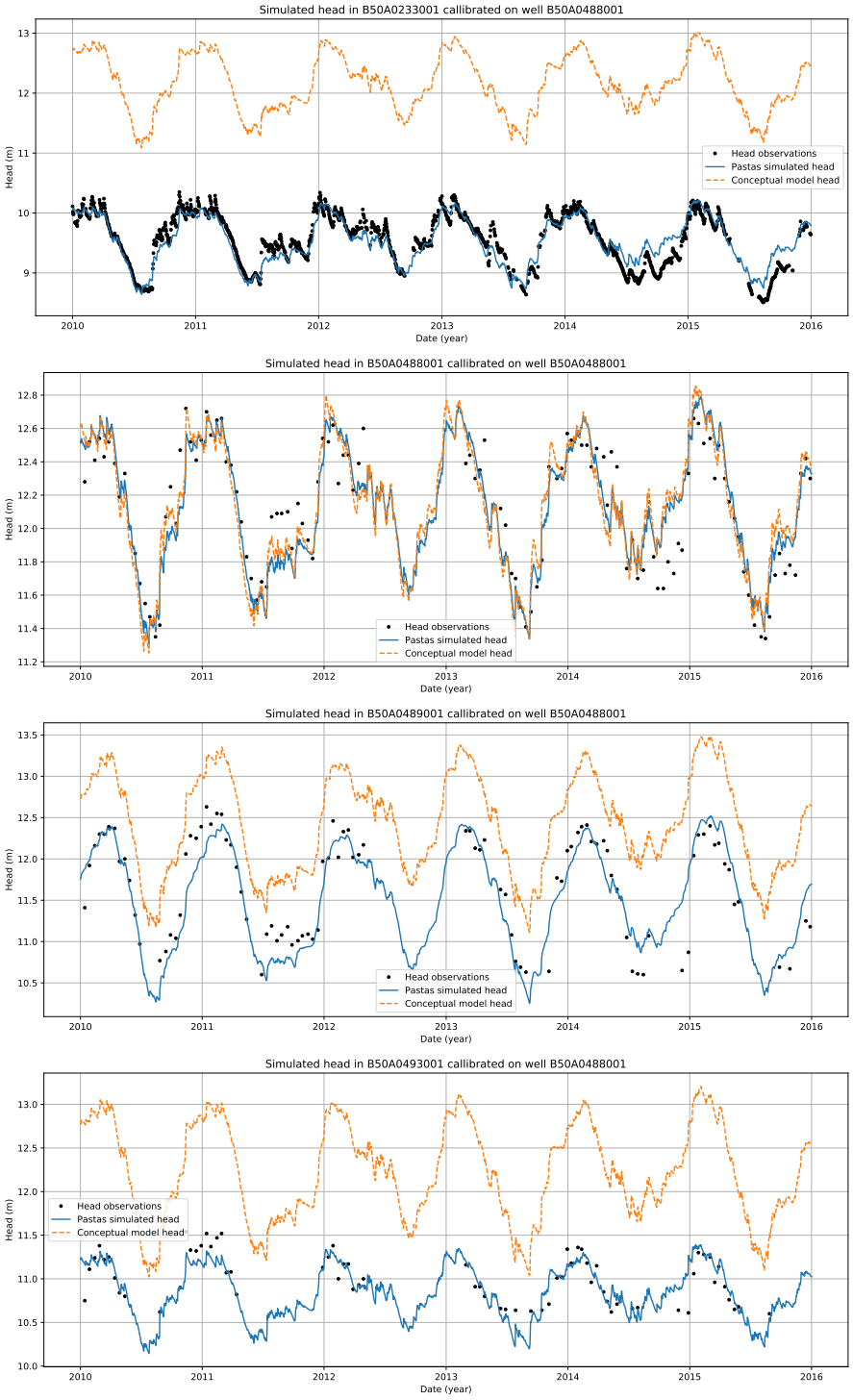

Figure C.3: The conceptual model simulation of well at the observations wells calibrated on well B50A0488001

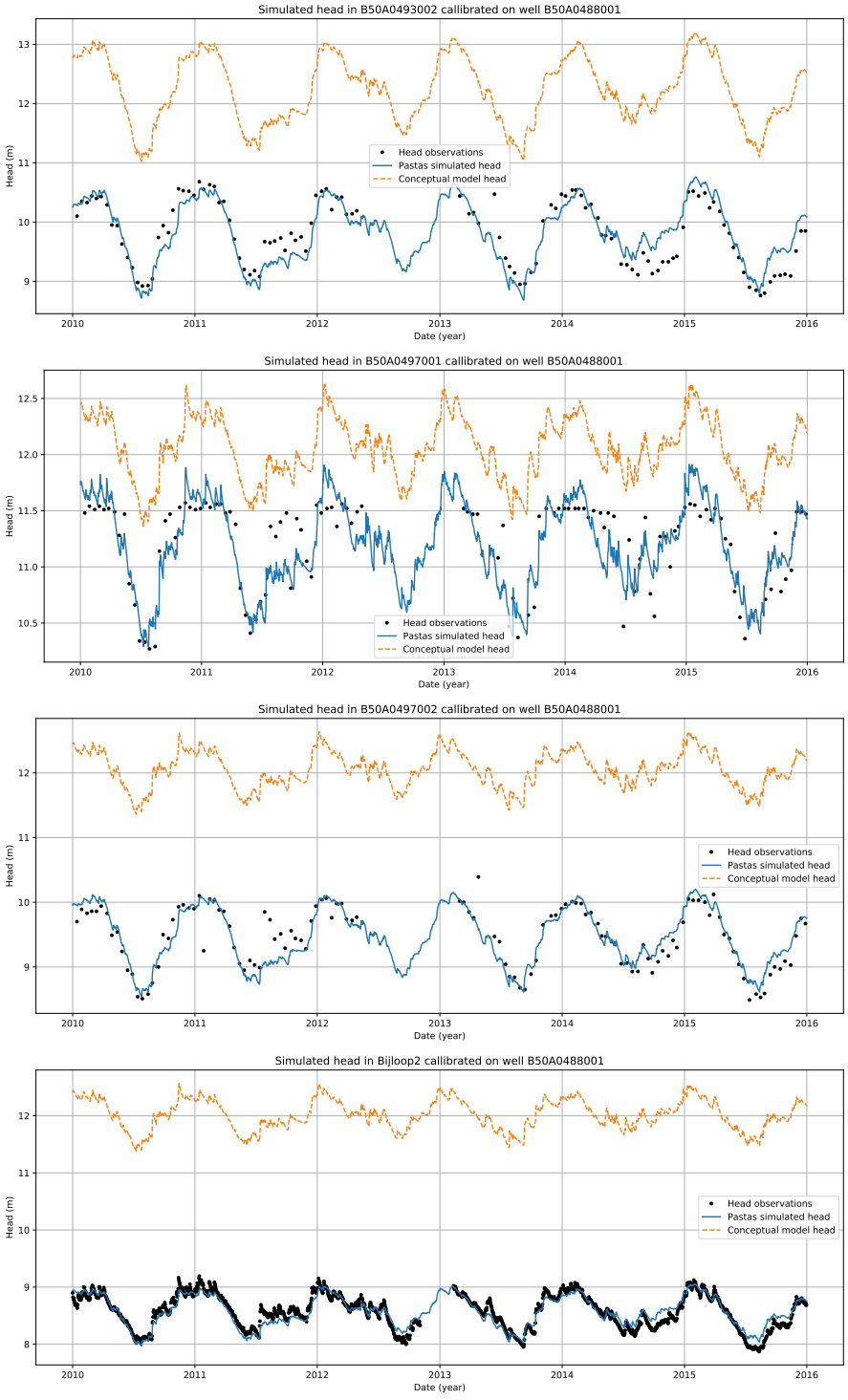

Figure C.3: Continued: The conceptual model simulation at the observations wells calibrated on well B50A0488001

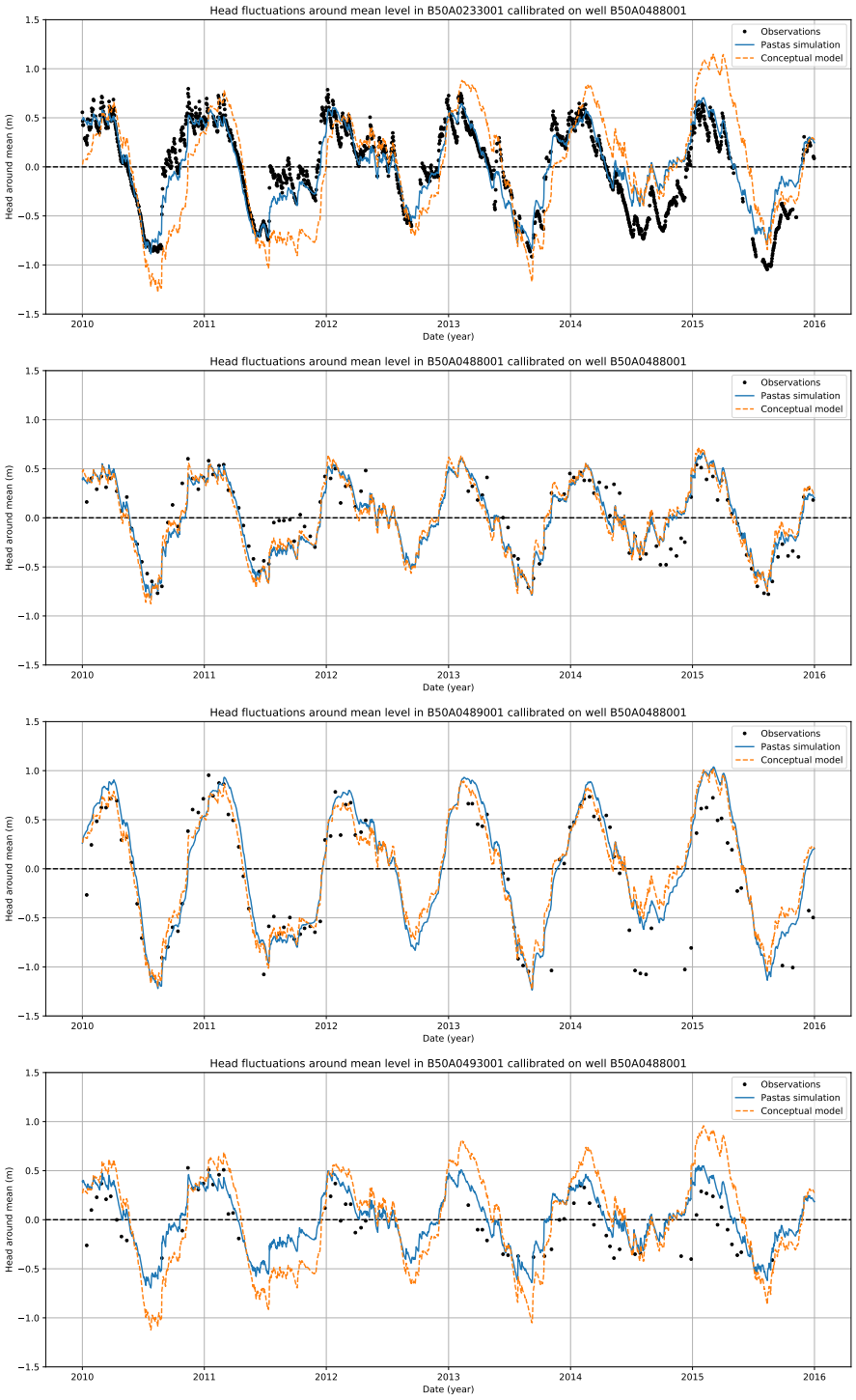

Figure C.4: Fluctuations of the observations, Pastas simulation and conceptual model simulation in well B50A0488001

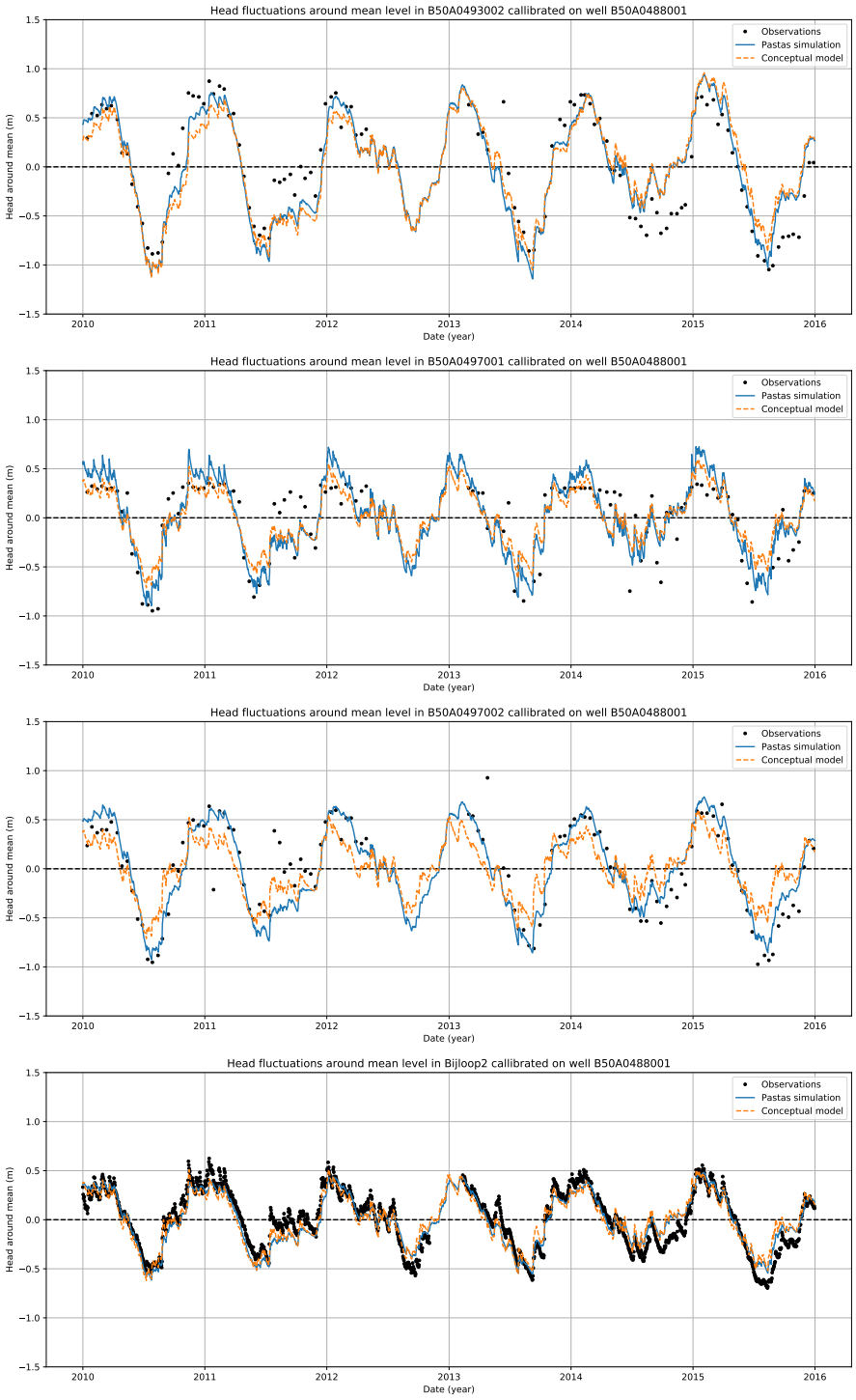

Figure C.4: Continued: Fluctuations of the observations, Pastas simulation and conceptual model simulation in well B50A0488001

Well B50A0489001

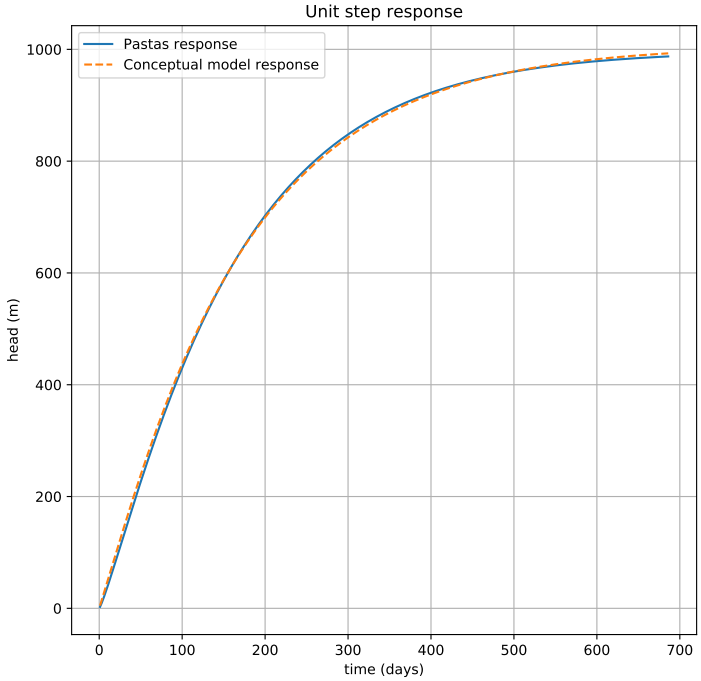

Figure C.5: The calibration result of the conceptual model to the Pastas step response of well B50A0489001

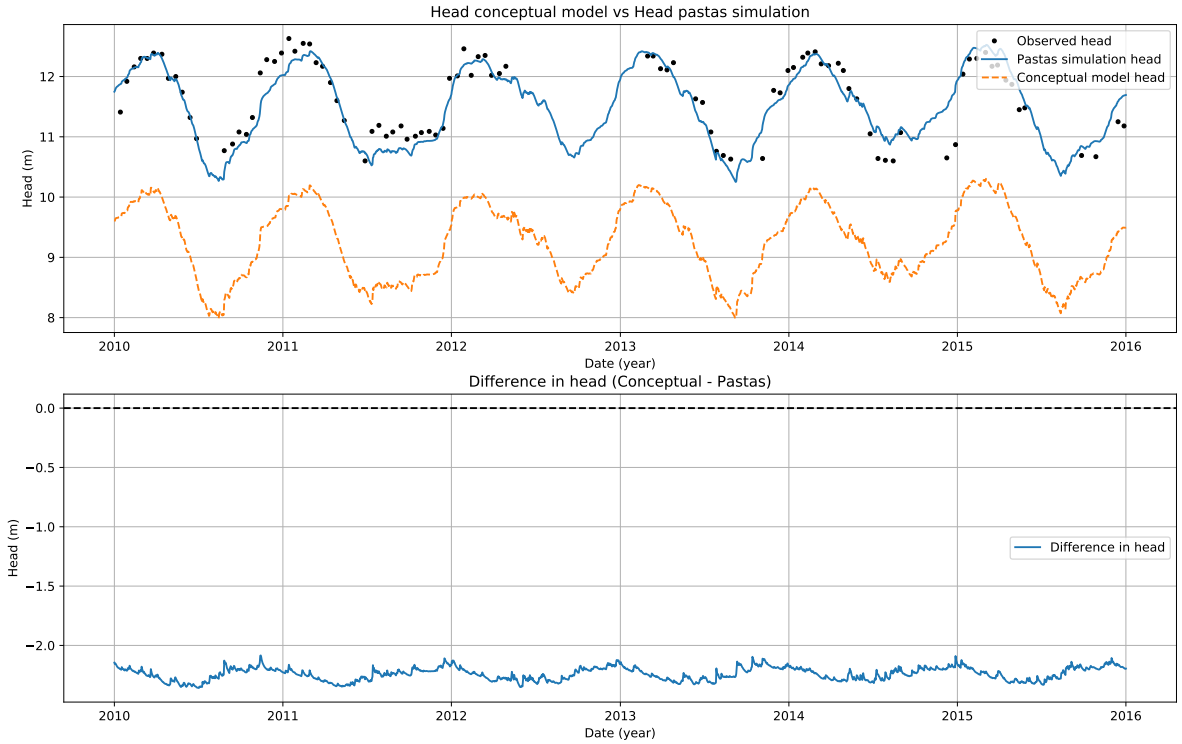

Figure C.6: Simulated head in well B50A0489001, compared with the observations and the time series simulation

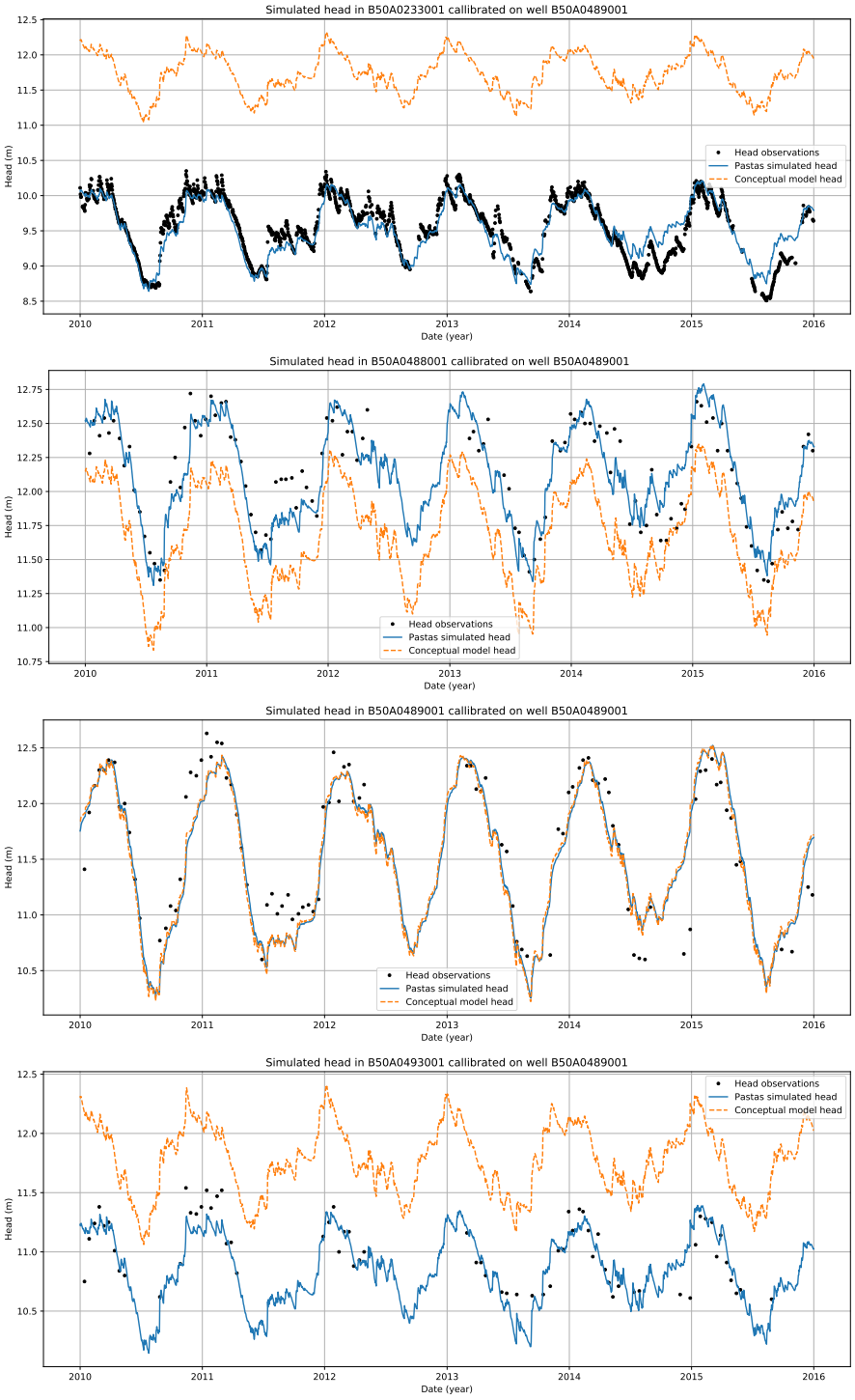

Figure C.7: The conceptual model simulation of well at the observations wells calibrated on well B50A0489001

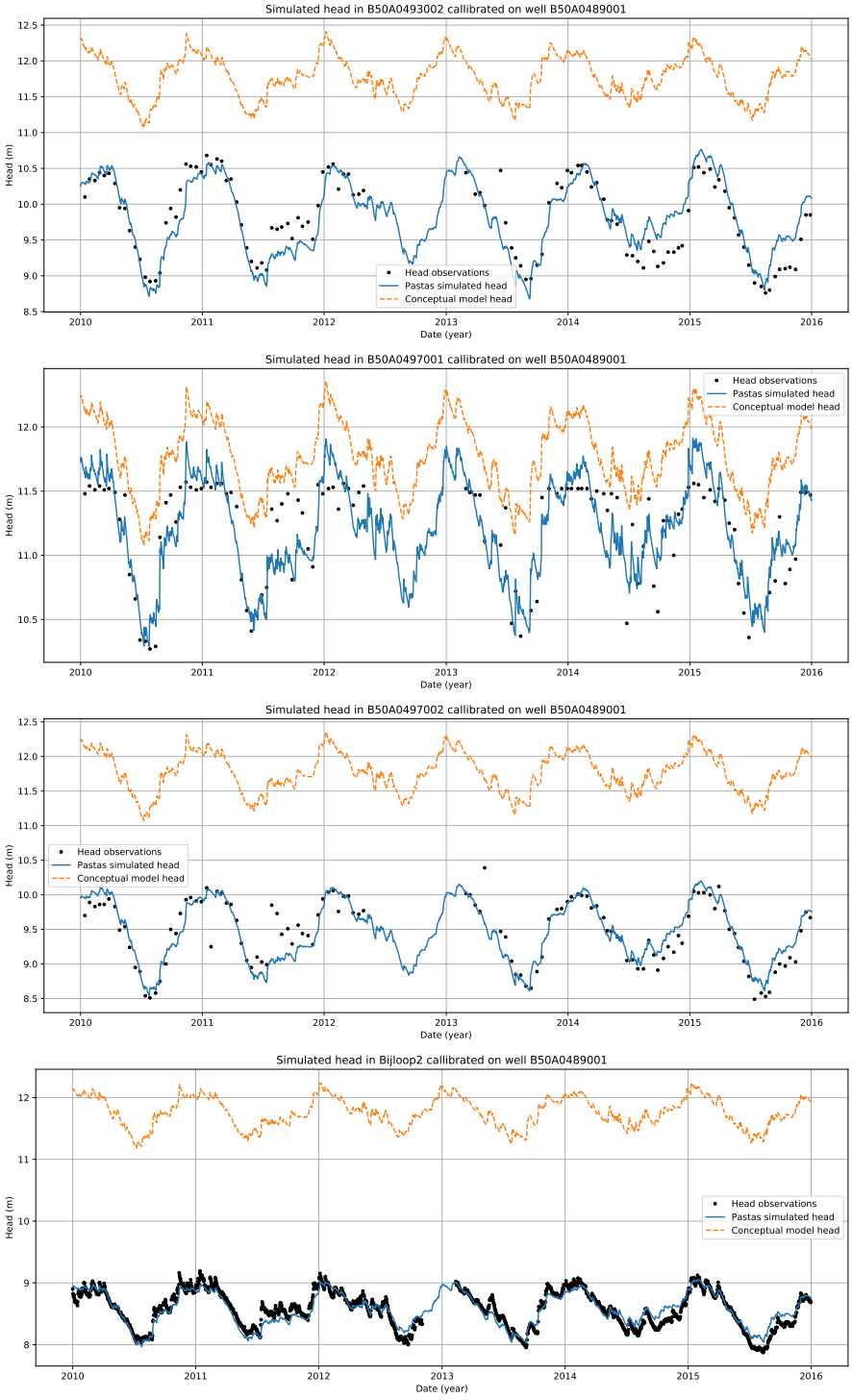

Figure C.7: Continued: The conceptual model simulation at the observations wells calibrated on well B50A0489001

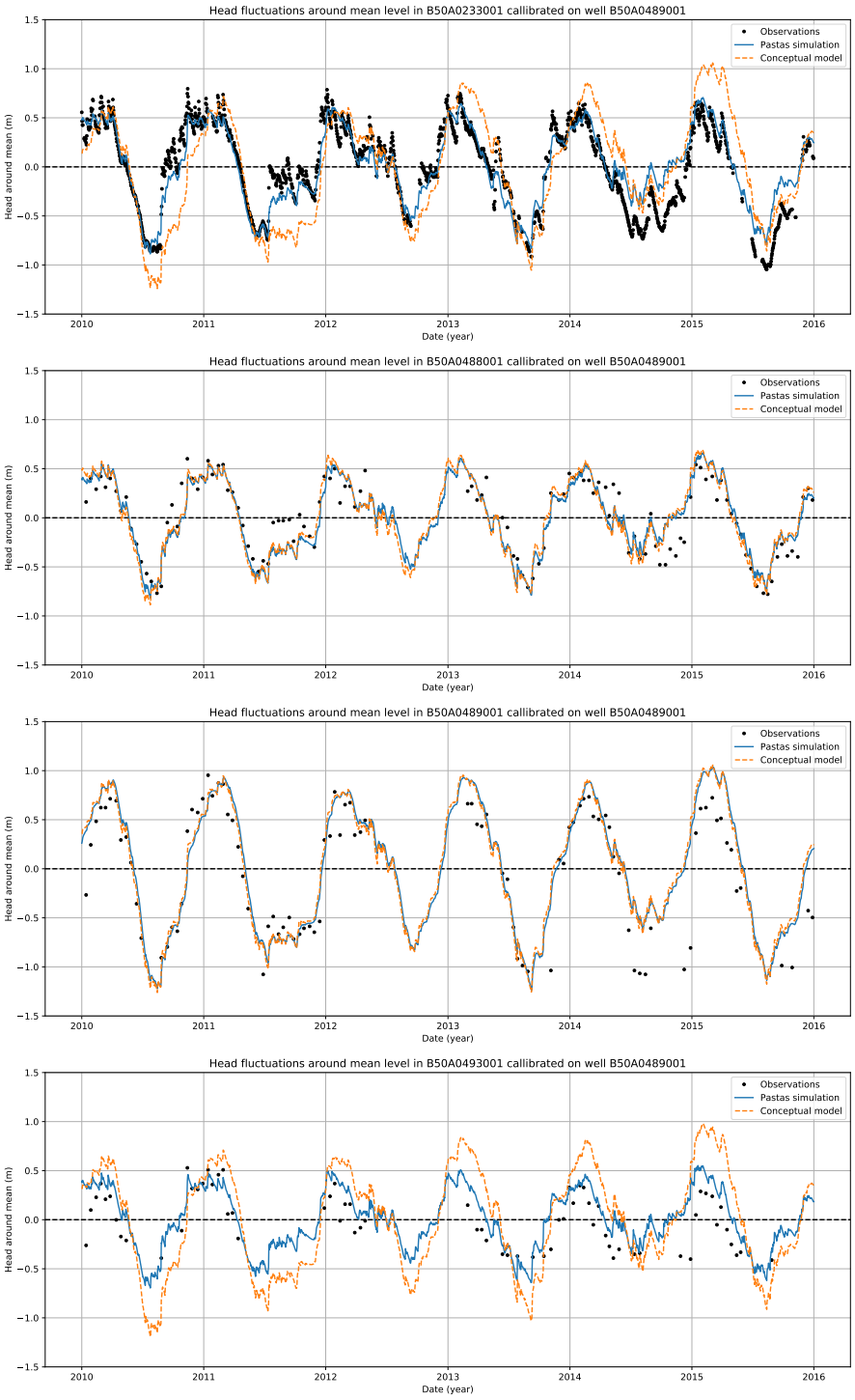

Figure C.8: Fluctuations of the observations, Pastas simulation and conceptual model simulation in well B50A0489001

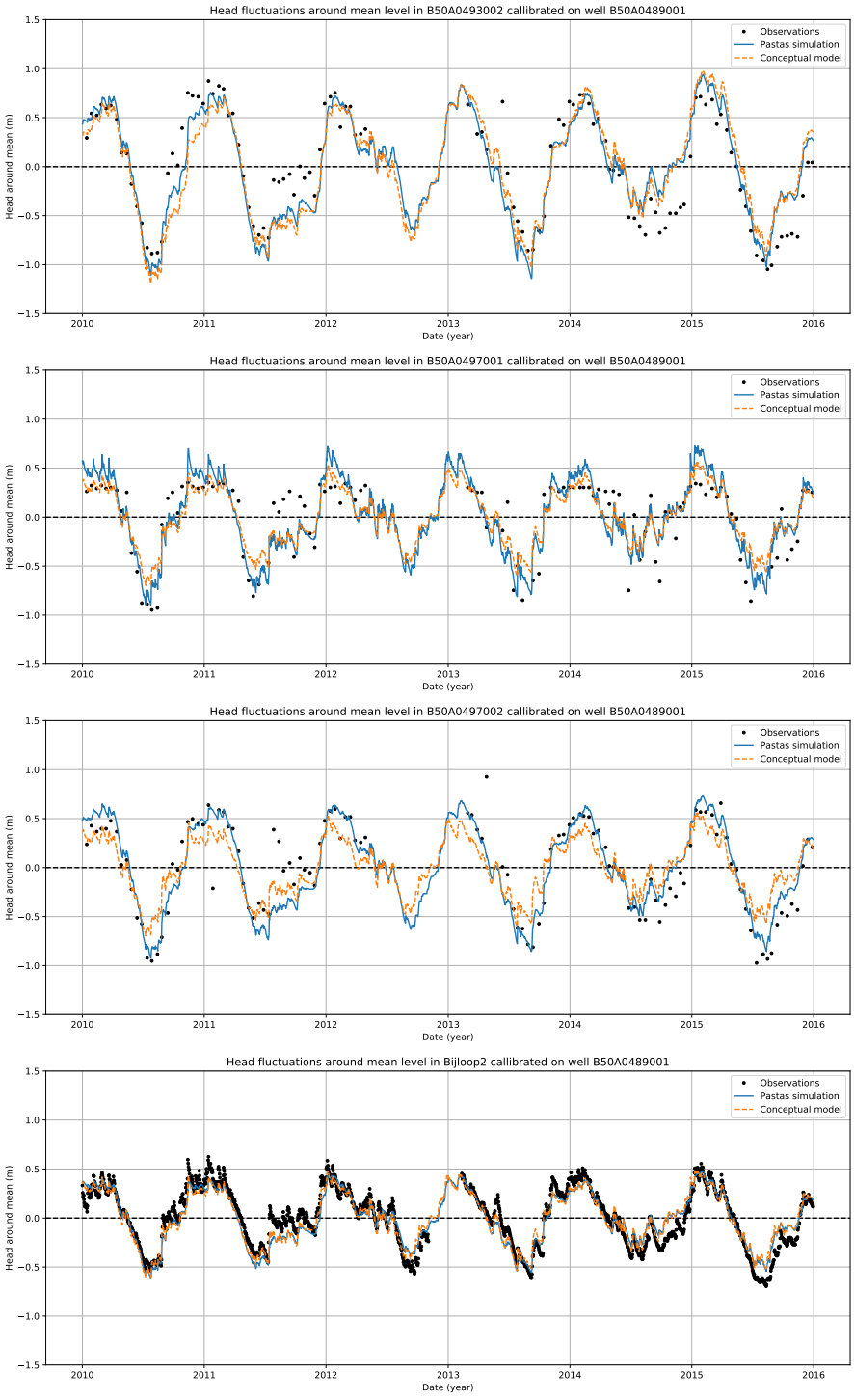

Figure C.8: Continued: Fluctuations of the observations, Pastas simulation and conceptual model simulation in well B50A0489001

Well B50A0493001

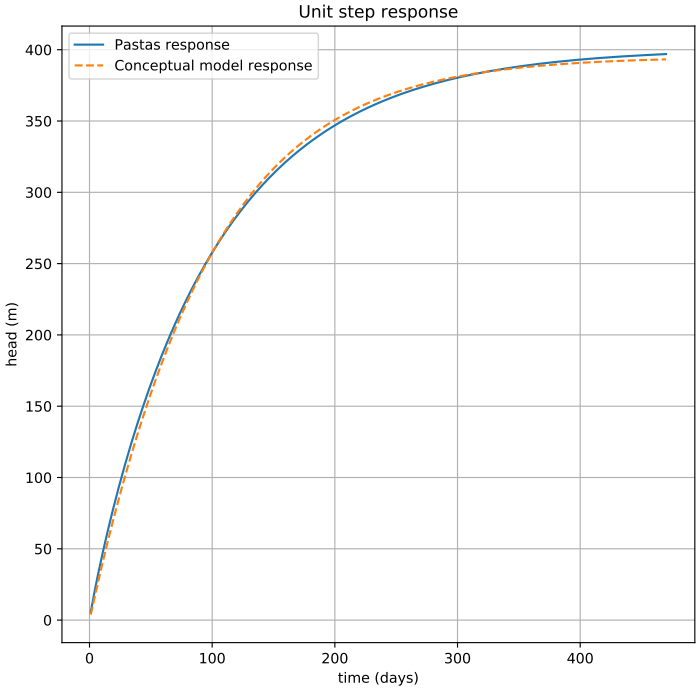

Figure C.9: The calibration result of the conceptual model to the Pastas step response of well B50A0493001

Figure C.10: Simulated head in well B50A0493001, compared with the observations and the time series simulation

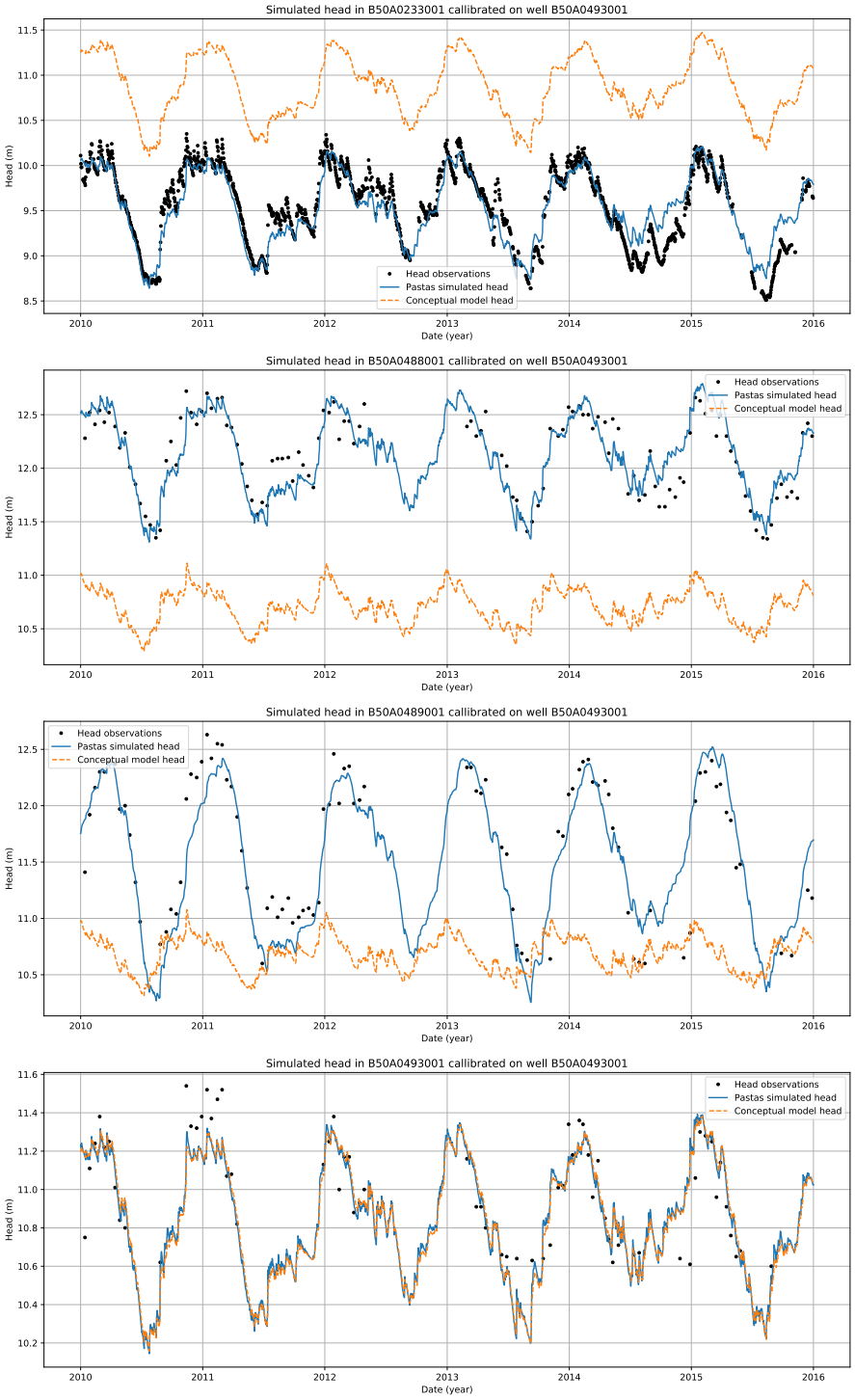

Figure C.11: The conceptual model simulation of well at the observations wells calibrated on well B50A0493001

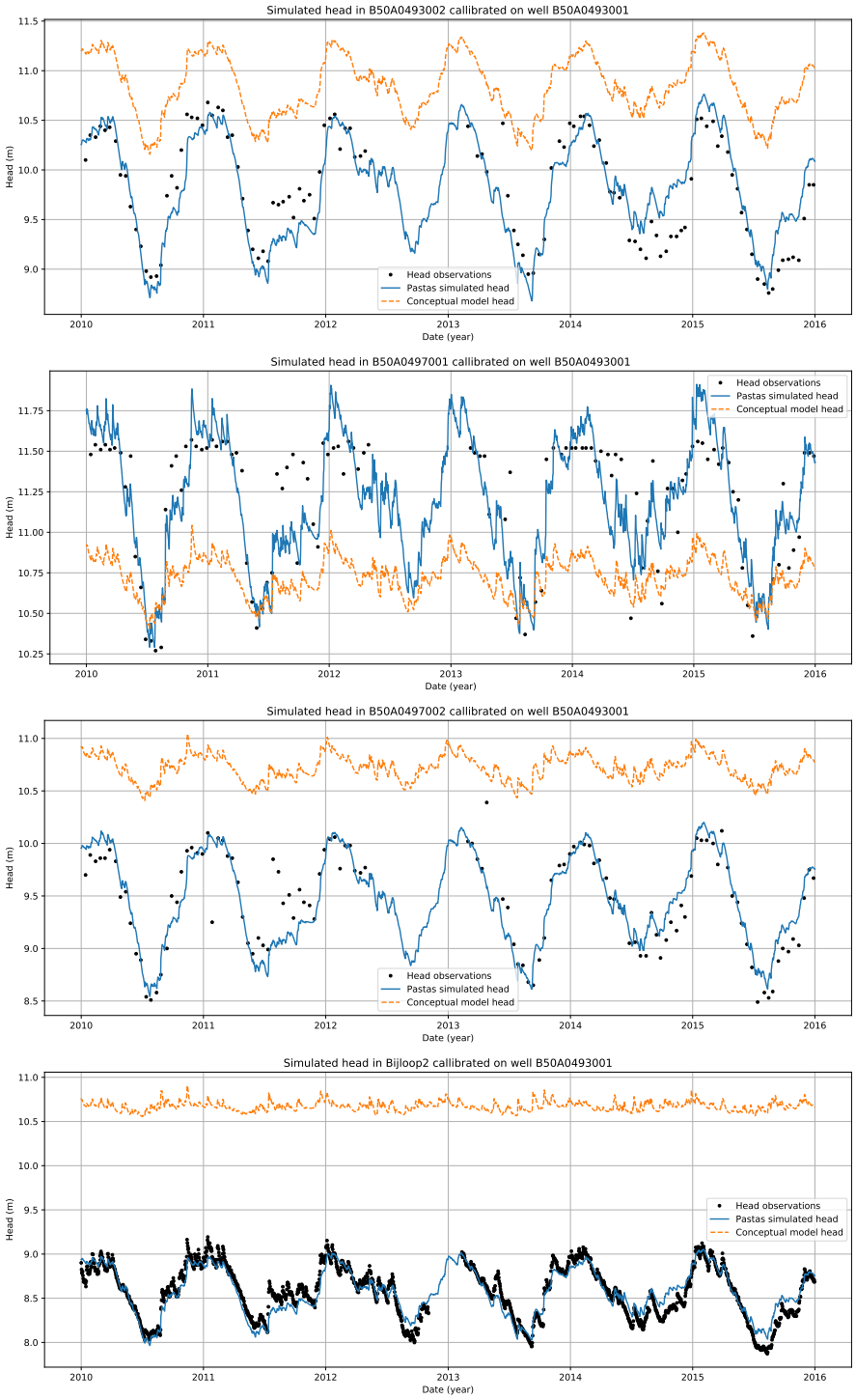

Figure C.11: Continued: The conceptual model simulation at the observations wells calibrated on well B50A0493001

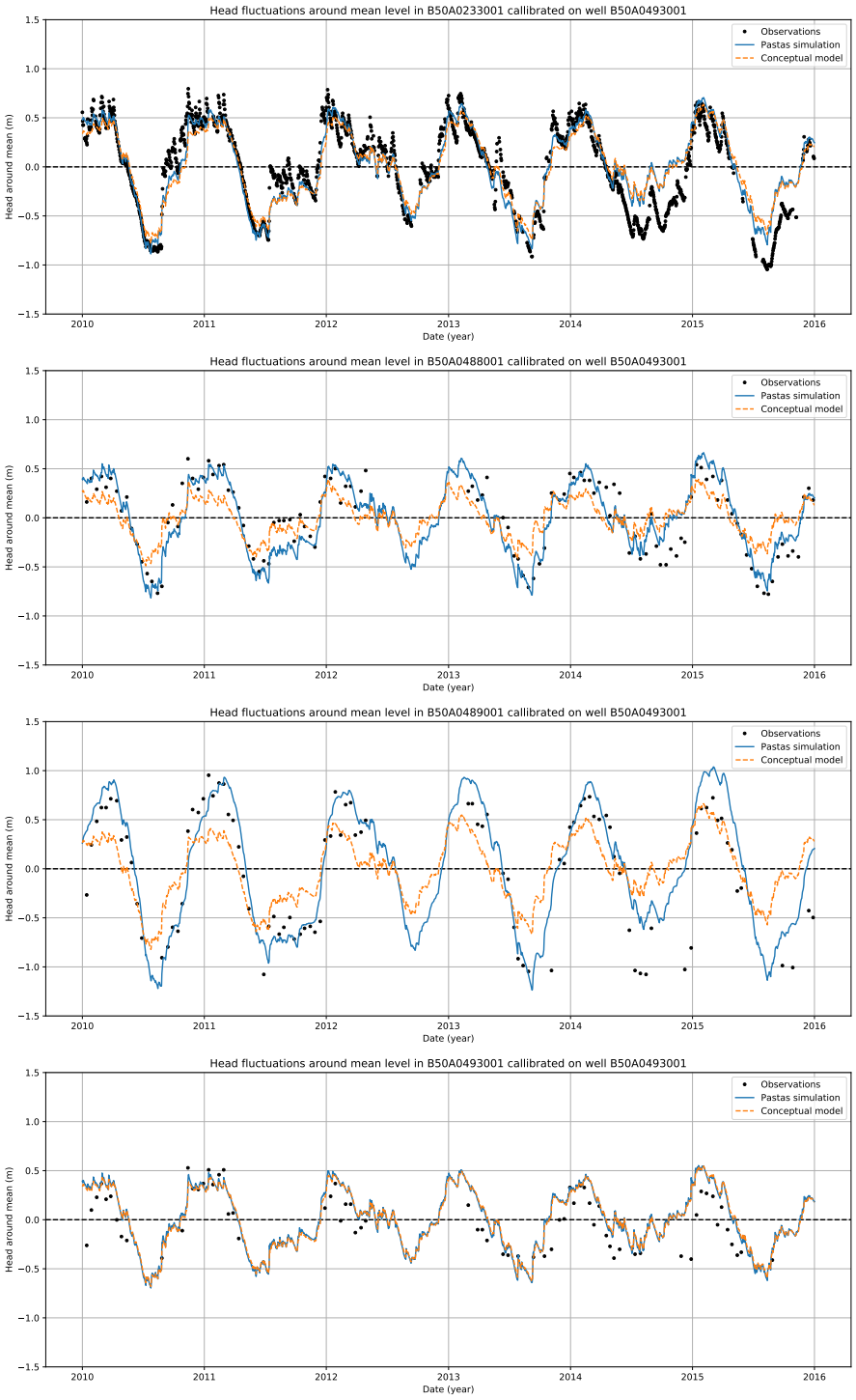

Figure C.12: Fluctuations of the observations, Pastas simulation and conceptual model simulation in well B50A0493001

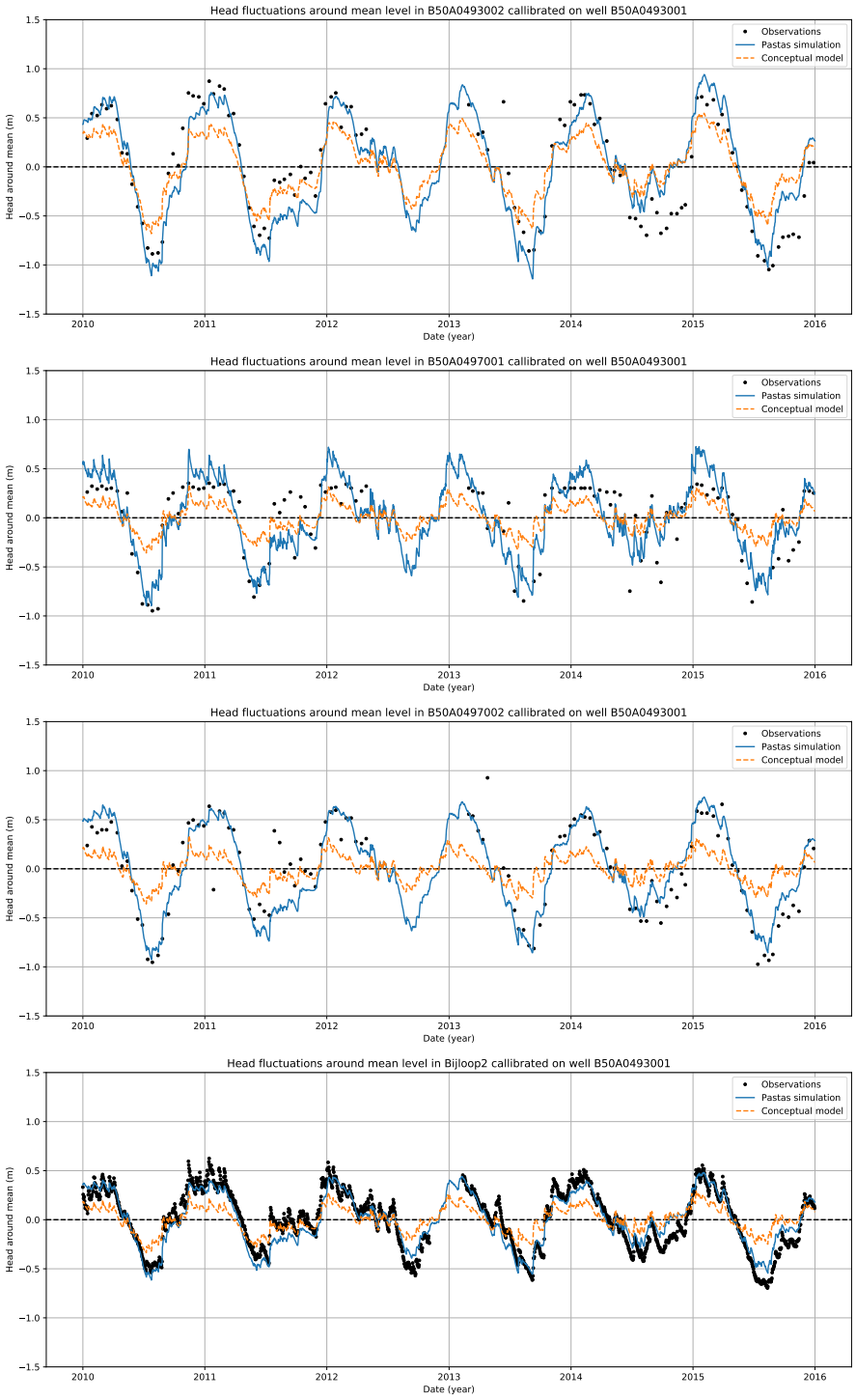

Figure C.12: Continued: Fluctuations of the observations, Pastas simulation and conceptual model simulation in well B50A0493001

Well B50A0493002

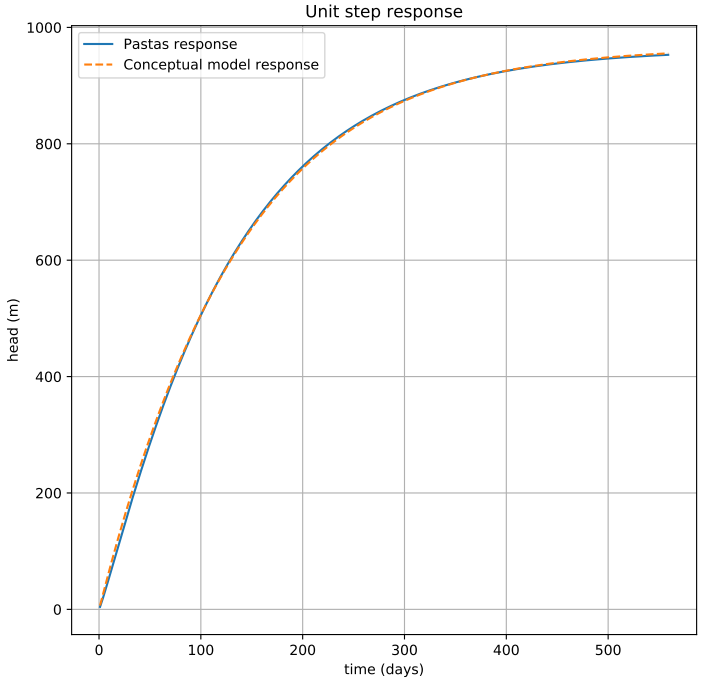

Figure C.13: The calibration result of the conceptual model to the Pastas step response of well B50A0493002

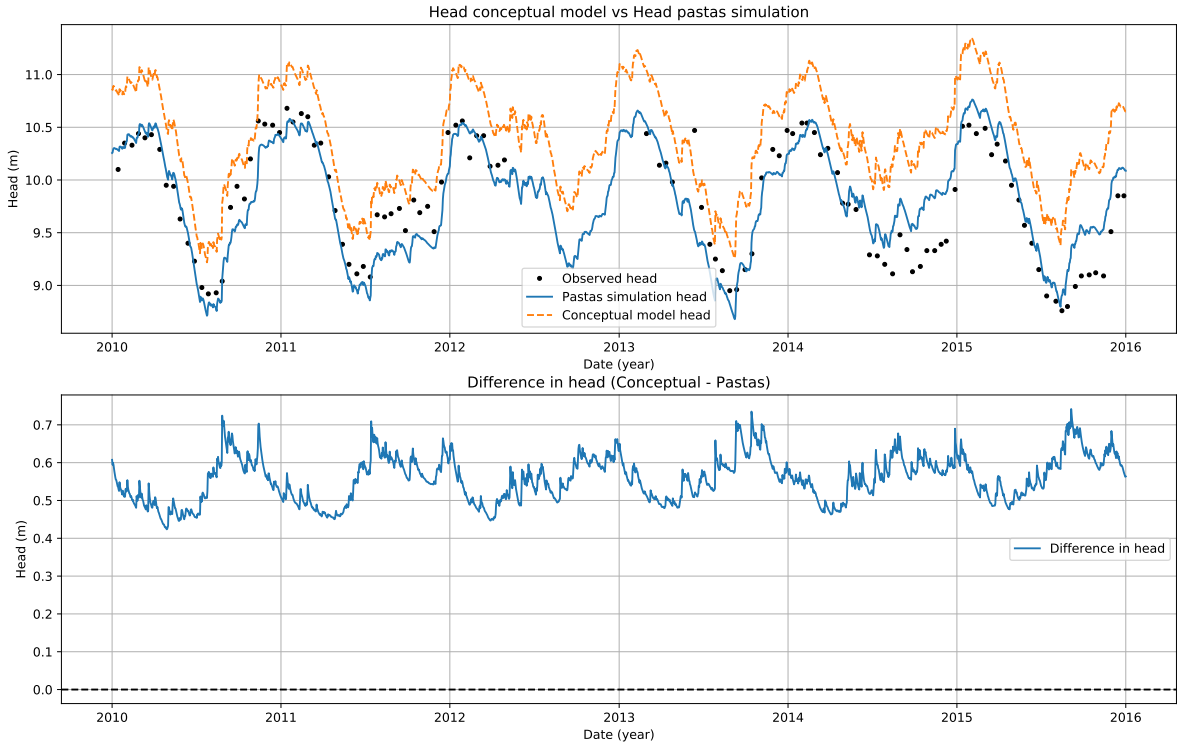

Figure C.14: Simulated head in well B50A0493002, compared with the observations and the time series simulation

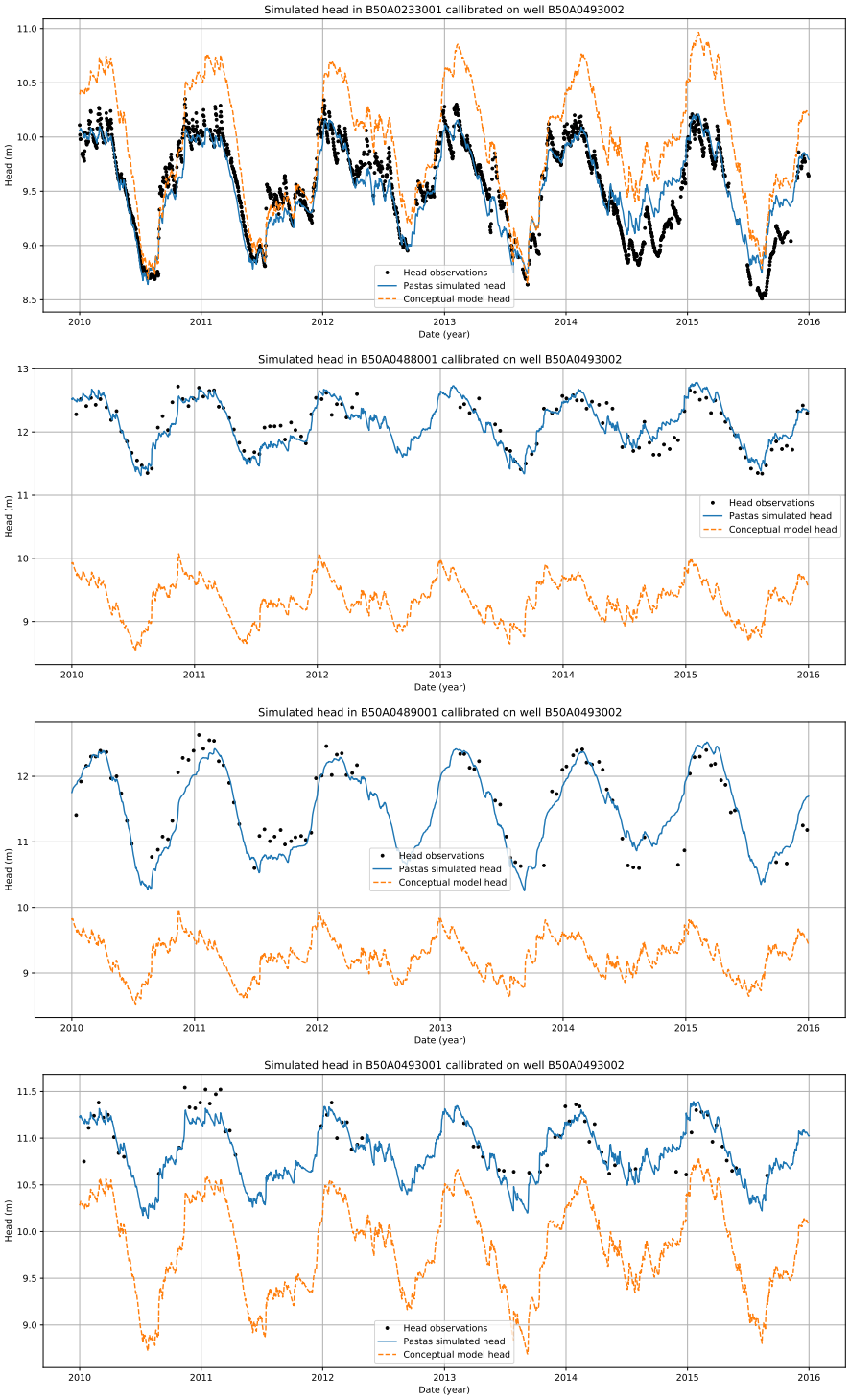

Figure C.15: The conceptual model simulation of well at the observations wells calibrated on well B50A0493002

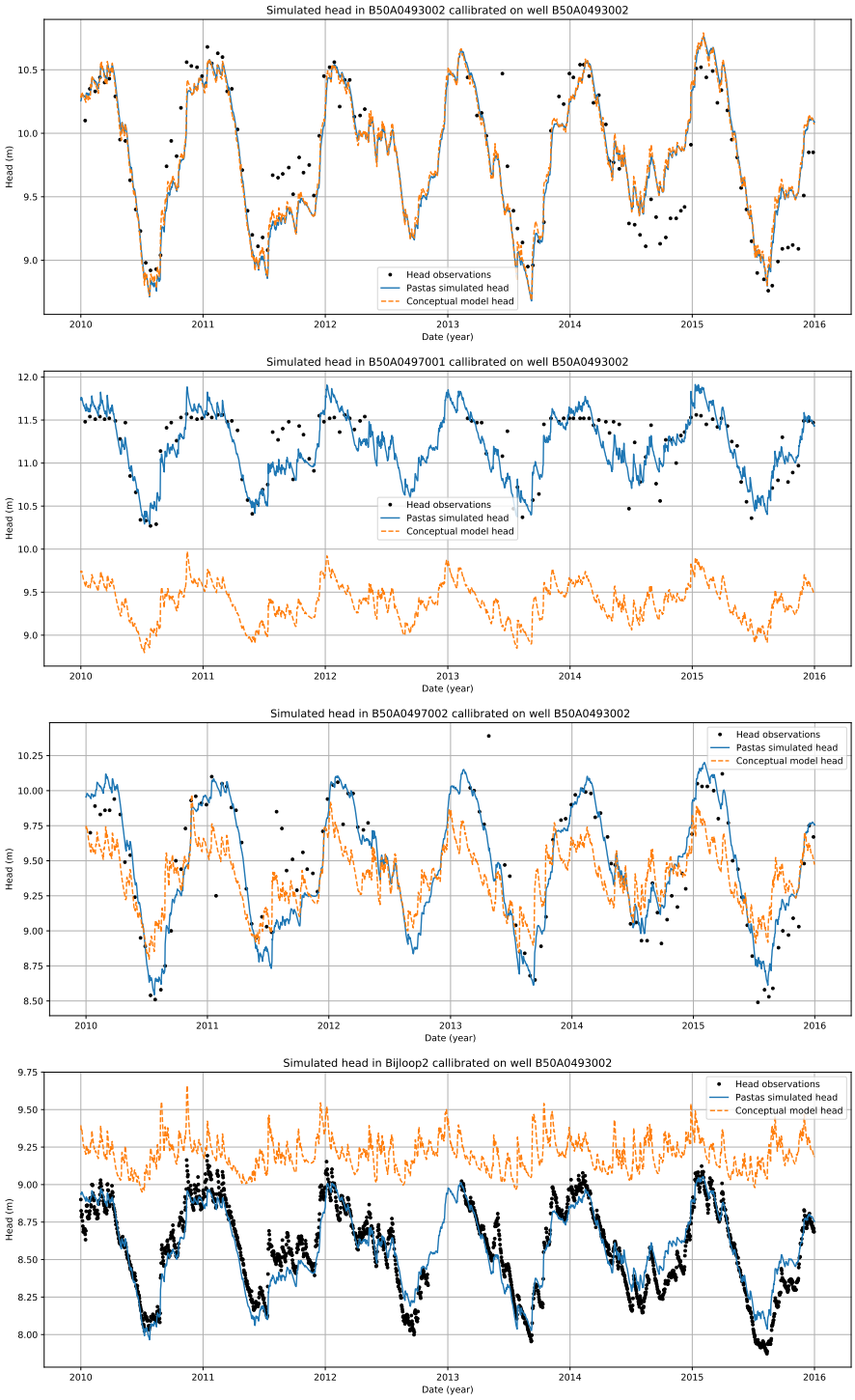

Figure C.15: Continued: The conceptual model simulation at the observations wells calibrated on well B50A0493002

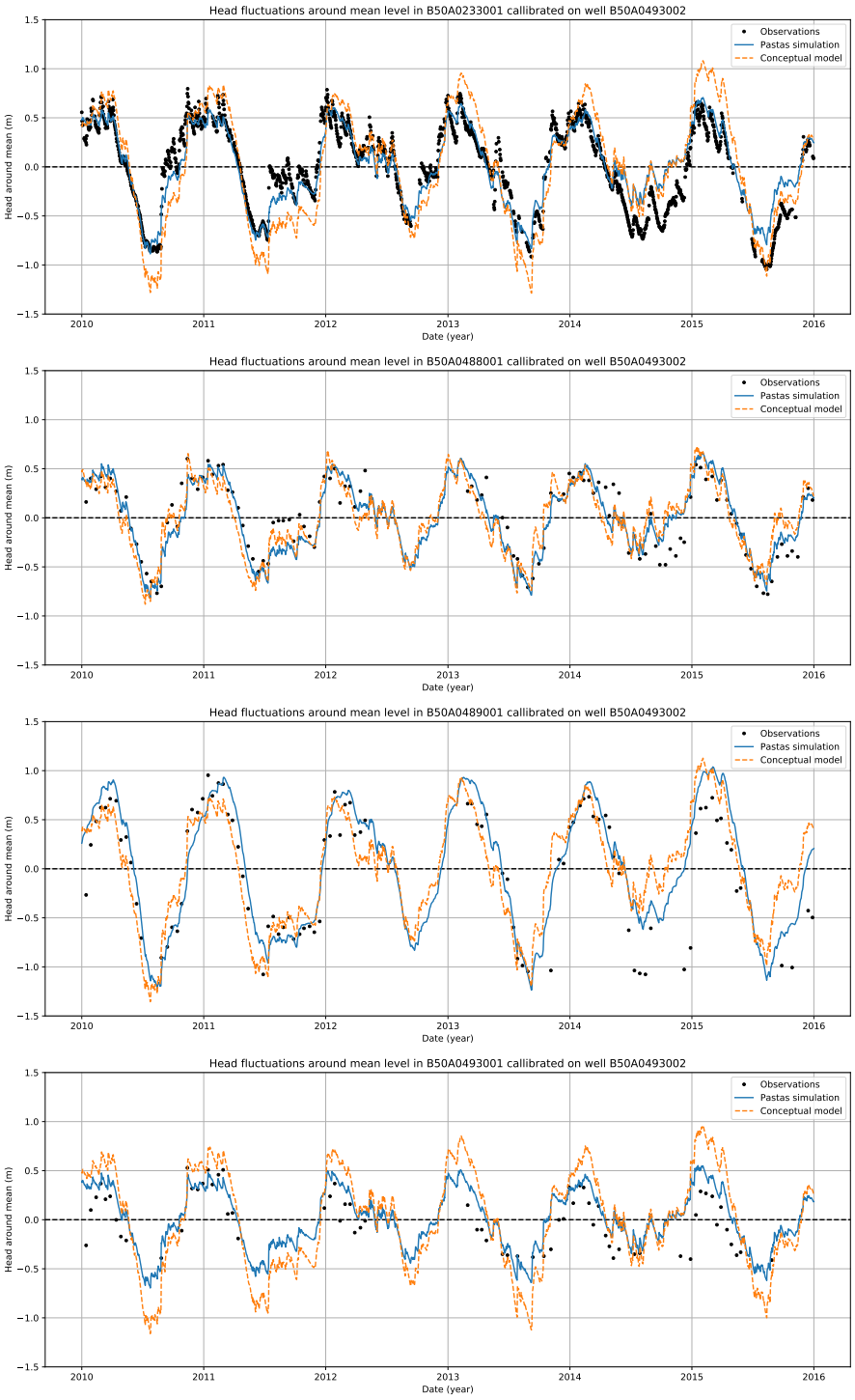

Figure C.16: Fluctuations of the observations, Pastas simulation and conceptual model simulation in well B50A0493002

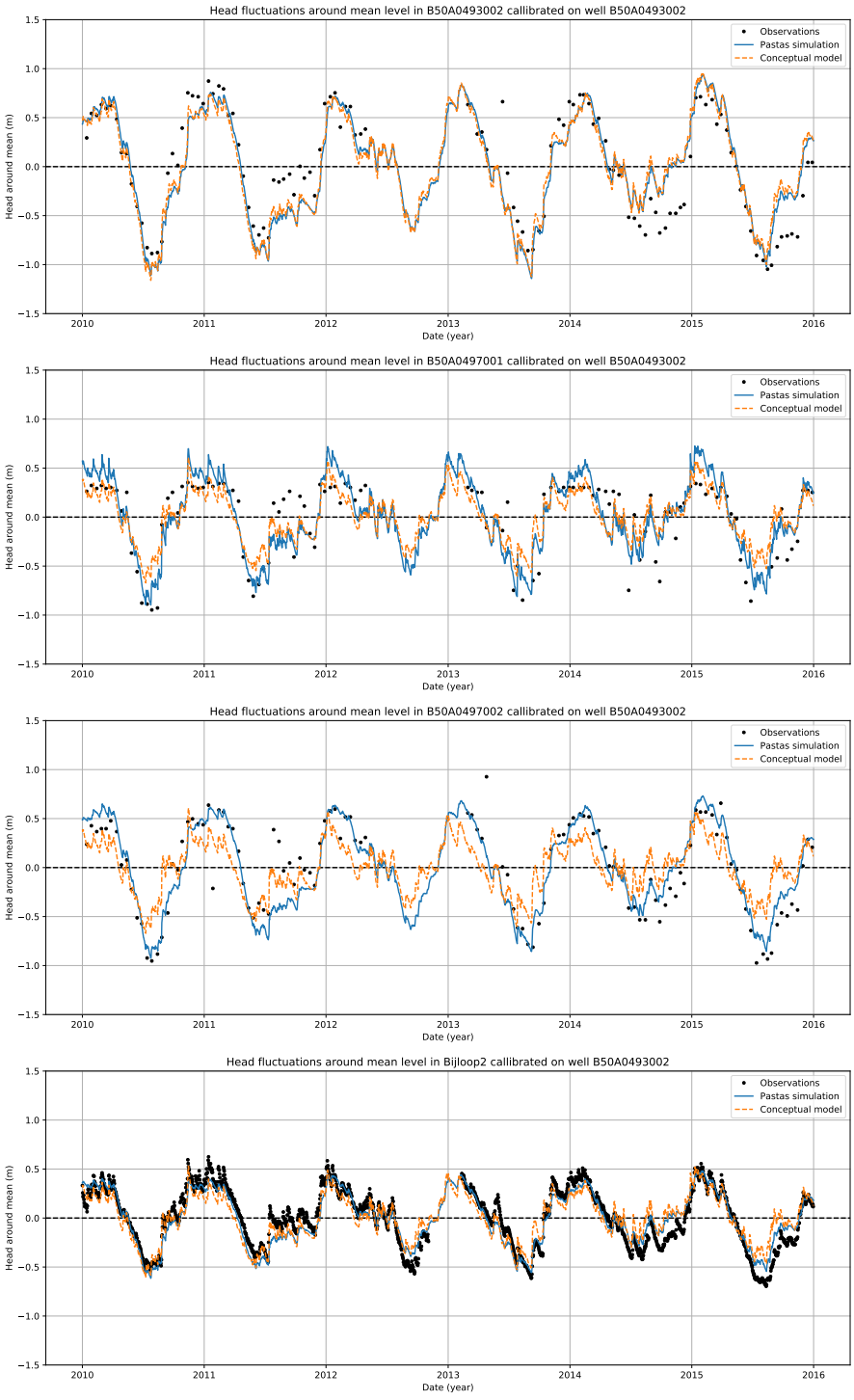

Figure C.16: Continued: Fluctuations of the observations, Pastas simulation and conceptual model simulation in well B50A0493002

Well B50A0497001

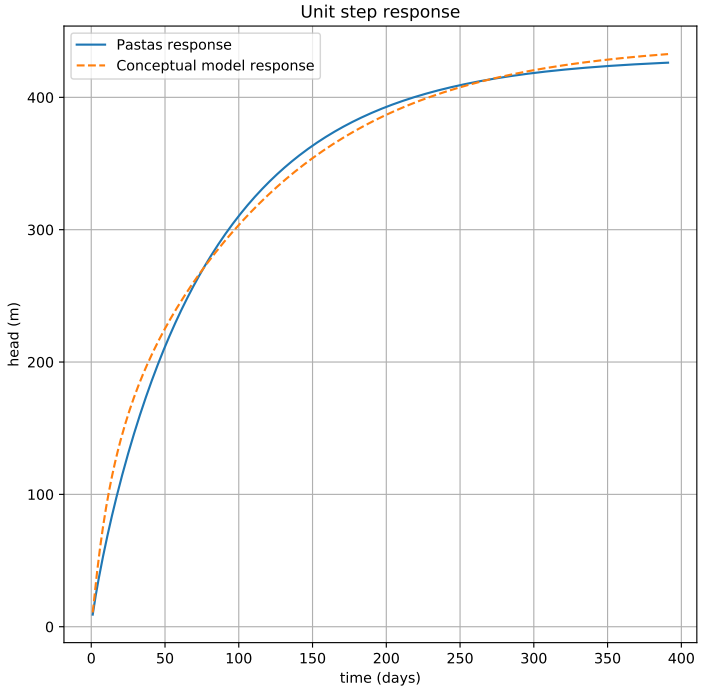

Figure C.17: The calibration result of the conceptual model to the Pastas step response of well B50A0497001

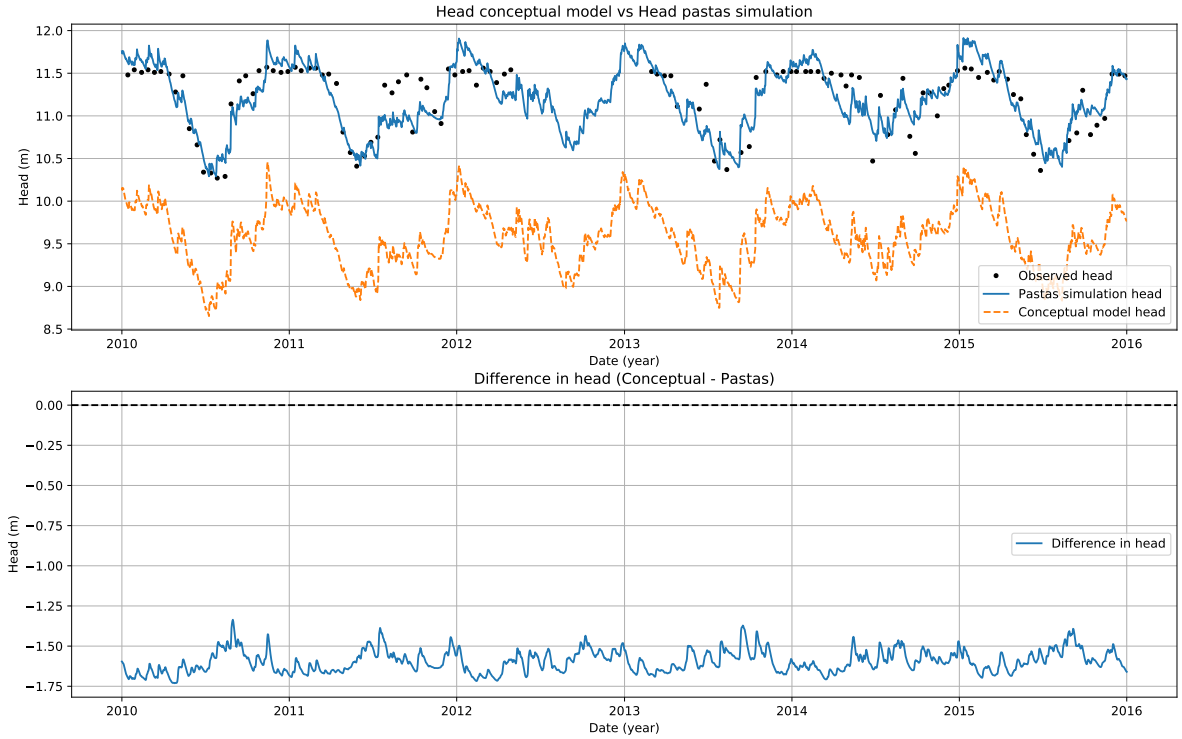

Figure C.18: Simulated head in well B50A0497001, compared with the observations and the time series simulation

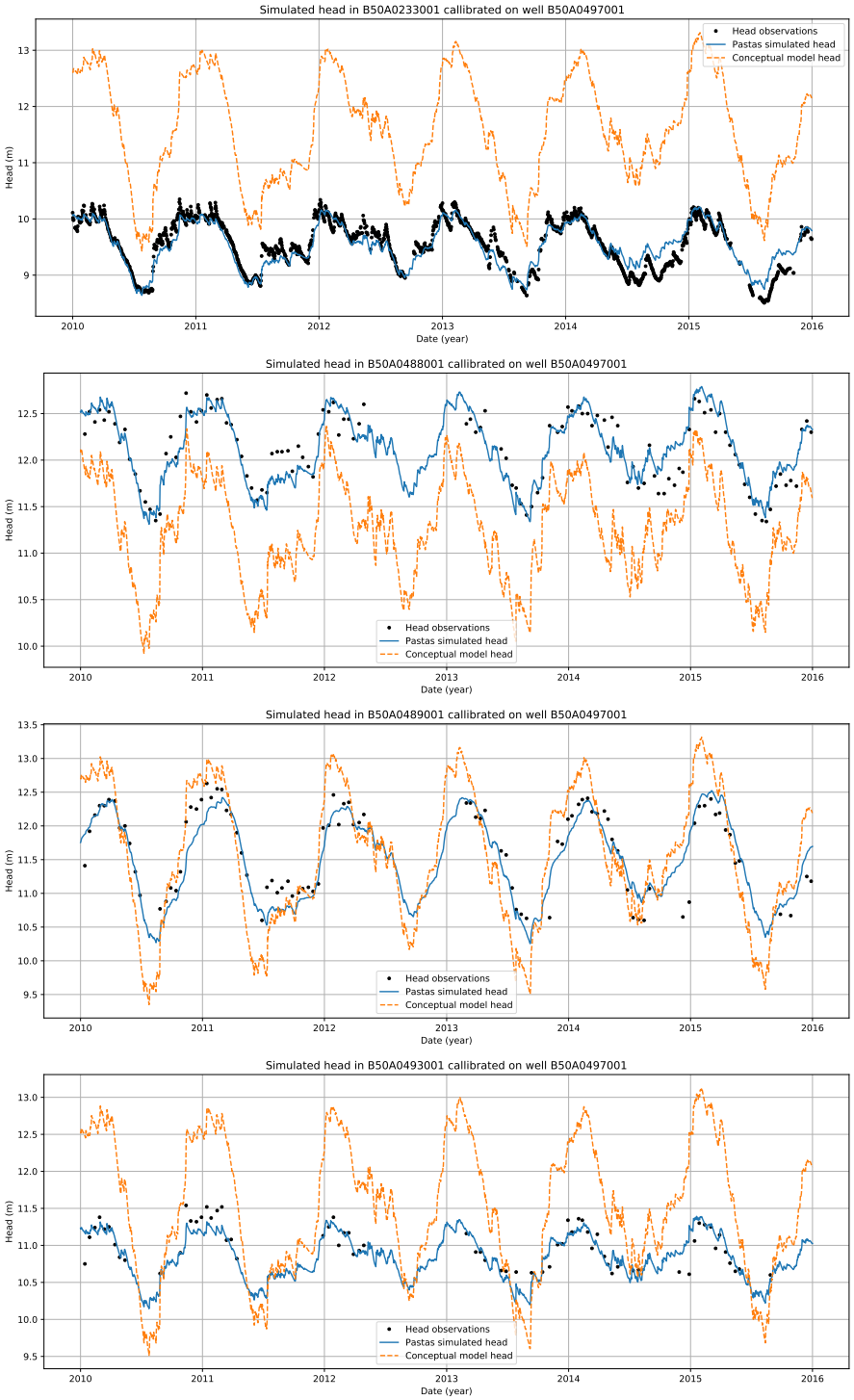

Figure C.19: The conceptual model simulation of well at the observations wells calibrated on well B50A0497001

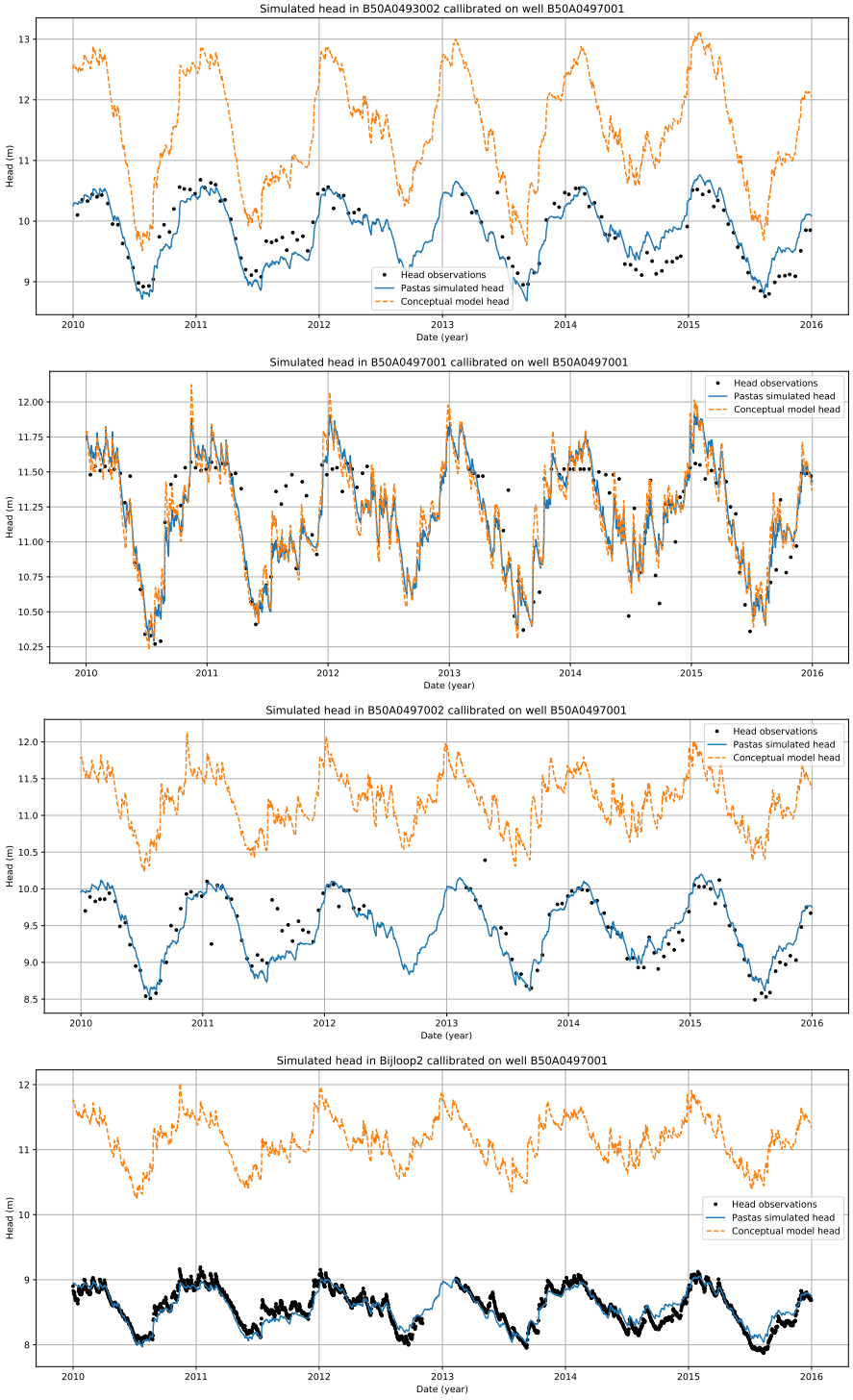

Figure C.19: Continued: The conceptual model simulation at the observations wells calibrated on well B50A0497001

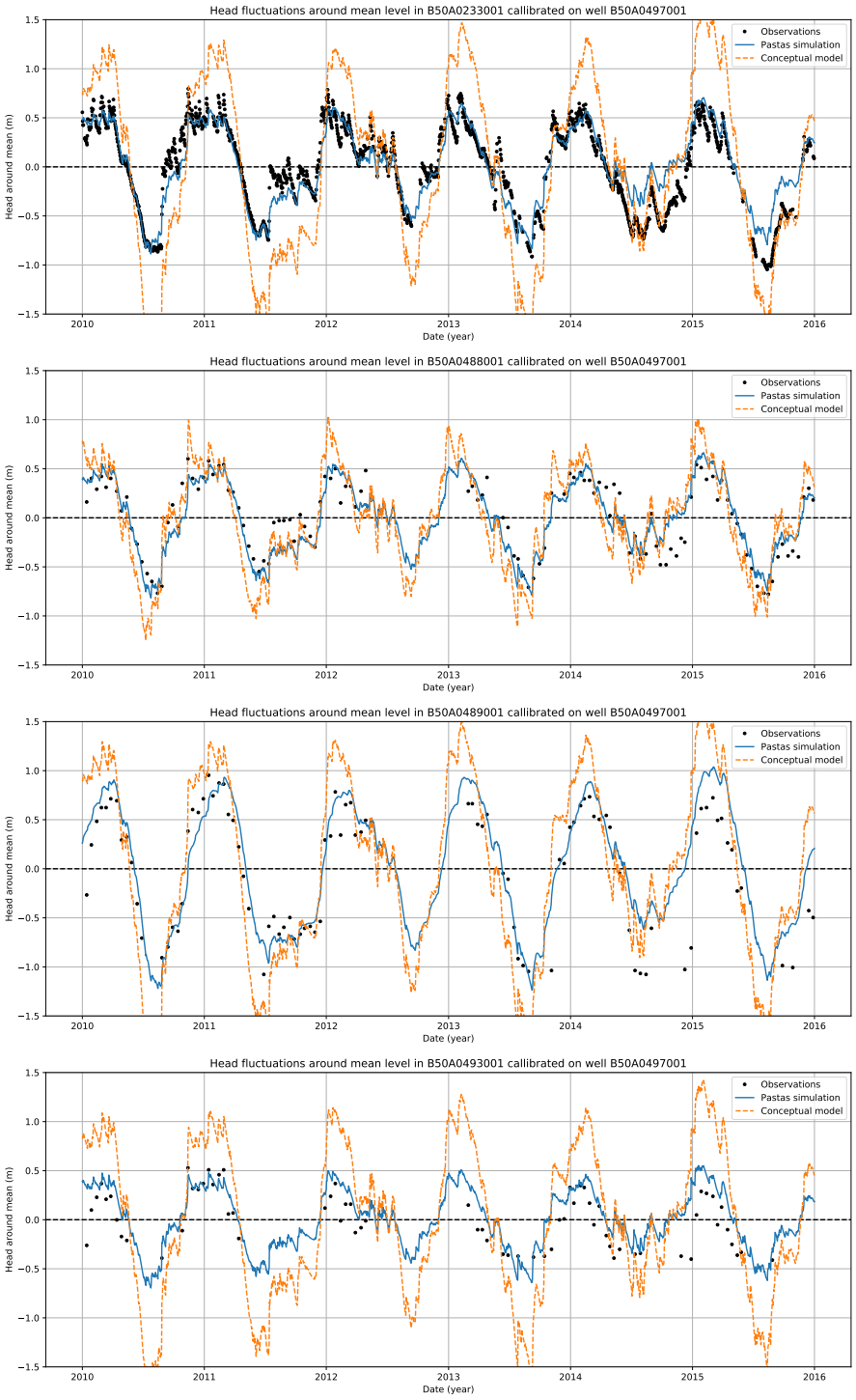

Figure C.20: Fluctuations of the observations, Pastas simulation and conceptual model simulation in well B50A0497001

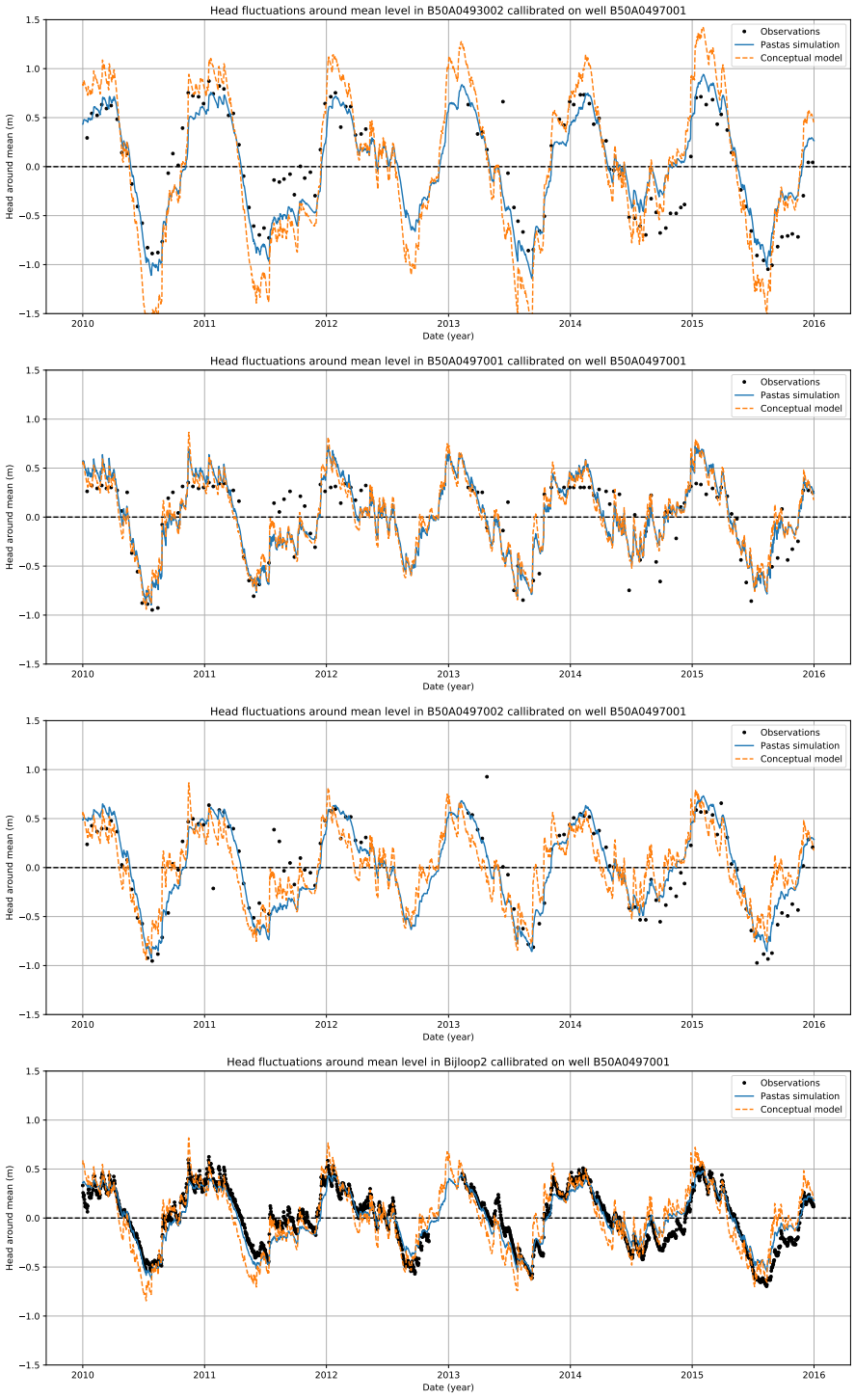

Figure C.20: Continued: Fluctuations of the observations, Pastas simulation and conceptual model simulation in well B50A0497001

Well B50A0497002

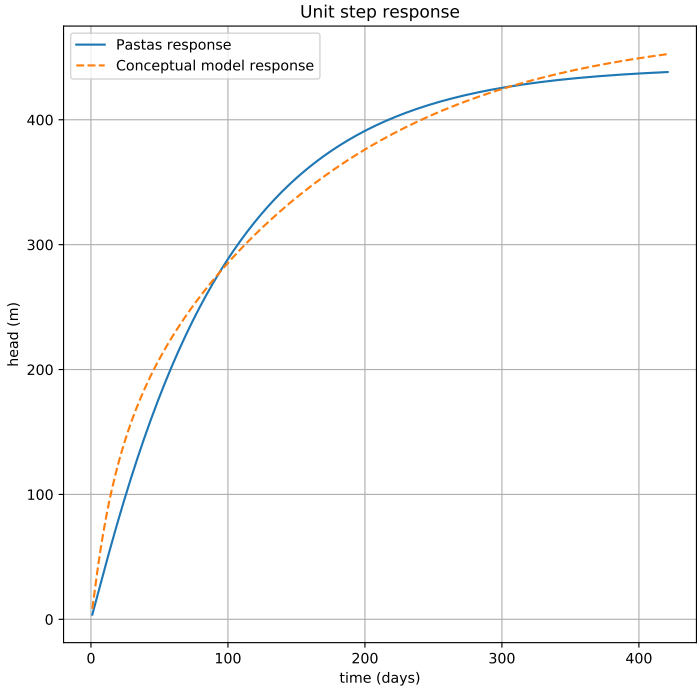

Figure C.21: The calibration result of the conceptual model to the Pastas step response of well B50A0497002

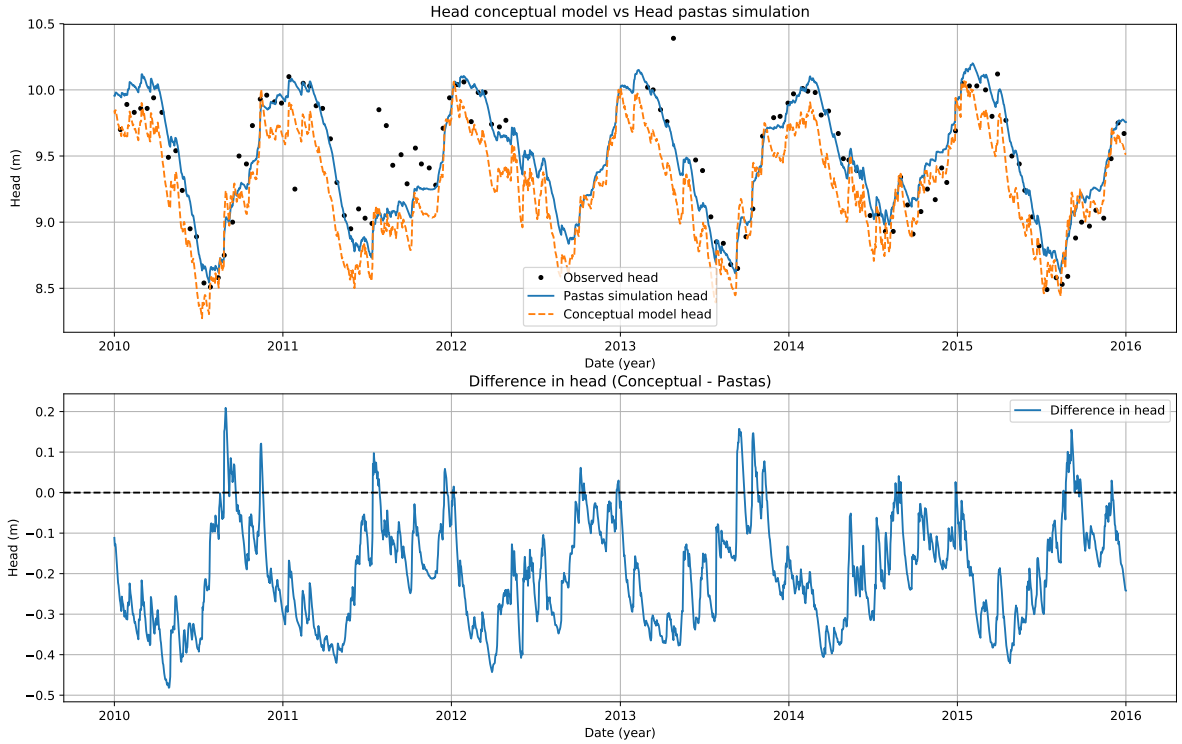

Figure C.22: Simulated head in well B50A0497002, compared with the observations and the time series simulation

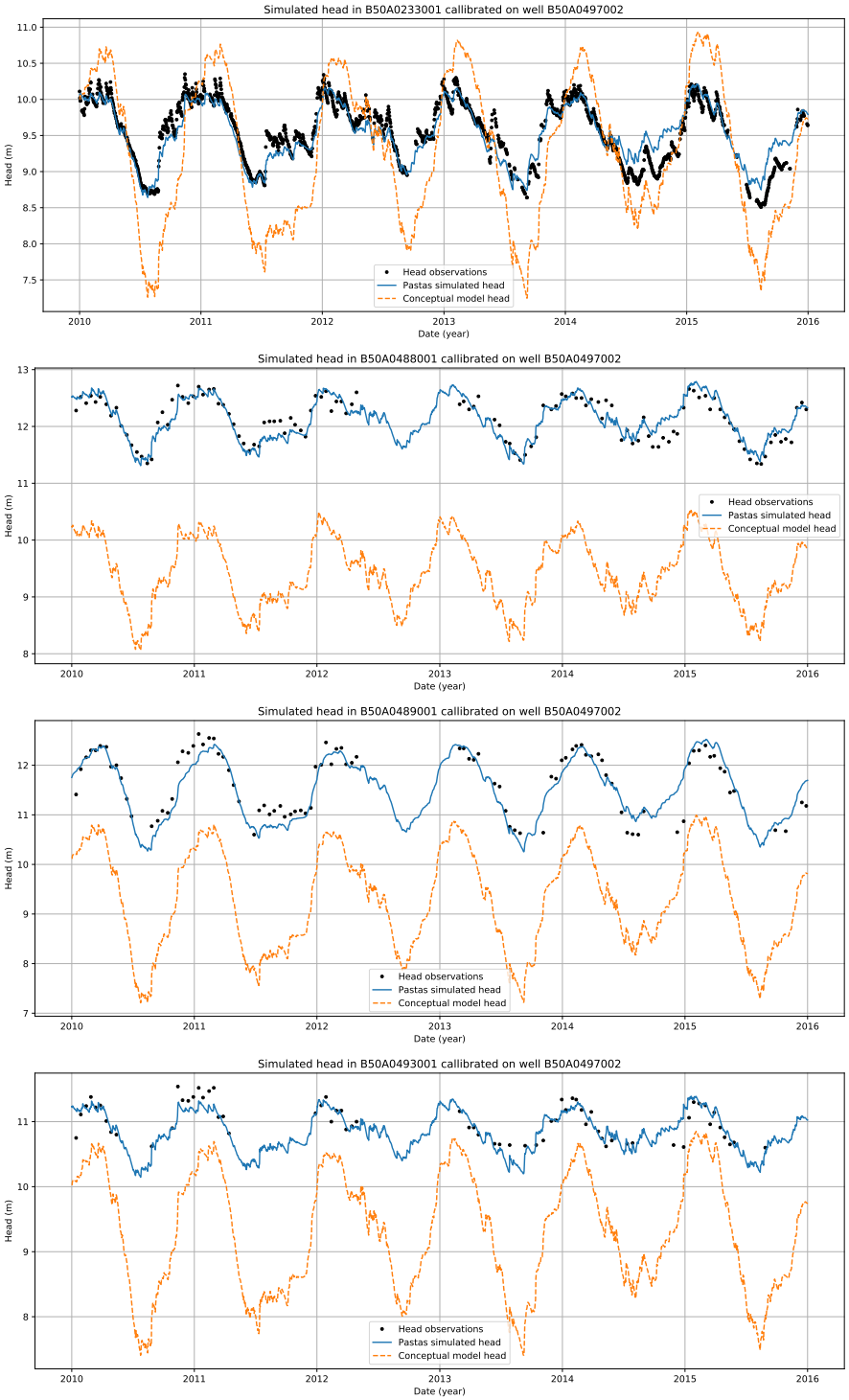

Figure C.23: The conceptual model simulation of well at the observations wells calibrated on well B50A0497002

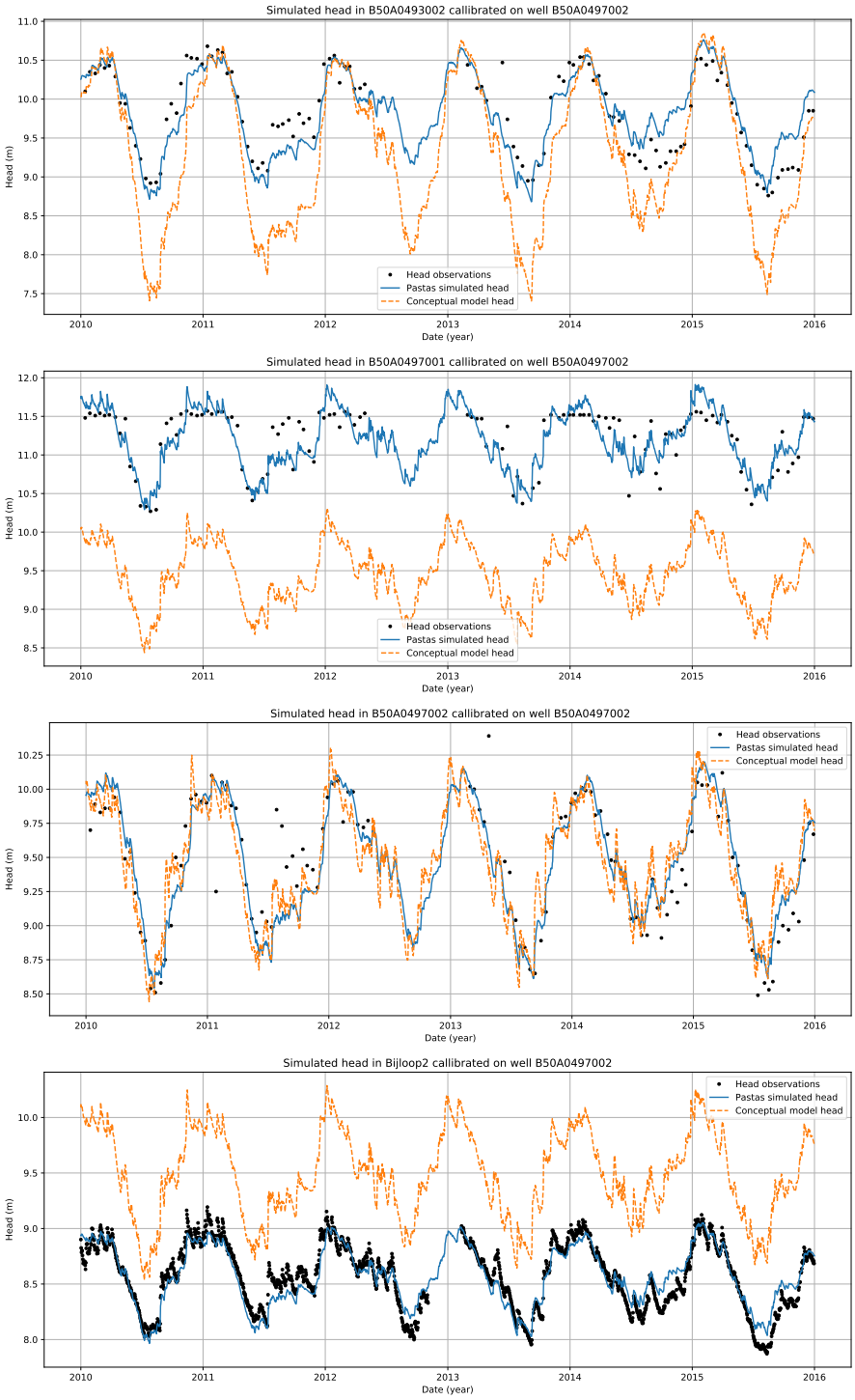

Figure C.23: Continued: The conceptual model simulation at the observations wells calibrated on well B50A0497002

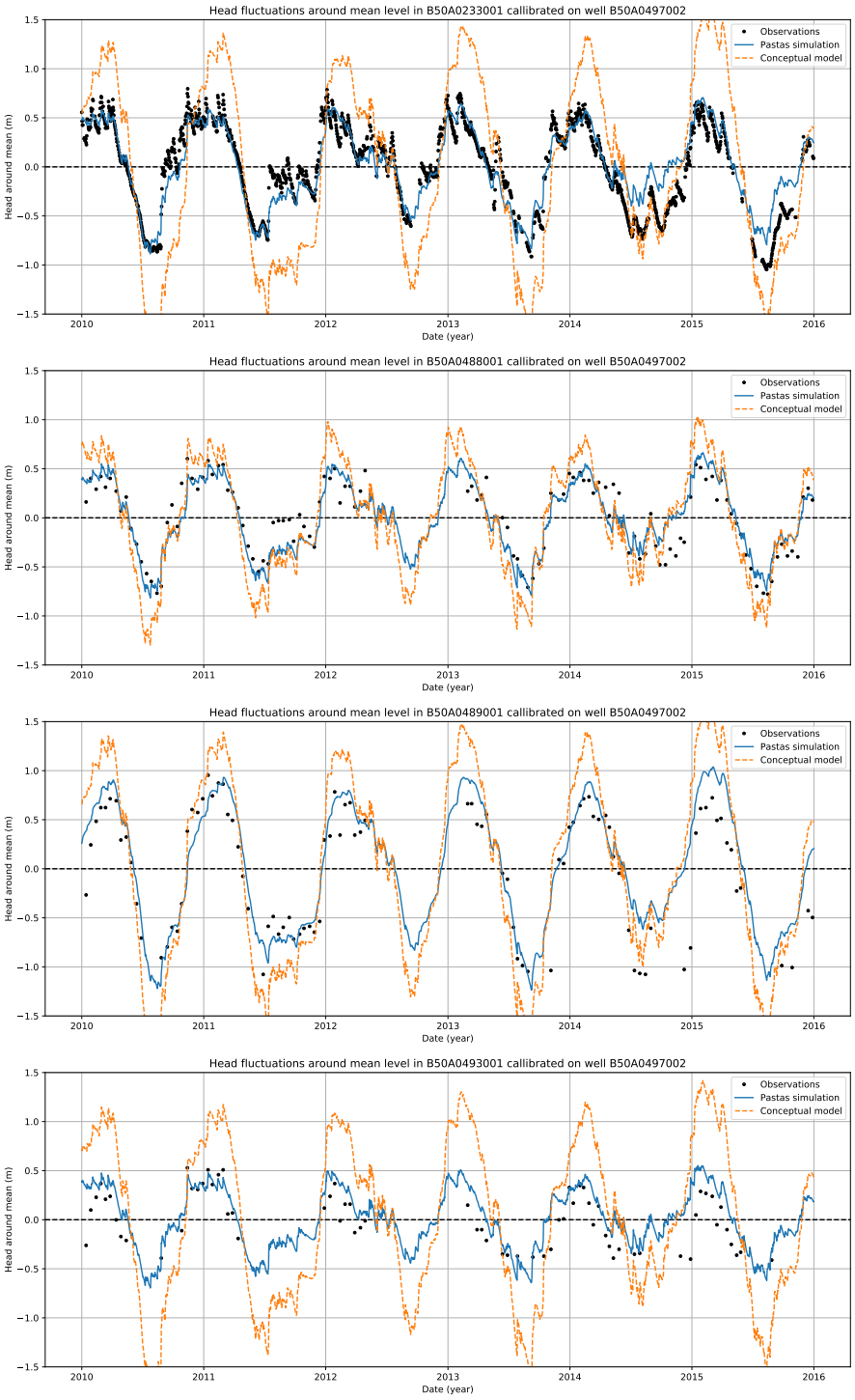

Figure C.24: Fluctuations of the observations, Pastas simulation and conceptual model simulation in well B50A0497002

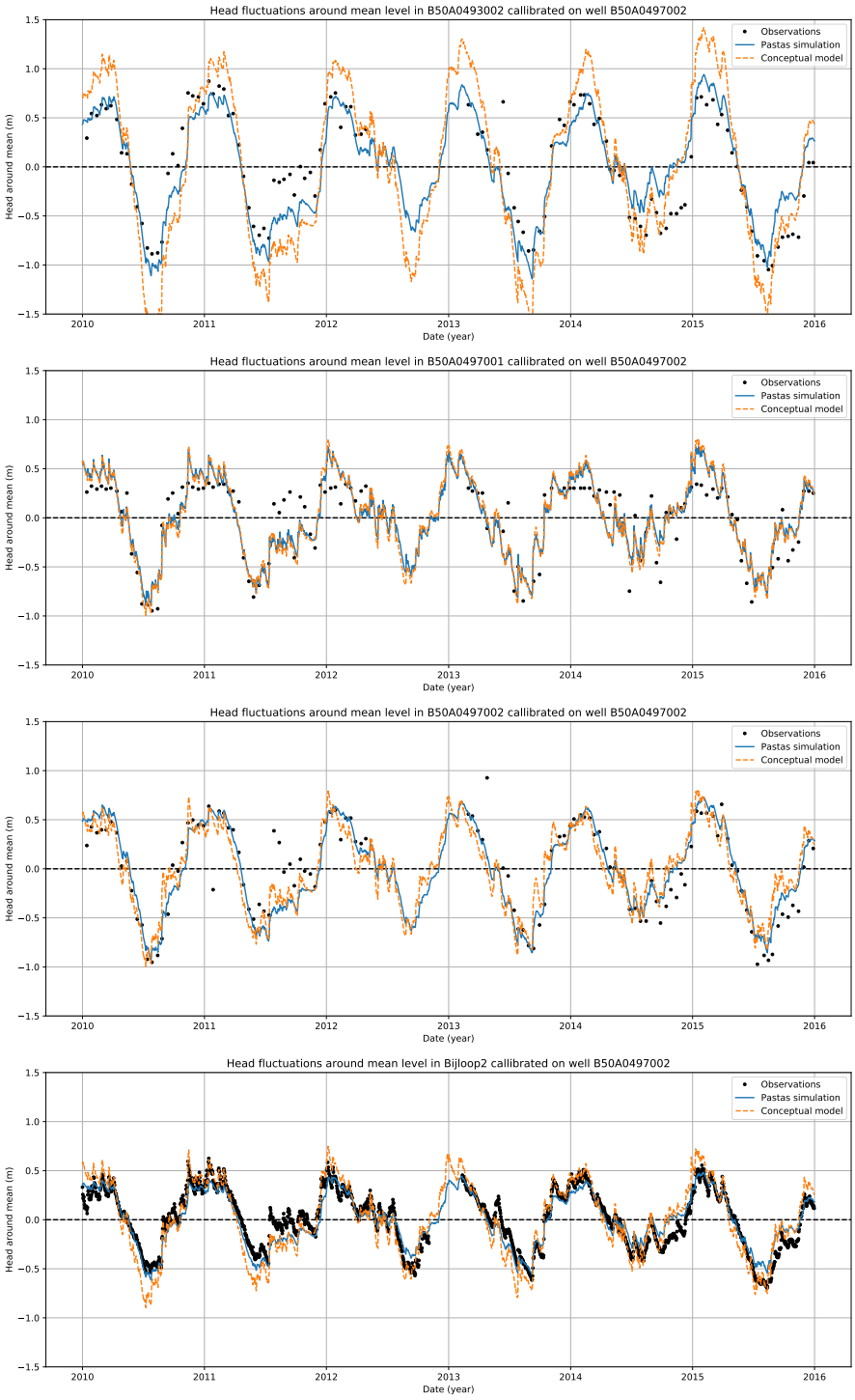

Figure C.24: Continued: Fluctuations of the observations, Pastas simulation and conceptual model simulation in well B50A0497002

Well B50A0233001

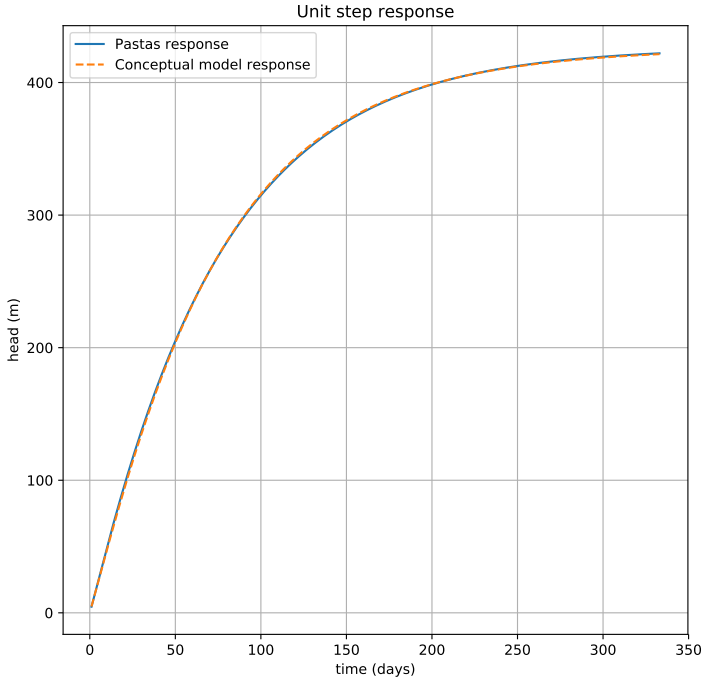

Figure C.25: The calibration result of the conceptual model to the Pastas step response of well B50A0233001

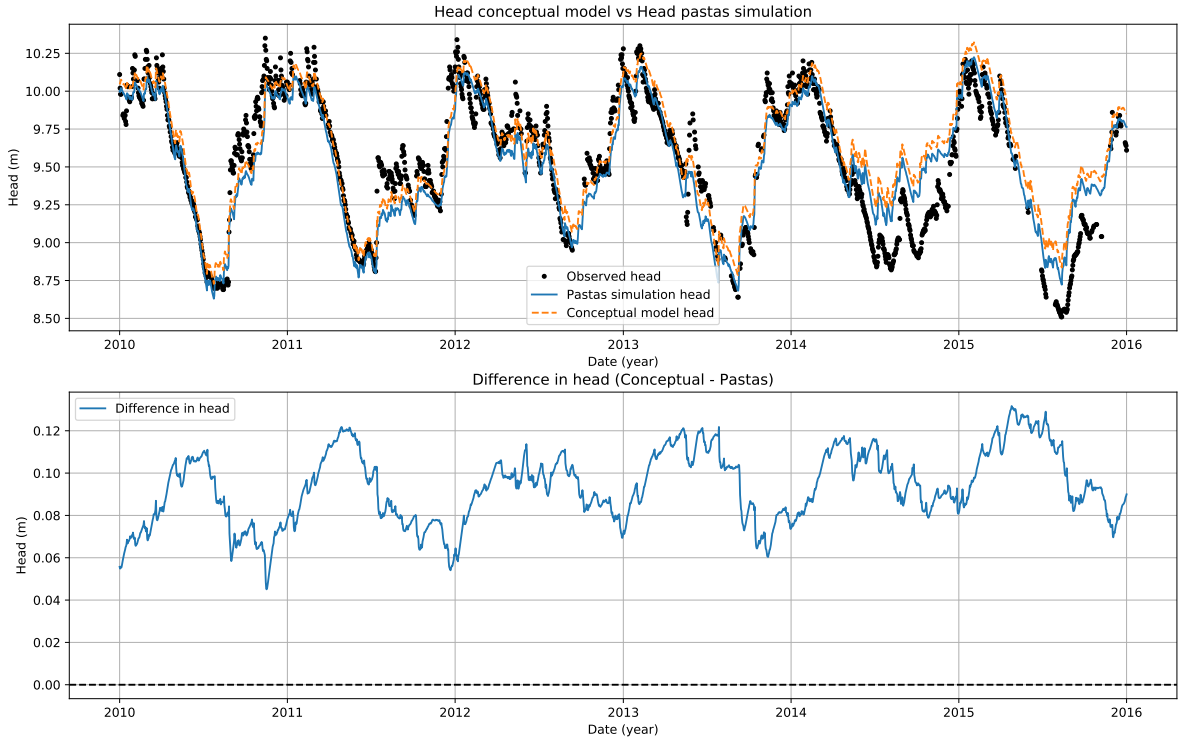

Figure C.26: Simulated head in well B50A0233001, compared with the observations and the time series simulation

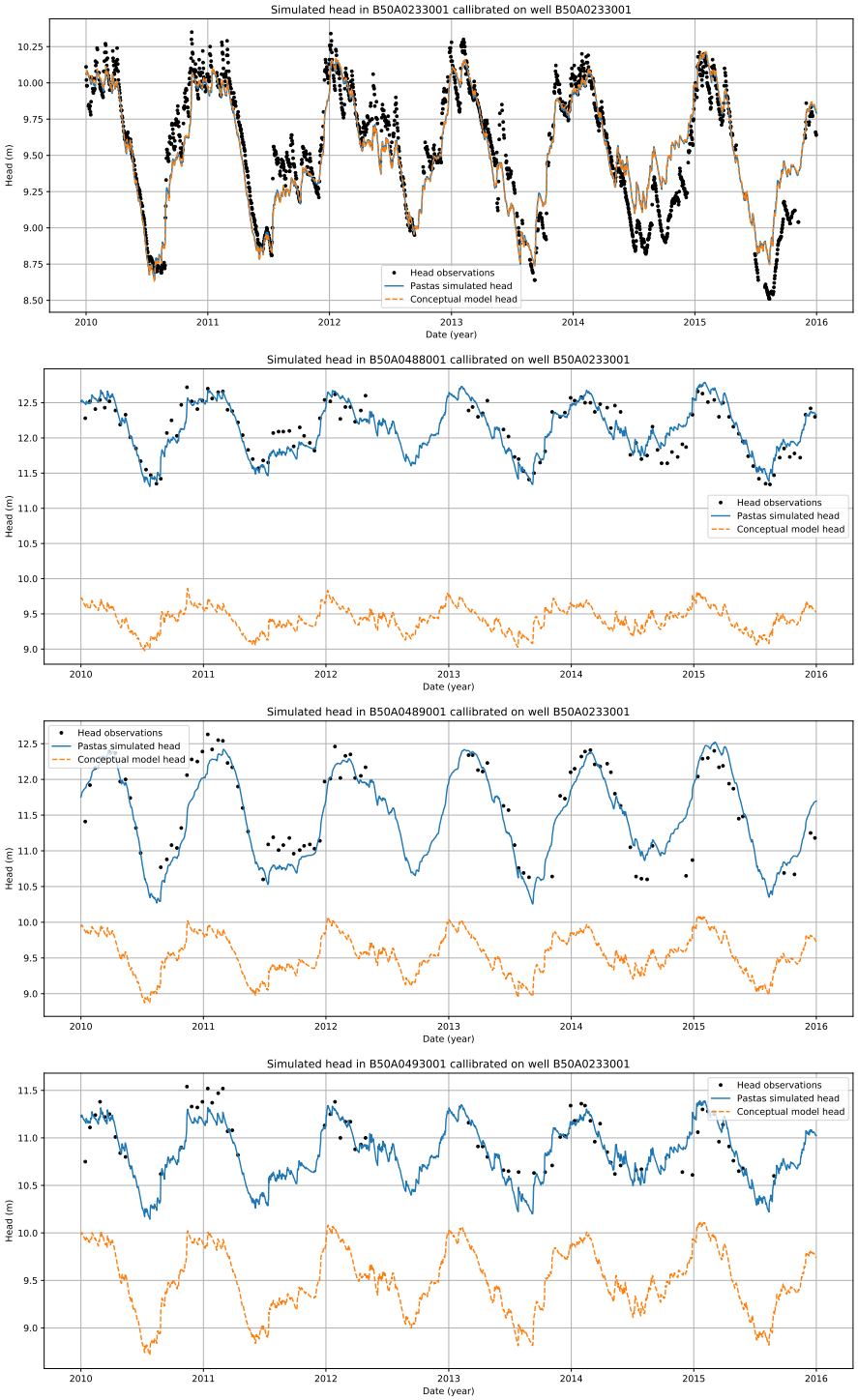

Figure C.27: The conceptual model simulation of well at the observations wells calibrated on well B50A0233001

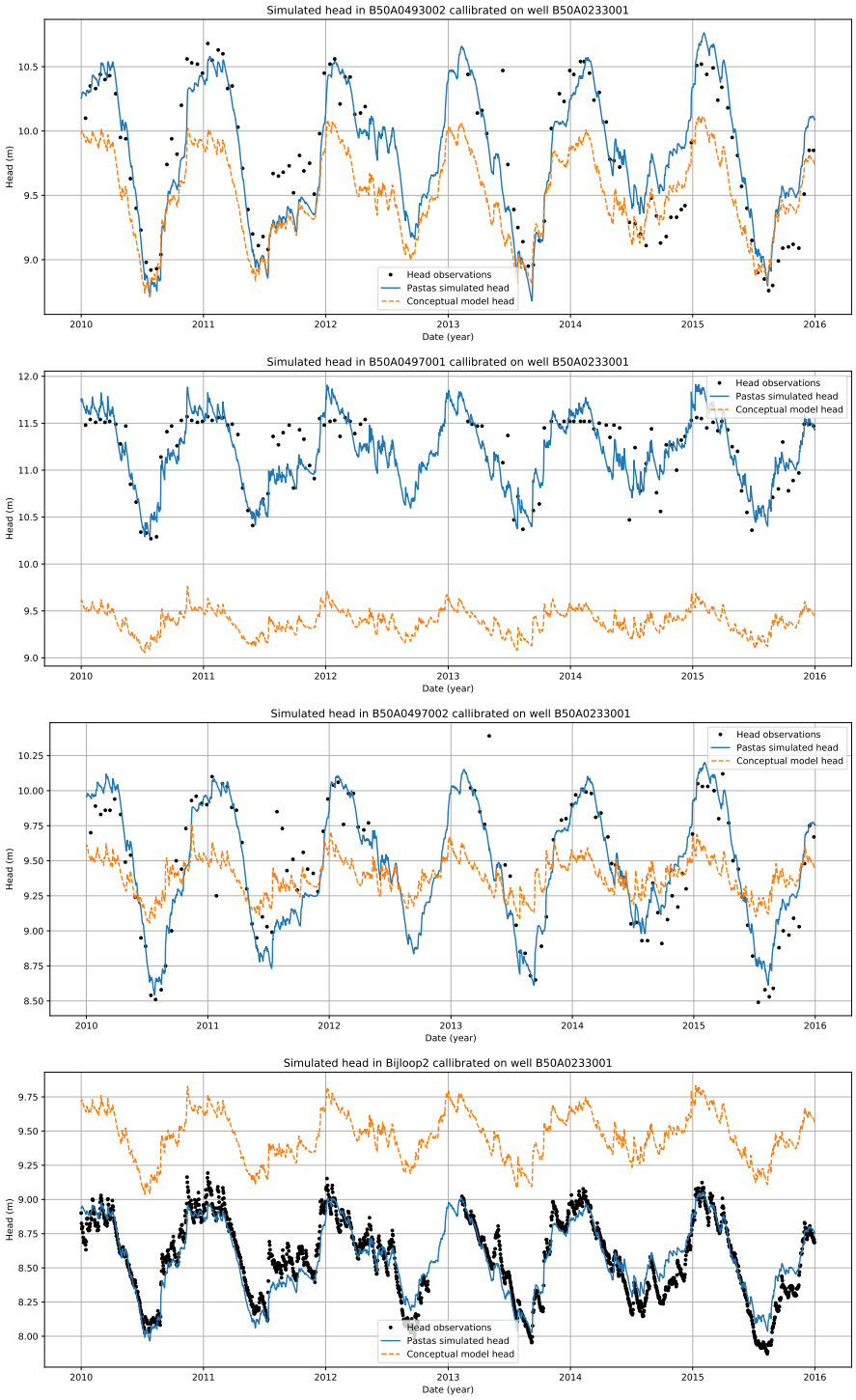

Figure C.27: Continued: The conceptual model simulation at the observations wells calibrated on well B50A0233001

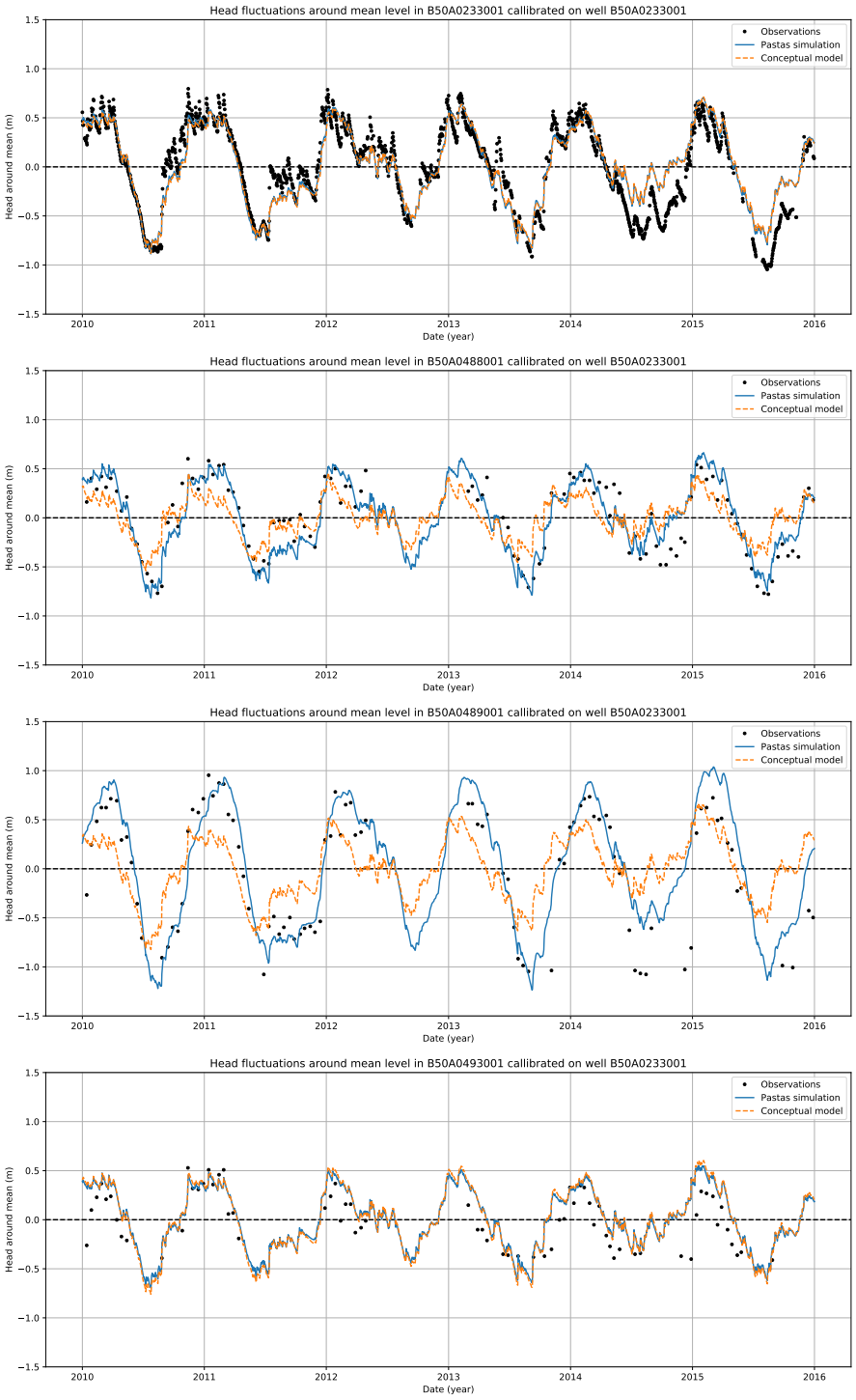

Figure C.28: Fluctuations of the observations, Pastas simulation and conceptual model simulation in well B50A0233001

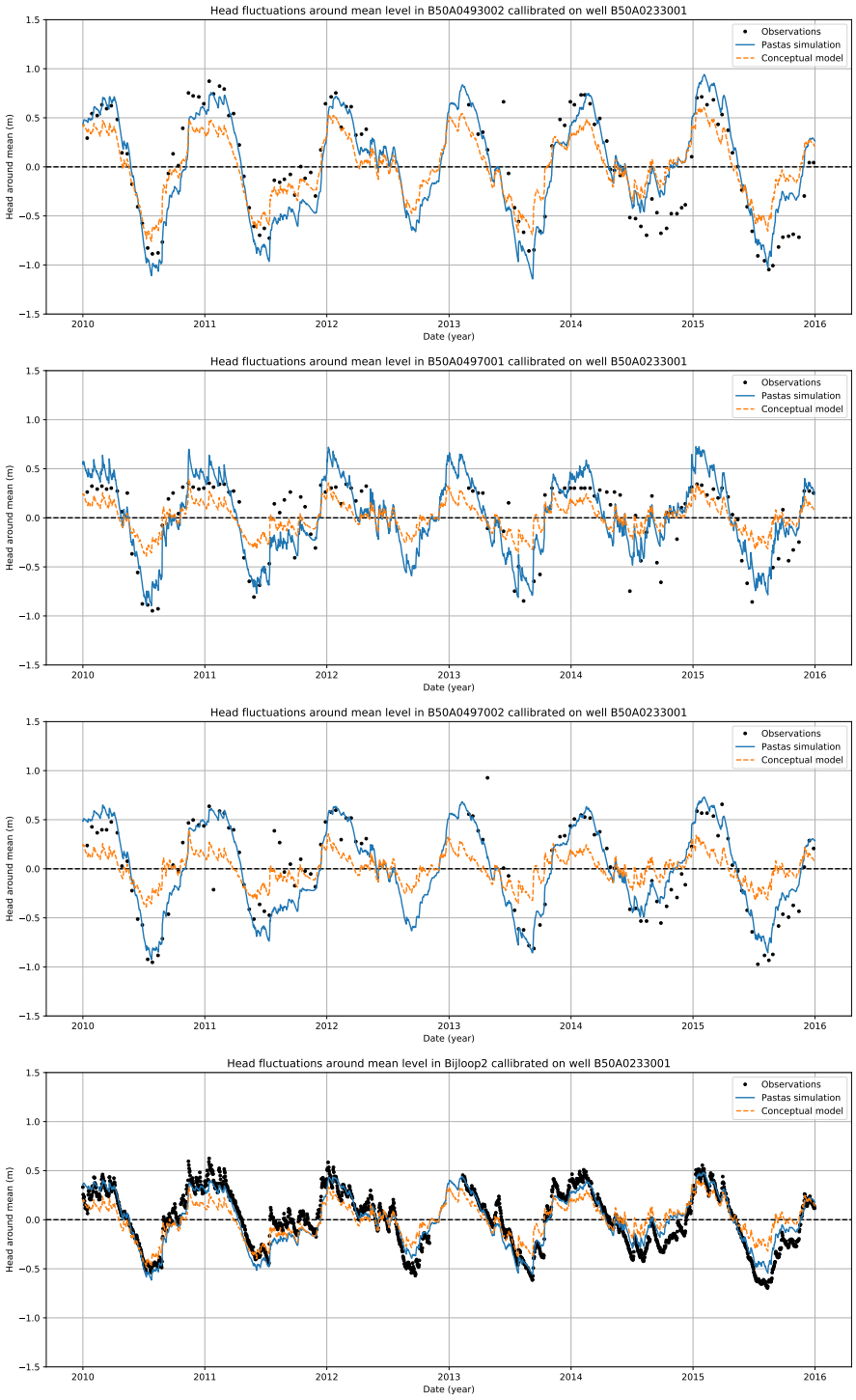

Figure C.28: Continued: Fluctuations of the observations, Pastas simulation and conceptual model simulation in well B50A0233001

Well Bijloop2

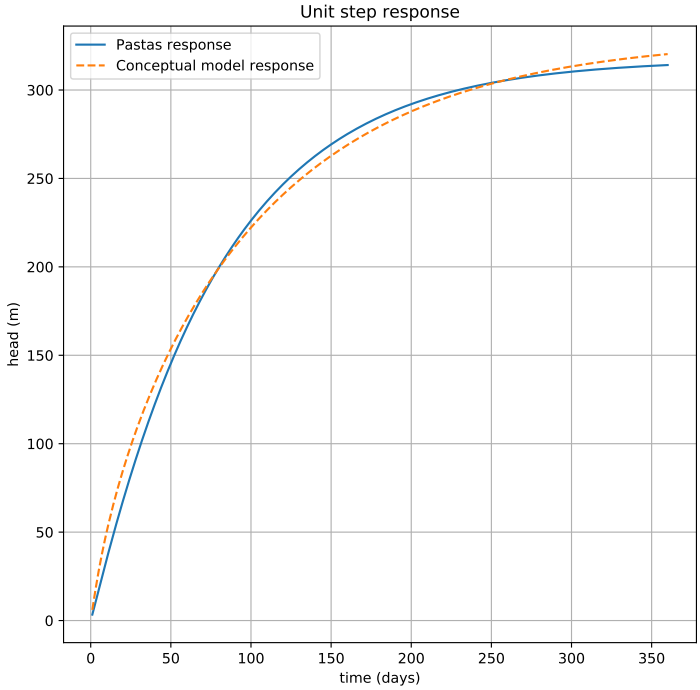

Figure C.29: The calibration result of the conceptual model to the Pastas step response of well Bijloop2

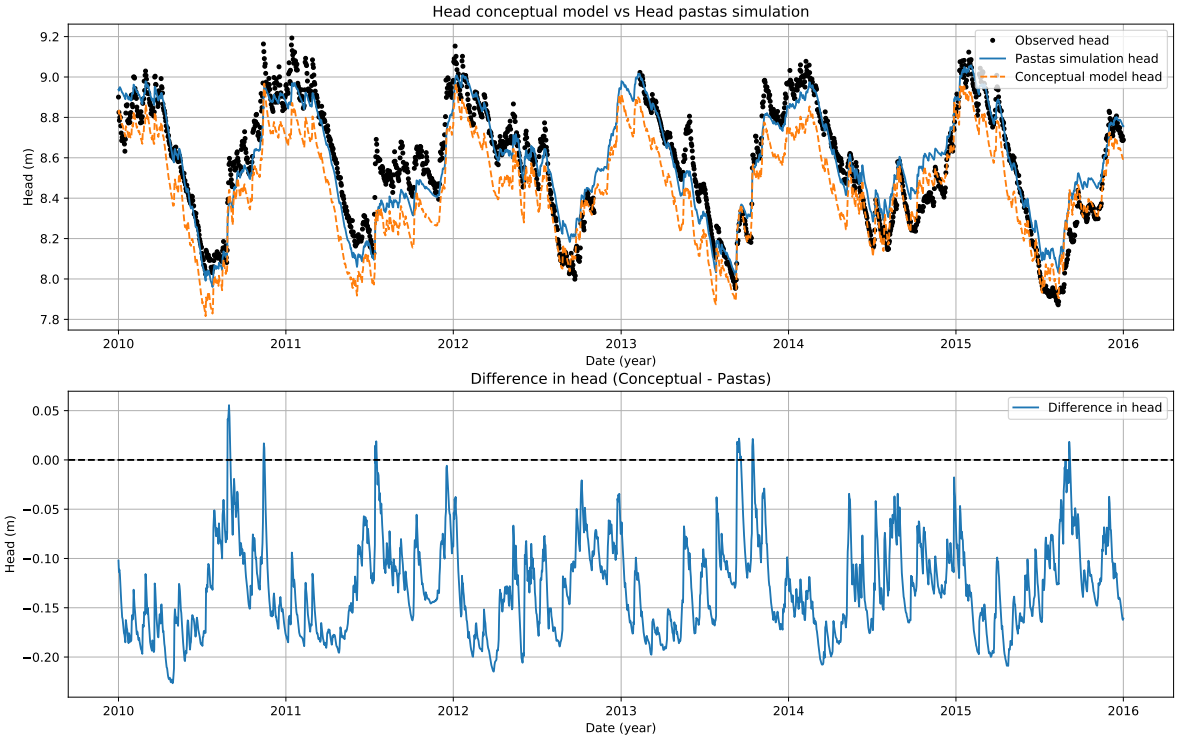

Figure C.30: Simulated head in well Bijloop2, compared with the observations and the time series simulation

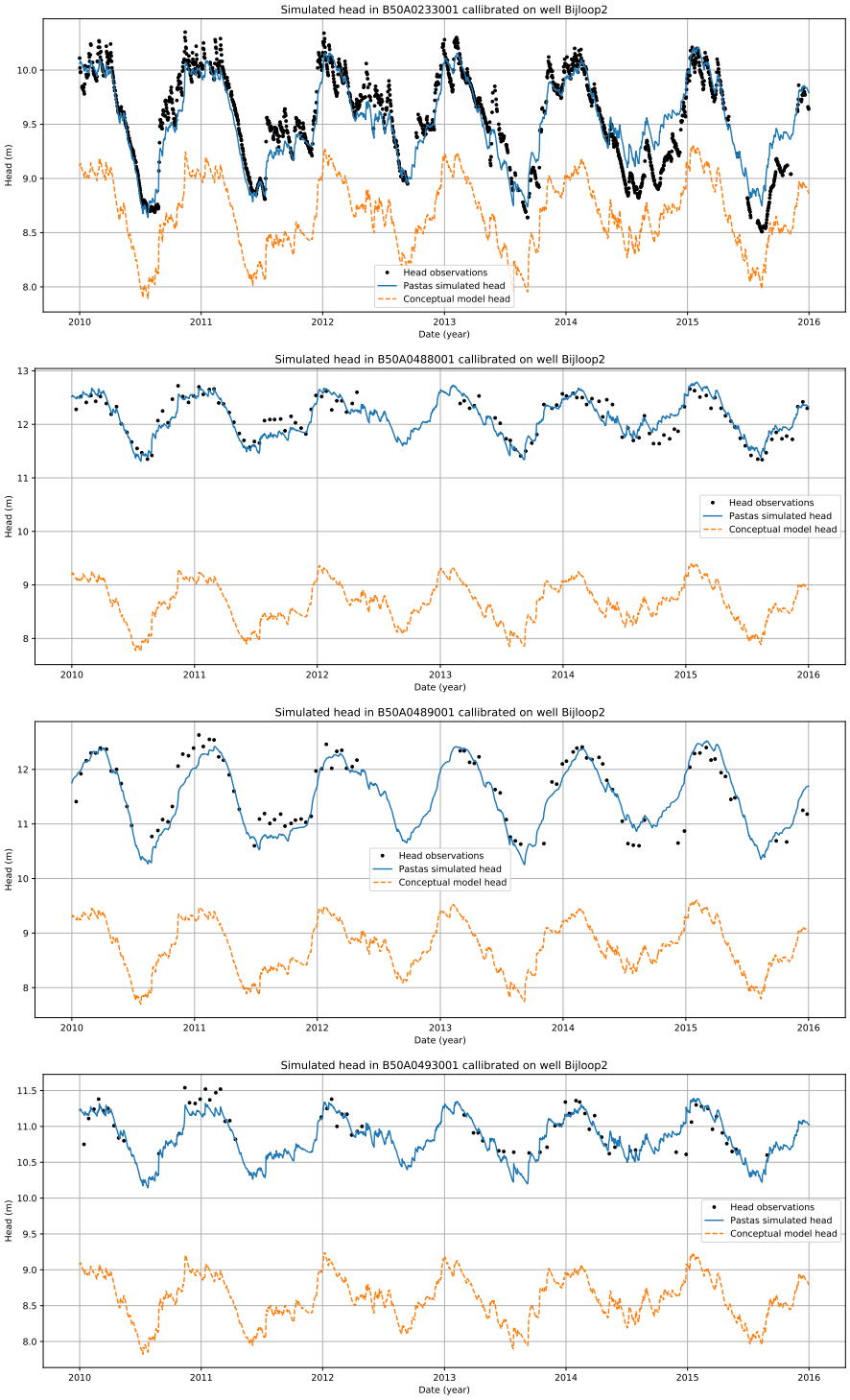

Figure C.31: The conceptual model simulation of well at the observations wells calibrated on well Bijloop2

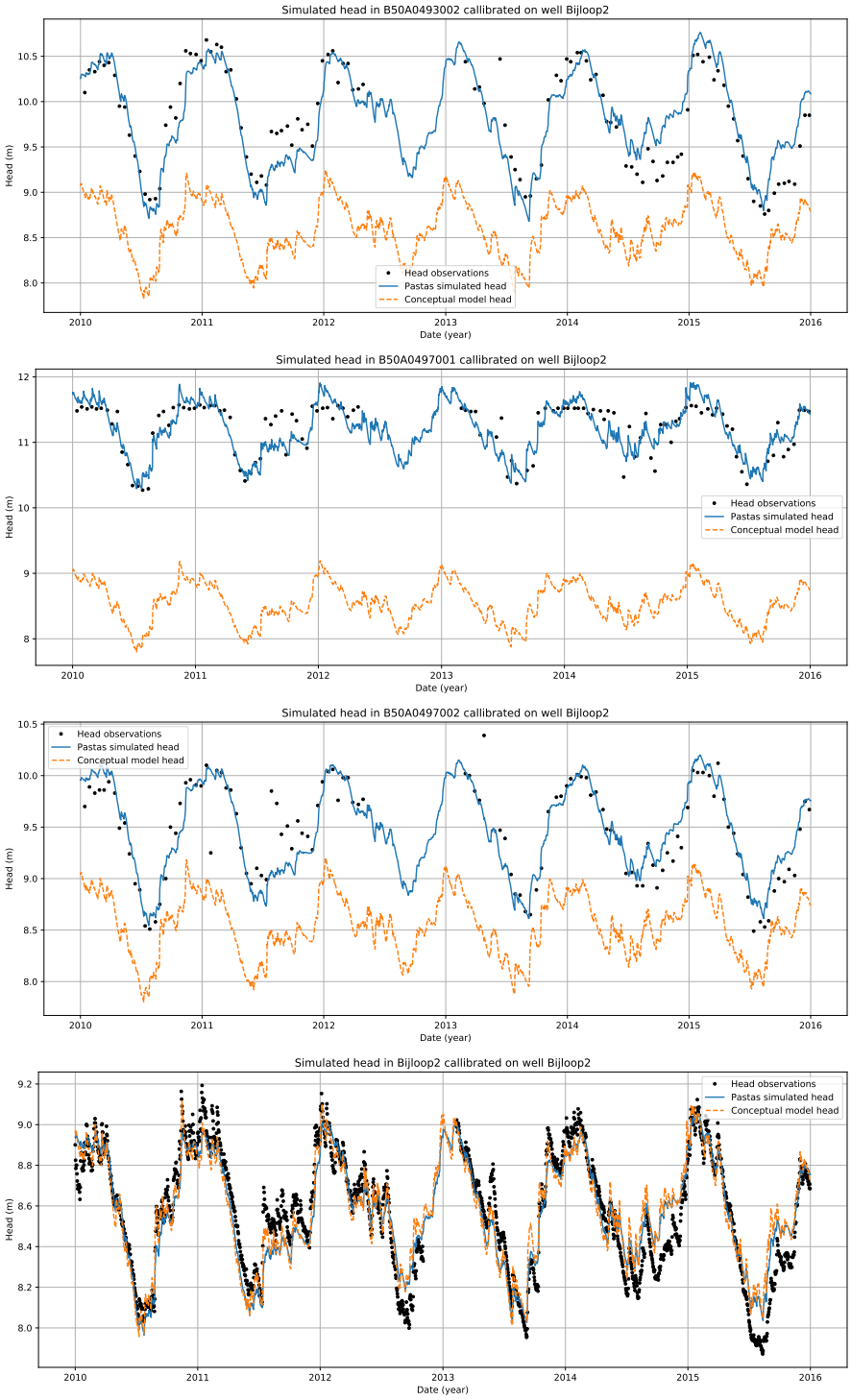

Figure C.31: Continued: The conceptual model simulation at the observations wells calibrated on well Bijloop2

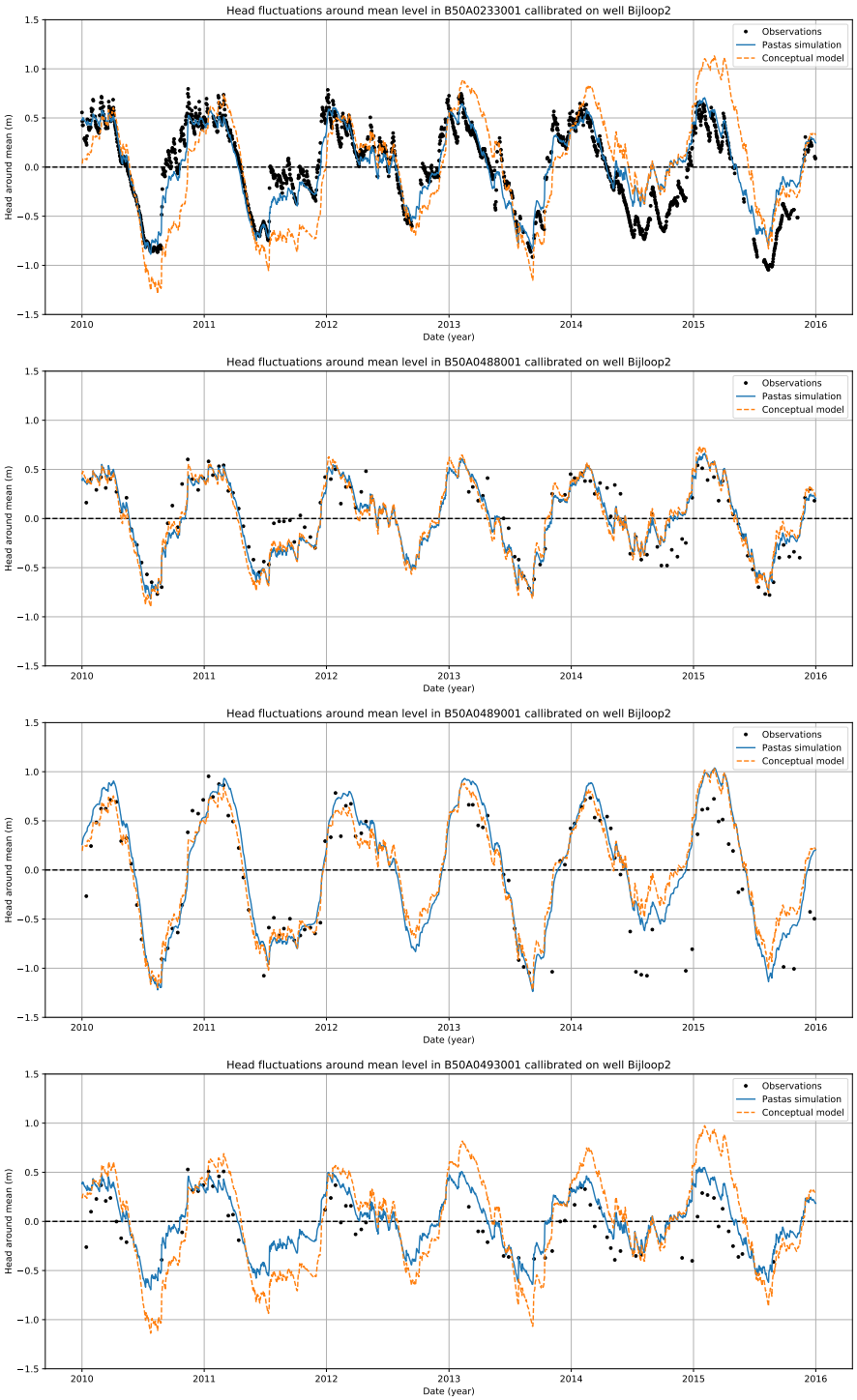

Figure C.32: Fluctuations of the observations, Pastas simulation and conceptual model simulation in well Bijloop2

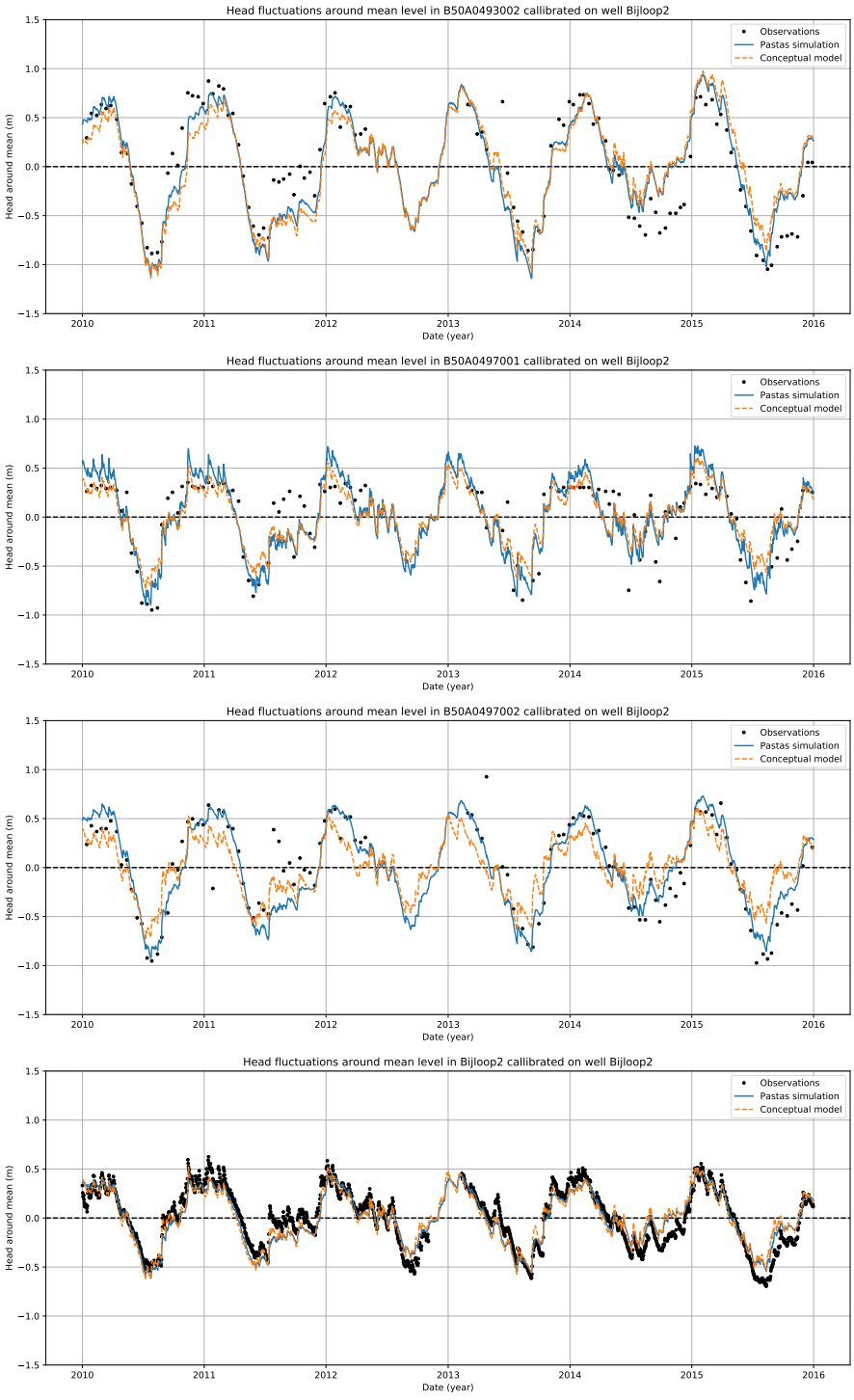

Figure C.32: Continued: Fluctuations of the observations, Pastas simulation and conceptual model simulation in well Bijloop2